PB81-185118

# Use and Limitations of In-Stack Impactors

Florida Univ.
Gainesville

Prepared for

Environmental Sciences Research Lab.
Research Triangle Park, NC

Feb 80

U.S. Department of Commerce
National Technical Information Service
NTIS

**TECHNICAL REPORT DATA**
*(Please read Instructions on the reverse before completing)*

| 1. REPORT NO. | 2 | 3. RECIPIENT'S ACCESSION NO. |
|---|---|---|
| EPA-600/2-80-048 | | |

| 4. TITLE AND SUBTITLE | 5. REPORT DATE |
|---|---|
| USE AND LIMITATIONS OF IN-STACK IMPACTORS | February 1980 |
| | 6. PERFORMING ORGANIZATION CODE |

| 7. AUTHOR(S) | 8. PERFORMING ORGANIZATION REPORT NO. |
|---|---|
| Dale A. Lundgren and W. David Balfour | |

| 9. PERFORMING ORGANIZATION NAME AND ADDRESS | 10. PROGRAM ELEMENT NO. |
|---|---|
| Department of Environmental Engineering Sciences<br>University of Florida<br>Gainesville, Florida 32611 | 1AD712 BA 28 (FY-77) |
| | 11. CONTRACT/GRANT NO. |
| | Grant R-803692 |

| 12. SPONSORING AGENCY NAME AND ADDRESS | 13. TYPE OF REPORT AND PERIOD COVERED |
|---|---|
| Environmental Sciences Research Laboratory - RTP, NC<br>Office of Research and Development<br>U.S. Environmental Protection Agency<br>Research Triangle Park, N.C. 27711 | Final |
| | 14. SPONSORING AGENCY CODE |
| | EPA/600/09 |

15. SUPPLEMENTARY NOTES

16. ABSTRACT

A systematic evaluation of the operating parameters for four commercially available in-stack cascade impactors was carried out with polydisperse test aerosols. Test aerosols used were polystyrene latex spheres, uranine, sodium chloride, dioctyl phthalate, or dinonyl phthalate. The effect upon the apparent measured size distribution of each polydisperse test aerosol was noted for various gas sampling rates (flow rates), types of impactor collection surfaces (glass fiber, uncoated aluminum, and aluminum coated with silicone), stage loadings and interstage losses. Collection surfaces were further characterized as to their weight loss during exposure to elevated temperatures and their tendency to be blown off by an impinging jet of air.

Measurements revealed that interstage losses may amount to 30% of the total collected mass; however, there is little effect upon the apparent measured size distribution when these losses are ignored. The useful range of flow rates available for the impactors was defined at the lower end by a loss of useful sizing data and at the upper end by the presence of particle bounce off the latter stages. In general, the impactors were found to give similar apparent measured size distributions when operated at various flow rates within this useful range.

Recommendations were made for: 1) optimum operation of the impactor when sampling various types of aerosols, and 2) accounting for observed or known errors in the data.

17. KEY WORDS AND DOCUMENT ANALYSIS

| a. DESCRIPTORS | b. IDENTIFIERS/OPEN ENDED TERMS | c. COSATI Field/Group |
|---|---|---|
| * Air pollution<br>* Evaluation<br>* Instruments<br>* Particle size distribution | In-Stack Cascade Impactor | 13B<br>14B |

| 18. DISTRIBUTION STATEMENT | 19. SECURITY CLASS (This Report) | 21. NO. OF PAGES |
|---|---|---|
| RELEASE TO PUBLIC | UNCLASSIFIED | 126 |
| | 20. SECURITY CLASS (This page) | 22. PRICE |
| | UNCLASSIFIED | |

EPA Form 2220-1 (Rev. 4-77) PREVIOUS EDITION IS OBSOLETE

United States
Environmental Protection
Agency

Environmental Sciences Research
Laboratory
Research Triangle Park NC 27711

EPA-600/2-80-048
February 1980

Research and Development

PB81-185118

EPA

# Use and Limitations of In-Stack Impactors

PRODUCT OF:
NATIONAL TECHNICAL
INFORMATION SERVICE
U.S. DEPARTMENT OF COMMERCE
SPRINGFIELD, VA. 22161

## RESEARCH REPORTING SERIES

Research reports of the Office of Research and Development, U.S. Environmental Protection Agency, have been grouped into nine series. These nine broad categories were established to facilitate further development and application of environmental technology. Elimination of traditional grouping was consciously planned to foster technology transfer and a maximum interface in related fields. The nine series are:

1. Environmental Health Effects Research
2. Environmental Protection Technology
3. Ecological Research
4. Environmental Monitoring
5. Socioeconomic Environmental Studies
6. Scientific and Technical Assessment Reports (STAR)
7. Interagency Energy-Environment Research and Development
8. "Special" Reports
9. Miscellaneous Reports

This report has been assigned to the ENVIRONMENTAL PROTECTION TECHNOLOGY series. This series describes research performed to develop and demonstrate instrumentation, equipment, and methodology to repair or prevent environmental degradation from point and non-point sources of pollution. This work provides the new or improved technology required for the control and treatment of pollution sources to meet environmental quality standards.

This document is available to the public through the National Technical Information Service, Springfield, Virginia 22161.

EPA-600/2-80-048
February 1980

# USE AND LIMITATIONS OF IN-STACK IMPACTORS

by

Dale A. Lundgren and W. David Balfour
Department of Environmental Engineering Sciences
University of Florida
Gainesville, Florida 32611

Grant No. R803692-02

Project Officer

Kenneth T. Knapp
Emissions Measurement and Characterization Division
Environmental Sciences Research Laboratory
Research Triangle Park, N.C. 27711

ENVIRONMENTAL SCIENCES RESEARCH LABORATORY
OFFICE OF RESEARCH AND DEVELOPMENT
U.S. ENVIRONMENTAL PROTECTION AGENCY
RESEARCH TRIANGLE PARK, N.C. 27711

## DISCLAIMER

This report has been reviewed by the Environmental Sciences Research Laboratory, U.S. Environmental Protection Agency, and approved for publication. Approval does not signify that the contents necessarily reflect the views and policies of the U.S. Environmental Protection Agency, nor does mention of trade names or commercial products constitute endorsement or recommendation for use.

## ABSTRACT

A systematic evaluation of the operating parameters for four commercially available in-stack cascade impactors was carried out with polydisperse test aerosols. The impactors tested included a MK III University of Washington source test cascade impactor, an Andersen MK III stack sampler, a Sierra Model 226 source cascade impactor and a modified Brink Model B cascade impactor. Test aerosols used, classified according to their collection characteristics, were hard and bouncy (polystyrene latex spheres), hygroscopic and medium bouncy (uranine and sodium chloride), or a sticky liquid (dioctyl phthalate and dinonyl phthalate). The effect upon the apparent measured size distribution of each polydisperse test aerosol was noted for various gas sampling rates (flow rates), types of impactor collection surfaces (glass fiber, uncoated aluminum, and aluminum coated with silicone), stage loadings and interstage losses. Collection surfaces were further characterized as to their weight loss during exposure to elevated temperatures and their tendency to be blown off by an impinging jet of air.

Based upon these observations the spray silicone was the only "grease" type collection surface coating found suitable for use at temperatures of up to 400°F and incident jet velocities up to 120 m/sec. At temperatures of 500°F and greater the only collection surfaces which gave acceptable results were the uncoated aluminum and the glass fiber. The type of collection surface coatings used was shown to have a definite effect upon the apparent measured size distribution. The observed increase in mass mean diameter (mmd) noted with the glass fiber collection surface was shown to be due, at least in part, to the increased collection efficiency of submicron particles for the upper stages of the impactor. Both the silicon spray and glass fiber collection surface coatings provided stable collection characteristics over a range of stage loadings up to 10 mg per stage.

Measurements revealed that interstage losses may amount to 30% of the total collected mass; however, there is little effect upon the apparent measured size distribution when these losses are ignored. The useful range of flow rates available for the impactors was defined at the lower end by a loss of useful sizing data and at the upper end by the presence of particle bounce off the latter stages. In general, the impactors were found to give similar apparent measured size distributions when operated at various flow rates within this useful range.

Recommendations were made for: 1) optimum operation of the impactor when sampling various types of aerosols, and 2) accounting for observed or known errors in the data.

CONTENTS


Abstract . . . . . iii
Figures . . . . . vi
Tables . . . . . x
Symbols . . . . . xii

1. Introduction . . . . . 1
2. Discussion and Conclusions . . . . . 3
   A. Introduction . . . . . 3
   B. Collection Surface Coatings . . . . . 3
   C. Flow Rate . . . . . 5
   D. Stage Loadings . . . . . 7
   E. Interstage Losses . . . . . 8
   F. Summary and Recommendations . . . . . 8
3. Theoretical Background and Literature Review . . . . . 12
   A. Introduction . . . . . 12
   B. Impactor Theory . . . . . 15
   C. Particle Adhesion . . . . . 18
   D. Previous In-Stack Impactor Studies . . . . . 20
4. Experimental Apparatus, Methods and Procedures . . . . . 25
   A. Introduction . . . . . 25
   B. General Experimental Setup . . . . . 25
   C. Description of the In-Stack Impactors . . . . . 27
      1. MK III University of Washington Source Test Cascade Impactor (Model D) . . . . . 27
      2. Sierra Model 226 Source Cascade Impactor . . . . . 27
      3. Andersen MK III Stack Sampler . . . . . 33
      4. Modified Brink Model B Cascade Impactor . . . . . 33
   D. Impactor Collection Surface Coatings . . . . . 43
   E. Aerosol Generation . . . . . 43
      1. Description of Test Aerosols . . . . . 43
      2. Vibrating Orifice Aerosol Generator . . . . . 48
      3. Three Jet Collison Atomizer . . . . . 49
   F. Techniques for Mass Determination . . . . . 49
      1. Fluorometric Technique . . . . . 49
      2. Gravimetric Technique . . . . . 50
   G. Determination of Collection Efficiency . . . . . 50
   H. Measurement of Flow Rate, Temperature, and Relative Humidity . . . . . 50
5. Experimental Results . . . . . 52
   A. Introduction . . . . . 52
   B. Analysis of Errors . . . . . 52
   C. Collection Surface Coatings . . . . . 54
      1. Suitability of Use at Elevated Temperatures and High Jet Velocities . . . . . 54

2. Effect of Collection Surface Coating on the Measured Size Distribution . . . . . 59
D. Effect of Flow Rate on the Measured Size Distribution . . 63
E. Stage Loading . . . . . 80
1. Effect of Stage Loading on Stage Collection Efficiency . . . . . 80
2. Effect of Stage Loading on the Measured Size Distribution . . . . . 89
F. Interstage Losses . . . . . 95
1. Interstage Losses as a Function of Particle Size . . 95
2. Effect of Interstage Losses on Size Distribution . . 95

References . . . . . 107
Appendix . . . . . 110

A. Guide for the Use of In-Stack Cascade Impactors . . . . . 110

FIGURES


| Number | | Page |
|---|---|---|
| 1 | Effect of collection surface on measured size distribution for polydisperse uranine aerosol using SRI $D_{p_{50}}$ cut-points calibrated for grease and glass fiber collection surfaces (Brink)..... | 6 |
| 2 | Total interstage loss versus particle diameter (U. of W.)..... | 9 |
| 3 | Basic design of an in-stack cascade impactor..... | 13 |
| 4 | Principle of operation of an impactor..... | 14 |
| 5 | Typical impactor efficiency curve..... | 14 |
| 6 | Impactor efficiency curves showing the effect of jet-to-plate distance, Reynolds number and throat length..... | 17 |
| 7 | Particle sizing data presented as differential and cumulative plots..... | 19 |
| 8 | General arrangement of test equipment..... | 26 |
| 9 | MK III University of Washington source test cascade impactor..... | 28 |
| 10 | MK III University of Washington source test cascade impactor nomograph for determining $D_{p_{50}}$ cut-points..... | 31 |
| 11 | Sierra Model 226 source cascade impactor..... | 34 |
| 12 | Andersen MK III stack sampler..... | 38 |
| 13 | Modified Brink Model B cascade impactor..... | 42 |
| 14 | Test set-up for dynamic testing of collection surface coatings..... | 57 |
| 15 | Effect of collection surface on measured size distribution for polydisperse uranine aerosol (U. of W.) | 60 |

| Figure | | Page |
|---|---|---|
| 16 | Effect of collection surface on measured size distribution for polydisperse oil aerosol (U. of W.).... | 61 |
| 17 | Effect of collection surface on measured size distribution for polydisperse oil aerosol of increased mmd (U. of W.)..... | 62 |
| 18 | Deposition of uranine aerosol onto glass fiber collection surface at 0.5 cfm..... | 64 |
| 19 | Effect of collection surface on measured size distribution for polydisperse uranine aerosol (Brink)... | 66 |
| 20 | Measured size distributions for a polydisperse uranine aerosol obtained with the University of Washington, Andersen, Brink and Sierra impactors..... | 67 |
| 21 | Effect of flow rate on measured size distribution for polydisperse uranine aerosol sampled onto spray silicone (U. of W.)..... | 68 |
| 22 | Deposition of uranine aerosol onto spray silicone at 1.0 cfm..... | 69 |
| 23 | Effect of flow rate on measured size distribution for polydisperse uranine aerosol sampled onto glass fiber (U. of W.)..... | 71 |
| 24 | Effect of flow rate on measured size distribution for polydisperse oil aerosol sampled onto spray silicone (U. of W.)..... | 72 |
| 25 | Effect of flow rate on measured size distribution for polydisperse oil aerosol sampled onto glass fiber (U. of W.)..... | 73 |
| 26 | Deposition of oil aerosol..... | 74 |
| 27 | Effect of flow rate on measured size distribution for polydisperse oil aerosol of increased mmd sampled onto spray silicone (U. of W.)..... | 76 |
| 28 | Effect of flow rate on measured size distribution for polydisperse oil aerosol of increased mmd sampled onto glass fiber (U. of W.)..... | 77 |
| 29 | Deposition of polystyrene latex spheres..... | 78 |
| 30 | Effect of flow rate on measured size distribution for polydisperse uranine aerosol collected on glass fiber (Andersen)..... | 81 |

| Figure | | Page |
|---|---|---|
| 31 | Effect of flow rate on measured size distribution for polydisperse uranine aerosol collected on glass fiber (Sierra) | 82 |
| 32 | Effect of flow rate on measured size distribution for polydisperse uranine aerosol collected on glass fiber (Brink) | 83 |
| 33 | Effect of collection surface on measured size distribution of polydisperse uranine aerosol sampled at 1.0 cfm (U. of W.) | 84 |
| 34 | Effect of collection surface on measured size distribution of polydisperse uranine aerosol sampled at 0.25 cfm (U. of W.) | 85 |
| 35 | Effect of stage loading on penetration for polydisperse uranine aerosol | 86 |
| 36 | Effect of stage loading on penetration for polydisperse oil aerosol | 87 |
| 37 | Effect of stage loading on penetration for polydisperse oil aerosol | 88 |
| 38 | Effect of stage loading on penetration for polydisperse salt aerosol | 90 |
| 39 | Effect of stage loading on measured size distribution for polydisperse uranine aerosol sampled onto spray silicone (U. of W.) | 91 |
| 40 | Effect of stage loading on measured size distribution for polydisperse uranine aerosol sampled onto glass fiber (U. of W.) | 92 |
| 41 | Effect of stage loading on measured size distribution for polydisperse oil aerosol sampled onto glass fiber (U. of W.) | 93 |
| 42 | Effect of stage loading on measured size distribution for polydisperse oil aerosol sampled onto spray silicone (U. of W.) | 94 |
| 43 | Total interstage loss versus particle diameter(U of W). | 96 |
| 44 | Interstage losses for a polydisperse uranine aerosol at a total loading of 0.3 mg (U. of W.) | 97 |

| Figure | | Page |
|---|---|---|
| 45 | Interstage losses for a polydisperse uranine aerosol at a total loading of 10.0 mg (U. of W.)..... | 98 |
| 46 | Effect of interstage losses on measured size distribution of polydisperse uranine aerosol sampled onto spray silicone at low stage loading (U. of W.)... | 99 |
| 47 | Effect of interstage losses on measured size distribution for polydisperse uranine aerosol sampled onto spray silicone at high stage loading (U. of W.).. | 100 |
| 48 | Effect of interstage losses on measured size distribution for polydisperse uranine aerosol sampled onto glass fiber at low stage loading (U. of W.)..... | 101 |
| 49 | Effect of interstage losses on measured size distribution for polydisperse uranine aerosol sampled onto glass fiber at high stage loadings (U. of W.).... | 102 |
| 50 | Interstage losses for the Andersen, Sierra and Brink.. | 103 |
| 51 | Effect of interstage losses on measured size distribution for a polydisperse uranine aerosol (Andersen)..... | 104 |
| 52 | Effect of interstage losses on measured size distribution for a polydisperse uranine aerosol (Sierra)..... | 105 |
| 53 | Effect of interstage losses on measured size distribution for a polydisperse uranine aerosol (Brink)..... | 106 |

TABLES


| Number | | Page |
|---|---|---|
| 1 | Commercially Available In-Stack Cascade Impactors..... | 2 |
| 2 | Collection Surface Coatings Tested..... | 4 |
| 3 | Comparison of Measured Total Interstage Loss for Impactors Tested..... | 10 |
| 4 | Experimental Studies of In-Stack Impactors..... | 21 |
| 5 | Collection Surface Coatings Used with In-Stack Cascade Impactors..... | 23 |
| 6 | MK III University of Washington Source Test Cascade Impactor Critical Dimensions..... | 29 |
| 7 | MK III University of Washington Source Test Cascade Impactor Measured Pressure Drop at Various Flow Rates.... | 30 |
| 8 | Reported Values of $D_{P50}$ for the MK III University of Washington Source Test Cascade Impactor..... | 32 |
| 9 | Sierra Model 226 Source Cascade Impactor Critical Dimensions..... | 35 |
| 10 | Sierra Model 226 Source Cascade Impactor Measured Pressure Drop at Various Flow Rates..... | 36 |
| 11 | Reported Values of $D_{P50}$ for the Sierra Model 226 Source Cascade Impactor..... | 37 |
| 12 | Andersen MK III Stack Sampler Critical Dimensions..... | 39 |
| 13 | Andersen MK III Stack Sampler Measured Pressure Drop at Various Flow Rates..... | 40 |
| 14 | Reported Values of $D_{P50}$ for the Andersen MK III Stack Sampler..... | 41 |
| 15 | Modified Brink Model B Cascade Impactor Critical Dimensions..... | 44 |

| Number | | Page |
|---|---|---|
| 16 | Modified Brink Model B Cascade Impactor Measured Pressure Drop at Various Flow Rates | 45 |
| 17 | Reported Values of $D_{P50}$ for the Modified Brink Model B Cascade Impactor | 46 |
| 18 | Test Aerosols | 47 |
| 19 | Errors Associated with Mass Measurement | 53 |
| 20 | Collection Surface Coating Weight Loss for 1-Hour Exposures to Temperatures of 200°F and 500°F | 55 |
| 21 | Maximum Jet Velocities for Impactors Operated at Design Flow Rate | 56 |
| 22 | Observed Tendency of Collection Surface Coating to be Blown Off by an Impinging Jet of Varying Velocity and Temperature | 58 |
| 23 | Percent of Total Collected Mass Per Stage for a Polydisperse Uranine Aerosol | 65 |

## SYMBOLS

| | |
|---|---|
| $C$ | Cunningham slip correction factor, dimensionless |
| C.E. | collection efficiency |
| $D_d$ | droplet diameter, cm |
| $D_p$ | particle diameter, cm |
| $D_{P_{50}}$ | particle diameter associated with 50% collection efficiency, cm |
| $\ell_i$ | stopping distance, cm |
| $M_i$ | mass collected on stage i, gm |
| $\Delta M$ | mass collected on stage n, gm |
| mmd | mass mean diameter, cm |
| $P_a$ | atmospheric pressure, cm mercury |
| $\Delta P_m$ | pressure drop at the dry gas meter, cm mercury |
| $Q$ | gas sampling rate, cfm |
| Re | Reynolds number, dimensionless |
| STK | Stokes number, dimensionless |
| $STK_{50}$ | Stokes number associated with 50% collection efficiency, dimensionless |
| S/W | ratio of the jet-to-plate distance to the diameter or width of the jet, dimensionless |
| $T_a$ | temperature of the aerosol stream, $^oC$ |
| $T_m$ | temperature of the aerosol stream at the dry gas meter, $^oC$ |
| T/W | ratio of jet length to the diameter or width of the jet, dimensionless |
| $V_{acf}$ | actual volume of aerosol stream sampled, $cm^3$ |
| $V_m$ | volume of aerosol stream measured by the dry gas meter, $cm^3$ |

| | |
|---|---|
| $V_o$ | single component of velocity, cm/sec |
| W | width or diameter of the jet, cm |
| $\rho_p$ | particle density, $gm/cm^3$ |
| $\mu$ | viscosity of the media, poise |
| $\delta_g$ | geometric standard deviation, dimensionless |

# SECTION 1

# INTRODUCTION

Design of particulate control equipment necessitates a knowledge of the chemical and physical nature of the aerosol stream, including the particle size distribution present in the process gas stream at the point of control. This requirement results because the effectiveness of any given physical mechanism for particle removal is a function of particle size. Thus, knowledge of the process stream particle size distribution allows for optimum design or selection of particulate control equipment.

At present, size distribution measurements of process gas streams are obtained mainly through the use of in-stack cascade impactors (1), a wide variety of which are commercially available (Table 1). However, many questions still exist concerning the most effective operation of these devices for a given set of stack conditions. Earlier studies have provided information as to the theoretical design, performance, and limitations of cascade impactors operating at ambient conditions, and recent reports have presented generalized guidelines for in-stack cascade impactor calibration, testing procedures and data analysis (1-6).

The wide variety of process streams (temperature, relative humidity, mass loading, stack gas velocity, type of particles, etc.) adds variables whose effects upon the operation of in-stack impactors have not yet been fully documented. This study was an attempt to evaluate systematically several operating parameters for four different models of in-stack impactors, by using polydisperse test aerosols of various composition. The impactors tested were a MK III University of Washington source test cascade impactor, an Andersen MK III stack sampler, a Sierra Model 226 source cascade impactor, and a modified Brink Model B cascade impactor. The parameters evaluated included: 1) gas sampling rate (flow rate); 2) impactor collection surface coating; 3) stage loading limits; 4) interstage losses; and 5) the effects of these above parameters upon the "indicated or apparent" particle size distribution of a polydisperse aerosol.

TABLE 1. COMMERCIALLY AVAILABLE IN-STACK CASCADE IMPACTORS

1. University of Washington Source Test Cascade Impactor
   Pollution Control Systems Corporation
   Renton, Washington 98055

2. Andersen Stack Sampler
   Andersen 2000, Inc
   Atlanta, Georgia 30320

3. Brink Model B Cascade Impactor
   Monsanto Enviro-Chem Systems, Inc
   St. Louis, Missouri 63166

4. MRI Model 1502 Cascade Impactor
   Meteorology Research, Inc
   Altadena, California 91001

5. Sierra Model 226 Cascade Impactor
   Sierra Instruments, Inc
   Carmel Valley, California 93924

6. Tag Sampler
   Sierra Instruments, Inc
   Carmel Valley, California 93924

## SECTION 2

## DISCUSSION AND CONCLUSIONS

### A. INTRODUCTION

This study has attempted to evaluate experimentally the effect of several parameters upon the operation of in-stack cascade impactors, including: type of collection surface, gas sampling rate (flow rate), stage loading and interstage losses. It was accomplished by sampling polydisperse aerosols of various composition and observing the effect of each of these parameters upon the resulting measured size distribution. Results were obtained based upon extensive testing using a MK III University of Washington source test cascade impactor. Further testing utilized an Andersen MK III stack sampler, a Sierra Model 226 source cascade impactor and a modified Brink Model B cascade impactor. In addition, tests were conducted to establish the suitability of various collection surface coatings to operation at: (1) elevated temperatures and (2) high jet velocities.

### B. COLLECTION SURFACE COATINGS

Of the collection surfaces tested (Table 2) only the uncoated aluminum and glass fiber were suited to operation at temperatures of 500°F or greater. At temperatures below 400°F the industrial spray silicone was the only "grease-type" coating which had low, reproducible weight loss and showed no tendency to be blown off the surface to which it was applied. This coating is highly recommended when working temperatures permit its use.

When the uncoated aluminum, glass fiber or spray silicone collection surfaces were used, results of this study show a true need for proper preconditioning of the surface coatings. Several techniques for preconditioning surfaces have been previously cited (4,7,8) and will not be repeated here. With proper preconditioning, both the absolute weight loss and the variability of the coating are minimized. This decreases the collected mass required for given statistical accuracy of the sizing.

When glass fiber collection surfaces were used, the measured size distribution had mmd's greater than distributions obtained when uncoated aluminum or spray silicone were used. This effect was observed for various types of aerosols (uranine, DOP, DNP) at various flow rates (0.25, 0.5, 1.0 cfm) and at various total loadings 5, 10, 15 and 30 mg). In all of the above cases the difference between distributions was approximately 30%. It is not known at this time if such a correction factor could be applied to aerosols of different mmd and $\delta_g$. Results of sampling a polydisperse aerosol which

TABLE 2. COLLECTION SURFACE COATINGS TESTED

1. White Petroleum Jelly
   Andrew Lewis Distributing Corporation
   Rochester, N.Y. 14604

2. High Vacuum Grease
   Dow Corning Corporation
   Midland, Michigan 48640

3. 200 Fluid
   Dow Corning Corporation
   Midland, Michigan 48640

4. Apeizon Grease T
   James G. Biddle Company
   Plymouth Meeting, Pennsylvania 19462

5. Industrial Spray Silicone
   Hercules Packing Corporation
   Alden, N.Y. 14004

6. Gelman Type A
   Gelman Instrument Company
   Ann Arbor, Michigan 48106

should have primarily penetrated to the final filter suggest that the observed difference be attributed at least in part to an increased collection efficiency for submicron particles by the upper stages when the glass fiber surfaces are used. It is believed that this increase in collection efficiency can be attributed to a filtering effect produced by the penetration of the boundary layer into the fibrous mat (9,10).

Several investigators have previously cited such differences when sampling monodisperse aerosols and thus reported the use of a different set of $Dp_{50}$ cut-points when interpreting particle sizing data. From the data obtained in this study, it appears that the differences between the distributions obtained with spray silicone and glass fiber collection surfaces could not be accounted for through the use of such experimentally derived monodisperse calibrations. It was neither the purpose of this study nor did time allow for such calibrations to be conducted for the impactors tested. A set of $Dp_{50}$ cut-points experimentally derived for the Brink impactor with both "grease" and glass fiber collection surfaces has been reported by SRI (3), and thus allowed for the plotting of the sizing data with these $Dp_{50}$ cut-points. Although the impactor used in this study was not the one calibrated at SRI, all modifications were the same, and testing was carried out under similar conditions (flow rate, temperature, pressure). Figure 1 shows the distributions obtained when plotting the sizing data using the SRI cut-points calibrated for both glass fiber and "grease" coated collection surfaces. The figure suggests that such a monodisperse calibration does not account for the difference noted for size distributions obtained with glass fiber collection surfaces.

It is recommended that further investigation of this effect be conducted in an attempt to quantitatively account for the observed differences in distributions for various mmd's and $\delta_g$. If an initial calibration is to be used to account for the shift in the measured distribution, it is suggested that a polydisperse calibration technique be developed. At present, investigators should be aware that distributions obtained using glass fiber collection surfaces may have mmd's 30% greater than those obtained using grease coated collection surfaces.

## C. FLOW RATE

Theoretically, the size distribution obtained from a given impactor should not be affected by operation at various flow rates. There are, however, practical limits within which an impactor will operate most effectively. The lower limit is established at the flow rate for which useful sizing data can no longer be obtained. For example, when operated at 0.125 cfm the Sierra has a stage 6 cut-point of approximately 1.5 µm. Operation at this low flow rate provides minimal information for an aerosol of mmd = 0.5 µm. Thus, an increased flow rate would be desired in order to allow for collection of particles in this size range. The upper limit is set at the flow rate for which particle bound and reentrainment becomes significant, since at this point the size distribution will become skewed. Within this range, experimental results showed little effect of the flow rate on the measured distribution when a uranine aerosol was sampled. There was, however, an apparent effect when an oil aerosol was sampled. A suitable

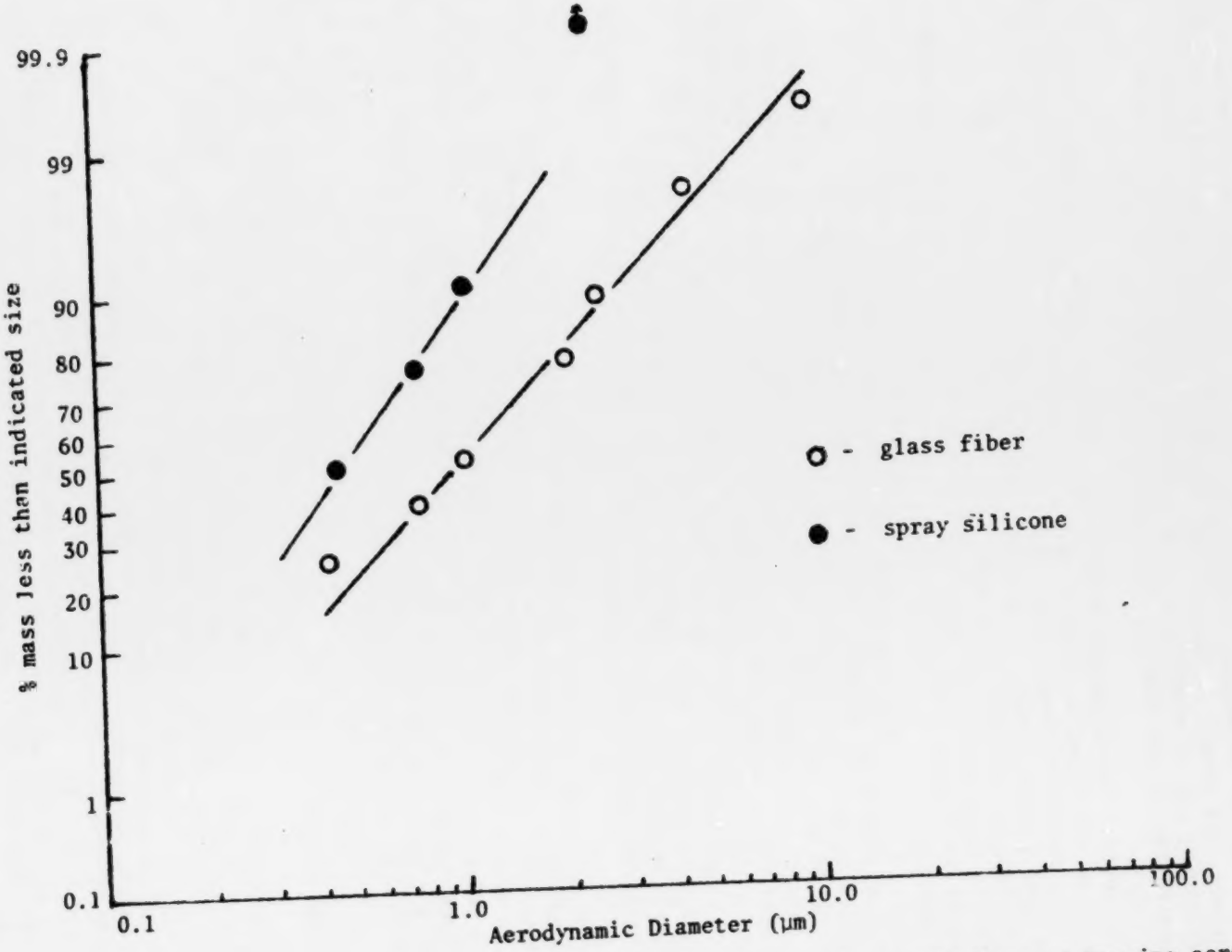


Figure 1. Effect of collection surface on measured size distribution for a polydisperse uranine aerosol with SRI $DP_{50}$ cut-points calibrated for spray and glass fiber collection surfaces (3). (Modified Brink Model B cascade impactor, 0.03 cfm, 70°F, 30.06 "Hg, 15.0 mg total loading, gravimetric analysis).

explanation for the observed shift in $\delta_g$ is not available at this time. The effect cannot be described as a result of particle reentrainment.

Experimental results show that particle reentrainment is influenced by not only jet velocity, but also the type of particle and collection surface. Examination of the data reveals that for hygroscopic solids (uranine) and liquids, particle bounce begins at jet velocities between 75-100 m/sec for submicron particles collected onto spray coated or glass fiber collection surfaces. This supports the findings of previous investigators (4,7). The specification of submicron particles is made, since larger particles may show a pronounced tendency to be reentrained at these high jet velocities, resulting in lowered collection efficiency. If the cascade impactor is operating in its normal configuration these larger particles will be removed from the stream onto the stage with the appropriate jet velocity and not be subjected to reentrainment.

Solid particles such as PSL spheres show a much more pronounced tendency to reentrainment at lower velocities. This was observed at velocities as low as 10 m/sec with uncoated aluminum surfaces. Spray silicone and glass fiber surfaces both showed the same effect between 40-50 m/sec for the PSL spheres.

The relative humidity of the test aerosol streams was approximately 45%. Previous studies have shown that at relative humidities of 75% or greater, the available moisture may act as an adhesive, preventing reentrainment at higher velocities or from uncoated surfaces. At the current test conditions, results may be interpreted as the lower threshold for reentrainment related problems. Increased humidity of the airstream may allow for increased collection efficiency at higher velocities or upon uncoated surfaces.

## D. STAGE LOADINGS

Experimental results have shown that increased collection efficiency (decreased reentrainment) may be expected after initial loading of particles on smooth collection surfaces; i.e., uncoated aluminum and spray silicone. Similar results were reported by Rao (9). It is assumed that the initial loading results in a roughened surface providing increased probability of interception and thus an overall increased collection efficiency.

The opposite may be assumed for the glass fiber surface, which is initially rough, and does in fact provide increased collection efficiency as both these and previous results have shown (9,10). Increased loading may tend to smooth over the surface, limiting the penetration of the impinging airstream into the fibrous mat and thus gradually decreasing the collection efficiency.

A practical upper limit for individual stage loadings appears to be 5-7 mg for hygroscopic solids. Uncoated aluminum, spray silicone and glass fiber surfaces seemed to provide stable collection characteristics up to this limit if other restrictions were met (i.e., velocity, etc.). Increased loading resulted in excessive losses onto the backside of the nozzle plate

and nonuniform deposition. The above limit on stage loading is slightly lower than the previously recommended value of 10 mg (4). When sampling a liquid oil aerosol, the uncoated aluminum surface is considered to be unacceptable due to highly variable collection characteristics. At stage loadings greater than 15-20 mg, the liquid deposits were observed to soak through the glass fiber surface. This suggests that loading be maintained below this amount. The spray silicone coating provides a stable collection surface for liquid aerosols when loadings were kept below 10-15 mg.

## E. INTERSTAGE LOSSES

Results of measuring the effect of particle diameter upon interstage loss agree closely with those obtained by SRI (3) (Figure 2). Interpretation of these results in predicting the interstage losses for a polydisperse aerosol having a mmd of 0.5 μm suggest approximately 2% of the total collected mass. The measured interstage losses for such an aerosol were found to be approximately that, when the total mass loading was 0.3 mg. However, upon increasing the total mass loading to 10.0 mg, a loading likely to be obtained during field testing, the interstage losses were found to increase to 10% of the total collected mass. It appears that a simple correlation cannot be assumed between the measured losses for a given sized particle, and those measured for a distribution having a similar mmd.

Of primary importance was the observation that exclusion of these losses from the particle size distribution did not appear to significantly alter the distribution. It was observed that losses occur primarily on the stages collecting the greatest mass. It is therefore not known if distributions of increased mmd will be affected in the same manner when excluding interstage losses from the calculations. Past operations of the impactors in the field have included painstaking efforts to recover all interstage losses. The present results indicate that such procedures may not be necessary to obtain a valid size distribution measurement. Because of the problems and errors in recovering losses in a field test, it may be more accurate to neglect the losses. It should be noted that if, however, the testing is to supply information as to the total mass output of the source, it does become necessary to recover these losses and include them as collected mass.

Present testing for interstage losses was only conducted at design flow rates. However, there was an indication that these losses tended to increase with increasing flow rates. It is not known if the high interstage losses recorded for the Brink are characteristic of single jet impactors in general, or due to its specific design. Similar consideration is true for the rectangular jet Sierra impactor, which exhibited very low losses at the flow rate tested. Interstage losses shown in Table 3 compare favorably to the results obtained by SRI (3), with the Brink showing the greatest losses.

## F. SUMMARY AND RECOMMENDATIONS

A guide to the use of current commercially available in-stack impactors is found in Appendix A. Recommendations are based upon the results presented

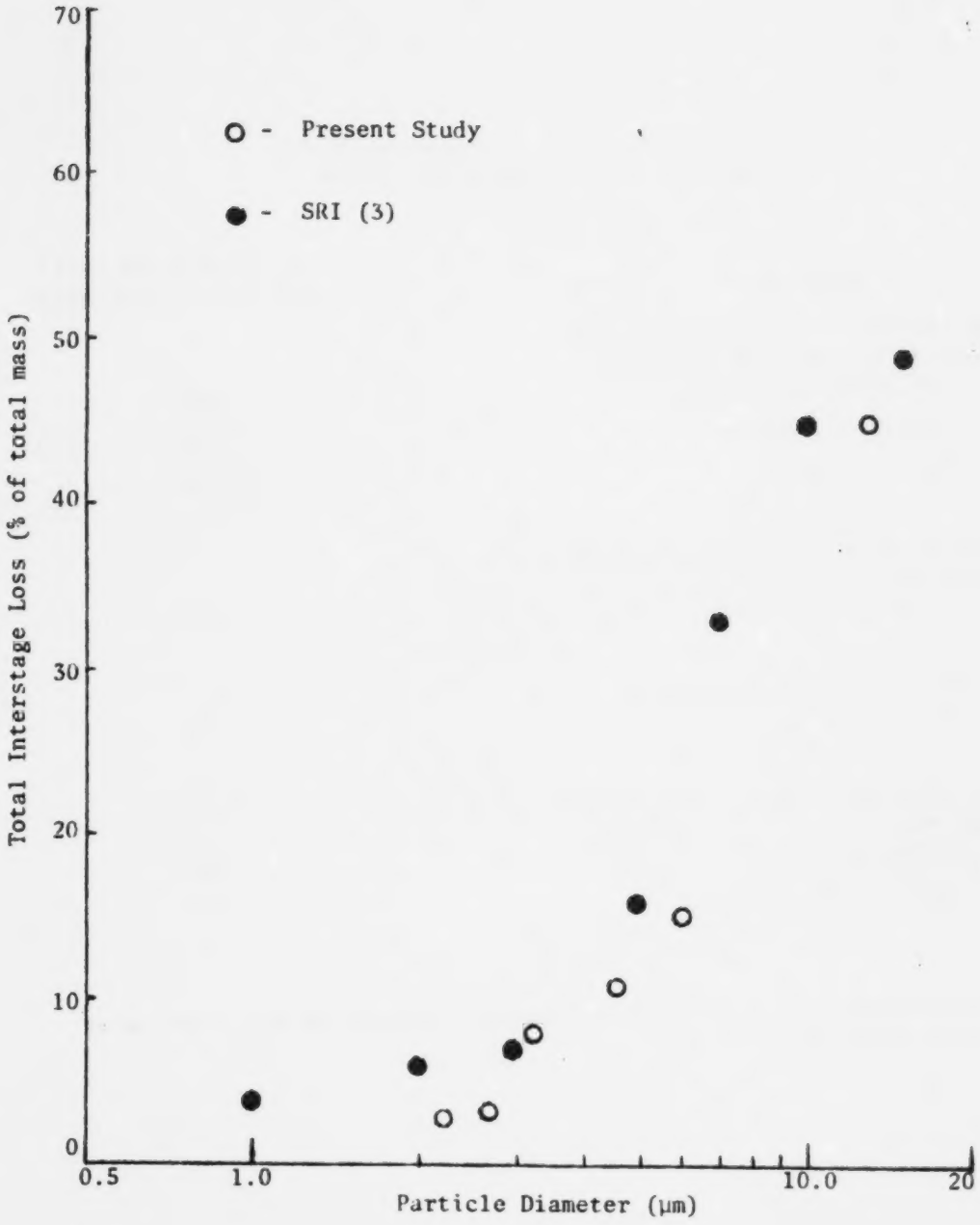


Figure 2. Total interstage loss versus particle diameter for the University of Washington MK III source test cascade impactor.

TABLE 3. COMPARISON OF MEASURED TOTAL INTERSTAGE LOSS FOR IMPACTORS TESTED

| Impactor | Total Interstage Loss* (% total collected mass) |
|---|---|
| MK III University of Washington Source Test Cascade Impactor | |
| (uncoated aluminum) | 20% |
| (spray silicone) | 13% |
| (glass fiber) | 12% |
| Sierra Model 226 Source Cascade Impactor | |
| (glass fiber) | 4% |
| Andersen MK III Stack Sampler | |
| (glass fiber) | 9% |
| Modified Brink Model B Cascade Impactor | |
| (glass fiber) | 36% |
| (spray silicone) | 31% |

*Measurements for a polydisperse uranine aerosol of mmd ≈ 0.56 μm at total loadings of 15 mg.

in this study and include information pertaining to: 1) the selection of a suitable collection surface coating, 2) operational flow rate, 3) limits on stage loadings, and 4) interstage losses. Investigators should be aware of the discrepancy in the particle size distribution obtained when using glass fiber collection surfaces. Further research is needed in order to correct accurately for this observed difference. Visual examination of individual collection surfaces can supply information to the operator of an impactor as to problems of particle bounce (flow rate) and/or overloading of the stage. Data obtained in this study indicate that interstage losses can be excluded from particle sizing data without significantly affecting the measured size distribution. It is recommended that testing be extended to include distributions of larger mmd in an attempt to further justify exclusion of interstage losses from sizing calculations. Recovered losses must, however, be included if information concerning the mass output of the source is desired. It is hoped that these findings will serve to allow for the more effective operation of in-stack impactors and thus provide a more valid instrument for assessing the particle size distributions of process gas streams.

## SECTION 3

## THEORETICAL BACKGROUND AND LITERATURE REVIEW

### A. INTRODUCTION

The cascade impactor as originated by May (11) classifies particles according to their aerodynamic diameter. This distinction is made since particles having the same physical size may behave differently in an airstream due to differences in shape and density. An irregular particle can be represented by an equivalent unit density sphere which, when moving through still air at low Reynolds numbers, will attain the same terminal settling velocity as the irregular particle. The diameter of this spherical particle is said to be the aerodynamic diameter of the actual particle under consideration.

The basic design of a cascade impactor consists of a series of alternating nozzles and impaction plates (Figure 3). In addition, an in-stack impactor is equipped with an array of entrance nozzles to allow for isokinetic sampling of the moving airstream, in order to minimize particulate sampling bias.

If one considers the movement of a particle-laden airstream through a typical impactor stage (Figure 4), it is seen that particles which have gained the required inertia will cross air streamlines and impact onto the collection plates. Particles with less inertia will not be impacted and will be carried by the airstream to the following stage. By increasing the velocity of the airstream in the succeeding stages, progressively smaller aerodynamic diameter particles are impacted and an inertial classification results. Ideally, for each stage all particles with an aerodynamic diameter greater than a critical diameter would be collected, while those smaller would not be collected.

Impaction efficiency as used in this report is defined as that fraction of incident particles of a given aerodynamic size which strike an impaction surface. This parameter can be calculated from theoretical considerations, or measured under ideal experimental conditions (12). The term collection efficiency is used to mean that fraction of the total aerosol mass actually collected (retained) by the impactor collection surface. The difference between the theoretical impaction efficiency and the experimental collection efficiency is often quite large and can be attributed to nonideal flow fields within the impactor and/or failure of the particles to adhere to the impaction surface.

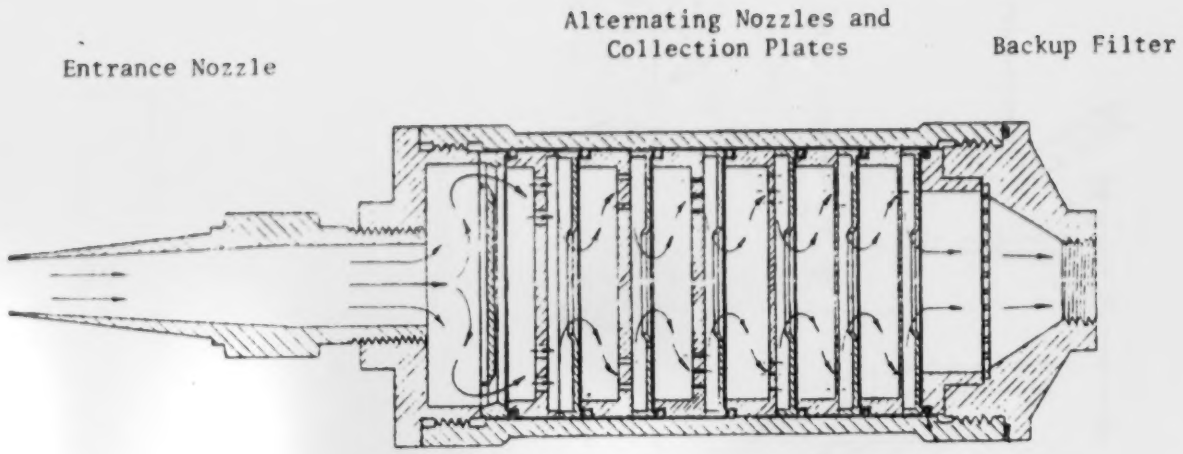


Figure 3. Basic design of an in-stack cascade impactor (MK III University of Washington source test cascade impactor).

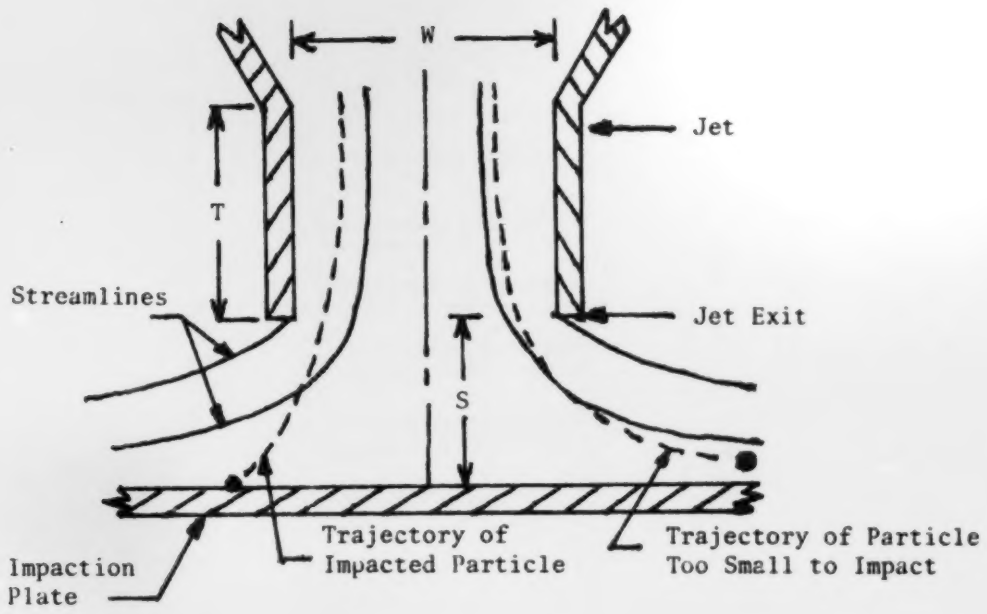


Figure 4. Principle of operation of an impactor, showing commonly referred to dimensions.

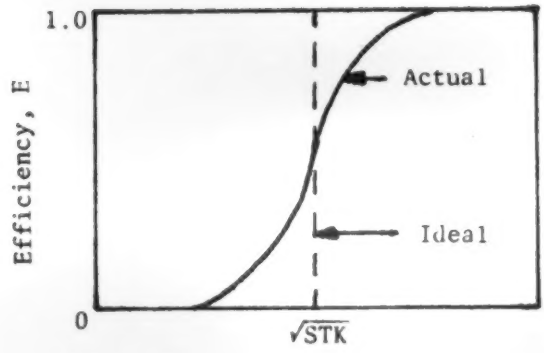


Figure 5. Typical impactor efficiency curve.

## B. IMPACTOR THEORY

In the theoretical analysis of inertial impaction, it is necessary to describe the flow field and then calculate the trajectories of particles within the flow field. Most earlier investigators assumed a simplified flow field when calculating impactor efficiency (13-17). By solving the Navier Stokes equations for the impactor flow field and then calculating particle motion within it, Marple (12) was able to obtain more exact solutions which he compared to experimental results. This method of analysis enabled him to account for the effects of several variables upon the overall performance of an impactor including: 1) the ratio of the jet-to-plate distance to the throat width (S/W); 2) the throat length to throat width ratio (T/W); 3) the jet Reynolds number (Re); and 4) the shape of the nozzle (see Figure 4). The corresponding effects of each of these parameters on both the flow field, and subsequently the impaction efficiency is discussed later in this section.

A particle trajectory in a flow field is calculated by equating Newton's second law with the fluid media resistance acting on the particle. While following a fluid streamline, a particle can be displaced by a distance equal to its stopping distance ($\ell_i$), defined by Fuchs (18) as the distance a particle with initial velocity, $V_o$, will travel in still air while that component of velocity ($V_o$) is lost due to the resistance of the media. When the fluid resistance force can be described by Stokes law, the stopping distance can be defined as:

$$\ell_i = \frac{\rho_p V_o C D_p^2}{18\mu} \qquad (1)$$

where:

$\ell_i$ = stopping distance (cm)

C = Cunningham slip correction factor (dimensionless)

$\rho_p$ = particle density ($gm/cm^3$)

$V_o$ = particle velocity (cm/sec)

$D_p$ = particle diameter (cm)

$\mu$ = viscosity of the media (poise)

If one assumes a uniform particle concentration across the jet plane, a given impactor geometry, and a constant flow rate, the impaction efficiency becomes a function of the ratio of a particle's stopping distance to the radius or half width of the nozzle; this is an inertial impaction parameter commonly referred to as the Stokes number (STK).

The Stokes number is then described as:

$$STK = \frac{\rho_p V_o C D_p^2}{18\mu\ W/2} \qquad (2)$$

where:

W = width for rectangular nozzle

= diameter for circular nozzle

The square root of the Stokes number ($\sqrt{STK}$) is a dimensionless particle size. The impactor stage can then be characterized by a plot of impaction efficiency versus the square root of the Stokes number ($\sqrt{STK}$) (Figure 5).

As mentioned earlier, deviation from ideal impactor behavior results when there is a nonideal flow field. Marple (12) stated that when the velocity profile is uniform across the jet exit, ideal impactor behavior can be obtained. However, the presence of a boundary layer at the walls of a nozzle prevents this criteria from being perfectly met and results in an actual impaction efficiency curve similar to the one shown in Figure 5.

Marple (8) investigated the effects of impactor geometry upon impaction efficiency curves for both round and rectangular nozzles by varying the three dimensionless parameters: S/W, T/W and Re, (Figure 6a,b,c) and has characterized these effects as stated below. Inspection of Figure 6b shows that except for low Reynolds numbers (Re < 500) and very high Reynolds numbers (Re > 25000), the shapes of the impactor efficiency curves are very similar. In the case of the low Reynolds numbers, the increased viscous boundary layer at the nozzle walls results in the poorer cut-offs. For Re = 25000 the knee in the curve appears to be due to the presence of a thin boundary layer in the area of the stagnation point at the impaction surface. The effect is to allow smaller particles to come in contact with the surface relative to areas where the boundary layer is thicker.

The effect of varying the S/W ratio is to alter the velocity profile at the jet exit. This is minimal for round nozzles with S/W ratio values greater than one-half and rectangular nozzles at values greater than one. For values of S/W smaller than those mentioned above it is seen that the position of the efficiency curve shifts towards smaller values of $\sqrt{STK}$, while the general shape of the curve remains the same (Figure 6a).

Variations in T/W over a range of values from 1 to 10 are seen to have little effect on either the shape of the efficiency curve or the position along the $\sqrt{STK}$ axis (Figure 6c).

The above considerations have been applied to a variety of impactor designs. Because of the inherent design of a rectangular nozzle, there are definite end effects. Ends of the rectangular nozzles act (more or less) as individual round nozzles, giving rise to variations in collection efficiency along the length of the nozzle. This effect can be minimized by limiting radial flow at the ends of the nozzle and by having a large aspect ratio (length-to-width ratio). Whether an impactor utilizes rectangular or round nozzles, if it has multiple nozzles it must be assumed that the velocity profile through each nozzle is identical.

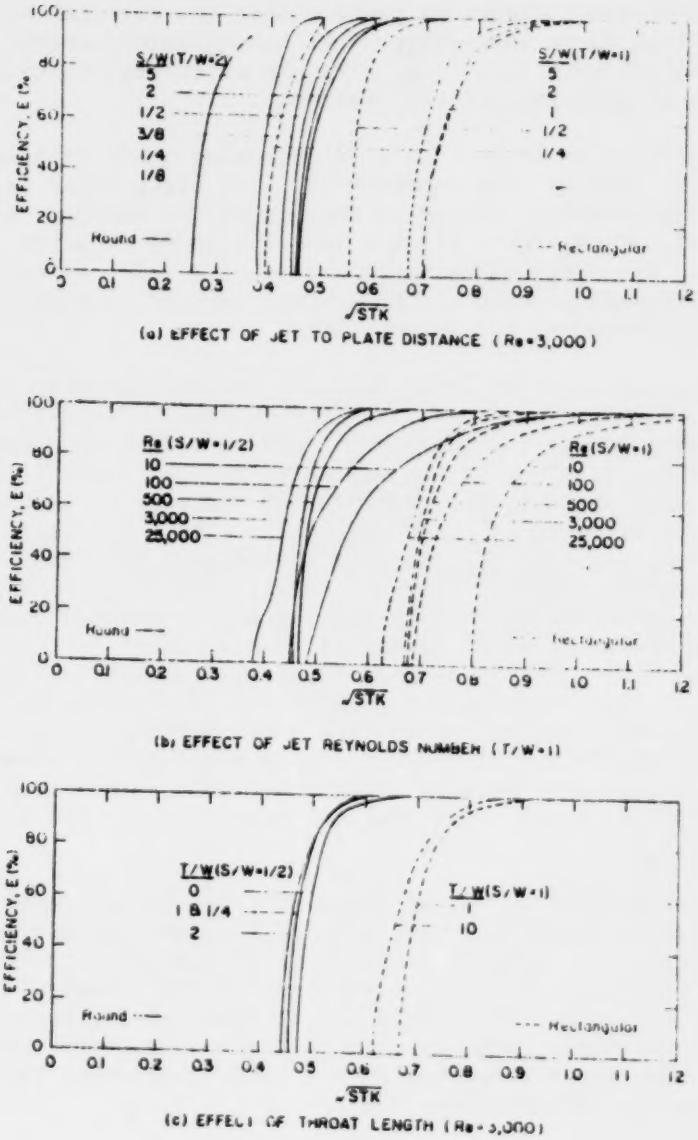


Figure 6. Impactor efficiency curves for the rectangular (broken line) and the round (solid line) impactors showing the effect of jet-to-plate distance, Reynolds number and throat length. (8)

Size distributions as measured by an impactor are, for the most part, based upon the $Dp_{50}$ method of data reduction. This method assumes an ideal, sharp cut point about the 50% efficiency, with all significant quantities of particles having aerodynamic diameters greater than the critical aerodynamic diameter assumed collected on that stage. The aerodynamic diameter corresponding to the 50% efficiency ($Dp_{50}$) may be calculated based upon theory, or obtained through an experimental calibration.

Theoretical calibration of $Dp_{50}$ involves assuming a 50% efficiency value for the Stokes number ($STK_{50}$) (see Equation 2). The $STK_{50}$ value is based upon considerations of the geometric design parameters of the impactor stage, as previously discussed. Thus, for a cascade impactor whose geometry differs from stage to stage, the $STK_{50}$ value would also vary (2,6). Agreement between theoretical and experimental values of $Dp_{50}$ would only be expected when the impactor flow field approaches ideal conditions.

Graphical presentation of impactor data may be based on either a differential or a cumulative particle size distribution. The differential particle size distribution is customarily plotted on either log-log or semi-log paper with $\Delta M/\Delta(\log Dp)$ as the ordinate and log Dp as the abscissa. The mass collected on stage n is designated by $\Delta M$ and represents the aerosol mass with diameters between $(Dp_{50})_n$ and $(Dp_{50})_{n-1}$. The term $\Delta(\log Dp)$ is then defined as $\log (Dp_{50})_{n-1} - \log (Dp_{50})_n$. The result is a histogram which is frequently represented by a best fit smooth curve. The cumulative particle size distribution is obtained by summing the stage mass catches plus the final filter and plotting the fraction of mass less than a given size versus particle size ($Dp_{50}$). The plot is made on log-normal probability paper and results in a straight line when the distribution is of a single mode and log-normally distributed. Figure 7 shows the same particle sizing data presented on both the differential and cumulative basis described above. In both cases the resulting distributions (since they are approximately log normal) may be characterized by a mass median diameter (mmd) and a geometric standard deviation ($\delta_g$).

The nonideal characteristics of an impactor necessarily result in a cross-sensitivity, which means that particles of a given size may be collected on more than one stage. Attempts have been made to characterize this cross-sensitivity based upon mathematical models (19-21). Natusch and Wallace, however, concluded that only when a large weight fraction of the collected mass is not made of particles close in size to the mmd do there occur any significant errors and that the mmd and $\delta_g$ are valid parameters for describing particle size distributions (21).

## C. PARTICLE ADHESION

The previous assessment of impaction theory has assumed that once a particle comes in contact with the impaction surface, it adheres to it. However, the greater the velocity of the incident particle, the greater the probability that the particle will not adhere. Theoretical estimates of the critical velocity at which a given size particle will reentrain rather than adhere have been made by Jordan (22) and Dahneke (23). The important forces

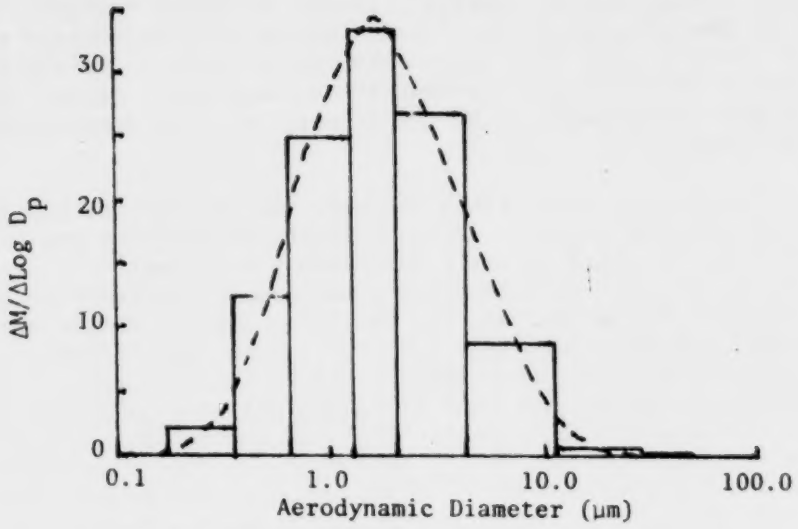


a. Differential particle size distribution plot.

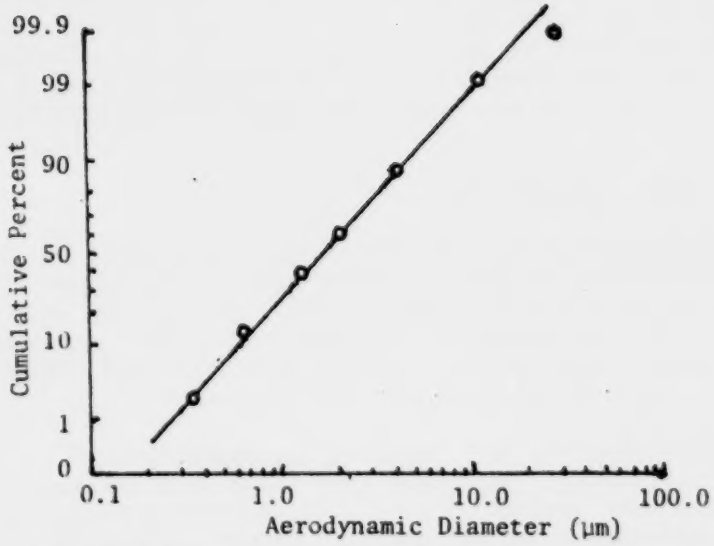


b. Cumulative particle size distribution plot.

Figure 7. Particle sizing data presented as differential and cumulative plots.

in the adhesion of the particle to the collection surface include: 1) intermolecular forces between the particle and surface (Van der Waal forces 2) electrostatic forces; and 3) capillary forces in liquid bridges. In an investigation of the adhesion of particles, Loffler (24) calculated that a 10 μm diameter particle with 1000 elementary charge units would still have a Van der Waal force 100 times greater than the electrostatic force. Thus, Van der Waal forces are assumed to be the primary adhering force between particle and surface.

To prevent bounce one must either decrease the velocity of the incident particles or increase the adhesive forces between the particle and collection surface. A decrease in stage velocity decreases the collection characteristics of the impactor; therefore, the desired alternative is to increase the adhesive forces between the particles and collection surface. In most cases this can be effectively accomplished by coating the collection surface with a grease or some other nonvolatile viscous substrate. While the coating may serve as nothing more than a cushion (24) for absorbing the kinetic energy of the particle, Buchhloz (25) and Berner (26) feel that the increased area of contact caused by the deformation of the coating does, in fact, increase the adhesion force. As a monolayer of particles accumulate upon the coating, the initial collection characteristics of the coating may be lost unless the coating substrate sufficiently wets the particles to achieve a coating of the newly formed surface (25). Excessive loading of the collection surface can lead to drastic losses in collection efficiency (27). Past studies indicate that when loadings exceed that of a monolayer deposit, reentrainment of the particles may result due to fluid drag forces (23,28). In a study of atmospheric aerosols, Winkler (29) determined that for relative humidities greater than 75%, high collection efficiencies were maintained without the use of an adhesive coating. The collection efficiency of uncoated surfaces was found to decrease rapidly as the relative humidity fell below 75%. For a more complete review of adhesive coatings and nonideal collection characteristics of impactors, the reader is referred to Rao (9).

## D. PREVIOUS IN-STACK IMPACTOR STUDIES

There are a large number of published papers concerning the use of impactors, and for a survey of basic impactor studies the reader is referred to the earlier works of Marple (12) and Rao (9). This review will consider studies of in-stack cascade impactors, a summary of which is presented in Table 4. This listing indicates the impactor model, the specific studies undertaken, and the type of test aerosols, if any, used.

As noted, several studies have compared the theoretical stage cut points of various commercial in-stack impactors with those obtained experimentally using a monodisperse test aerosol (2,3,6). Air Pollution Technology (A.P.T.), Incorporated has published a set of cascade impactor calibration guidelines which describes a calibration method involving atomization of polystyrene latex (PSL) spheres and particle detection utilizing an optical particle counter (2). Other methods of calibration include gravimetric or fluorometric analysis of stage catches after sampling of a monodisperse test aerosol (3,6). One important consideration pointed out by Willeke and

TABLE 4. EXPERIMENTAL STUDIES OF IN-STACK IMPACTORS

| Reference | Studies Conducted | Impactor Model | Aerosol Used |
|---|---|---|---|
| SRI (5) | 5,6,7 | a,b,d,e | Flyash |
| SRI (8) | 4 | --- | --- |
| SRI (7) | 4,7,3 | a,b,d | Ammonium Fluorescein, DOP |
| A.P.T., Inc (2) | 1,5 | a,f | PSL Spheres |
| SRI (3) | 1,2,3,4 | a,b,c,d,g | Ammonium Fluorescein, DOP |
| SRI (31) | 4 | --- | --- |

Impactor Models:

a) University of Washington
b) Andersen Stack Sampler
c) Sierra Model 226 Cascade Impactor
d) Brink Model B Cascade Impactor
e) TAG sampler
f) A.P.T. M-1 Cascade Impactor
g) MRI Model 1502 Cascade Impactor

Studies Conducted:

1) calibration against test aerosol
2) interstage losses
3) range of flow rates
4) collection surface coatings
5) data reduction
6) stage loadings
7) field tests

McFeters is that, in general, a single stage calibration will not give the stage characteristics of the completely assembled impactor due to the corresponding variations in the internal flow field (30). Thus, it is suggested that a calibration be conducted with the impactor assembled as it will be used in the field.

D. B. Harris has presented a set of nomographs which allows for the selection of isokinetic sampling conditions and sampling time based on the process stream mass loading (4). Included on the nomograph are the maximum recommended flow rates for several commercially available impactors ranging from 0.03 scfm for the Brink to 0.8 scfm for the University of Washington MK III. The upper limit for flow rate was based upon the maximum jet velocity at which deposition may be obtained without bounce or reentrainment. Studies at Southern Research Institute (SRI) suggest that jet velocities should be maintained below 65 m/sec for greased collection plates and below 35 m/sec for ungreased plates. Optimum results are reported at jet velocities of less than 10 m/sec (4,10).

Minimum single stage loadings are limited by the weighing accuracy attainable. Increased weighing accuracy may be gained by the use of light-weight collection plate inserts which reduce tare weights. Mass measurements with an accuracy of 0.01 mg or less are possible with several currently available microbalances. Maximum single stage loadings of 10 mg are suggested to avoid excessive reentrainment or loss of collection efficiency (3,4). Pre-cutters (cyclones) are often used upstream of the first impactor stage to avoid overloading the upper stages, yet allow sufficient sampling volumes to collect enough mass on the lower stages to maintain the desired weighing accuracy.

Suitability of the impactor collection plate surface to the sampling conditions is extremely important. Table 5 lists various surface coatings which have been suggested for increasing the collection efficiency of in-stack impactors. Previous studies indicate that collection efficiency is dependent upon the type of surface coating used (30,31). Several methods of preconditioning these surfaces have been suggested to prevent weight loss due to exposure to the process gas stream (3,4,7).

SRI has reported that various makes of glass fiber filters may gain weight when sampling a process stream with high $SO_2$ concentrations due to sulfate formation on the filter (3,7,8). Minimization of this effect can be accomplished through proper conditioning or choice of filter. At present, glass fiber filters are the only substrates commonly used at temperatures greater than 400°F (3,4).

SRI has also assessed the interstage losses for five different in-stack impactors (3). Their results show that for 15 μm particles interstage losses can amount to as much as 70% of the total stage catch. These losses are due mainly to deposition in the stage nozzles, and decrease to a minimum for 2 μm diameter particles.

In field work it is common practice to include any recovered stage losses with the catch for that stage (3,4). Results are then normally

TABLE 5. COLLECTION SURFACE COATINGS USED WITH IN-STACK CASCADE IMPACTORS

| Reference | Collection Surface Coatings |
|---|---|
| 1. SRI (3) | Teflon, Whatman GF/A, Whatman GF/D, Reeve Angel 934 AH, Gelman Type A, Gelman Spectro Grade Type A, MSA 1106 BH, Reeve Angel 900 AF, Dow Molykote III Compound |
| 2. APT, Inc (2) | Dow Corning High Vacuum Silicone Grease |
| 3. SRI ( 7) | Dow Corning High Vacuum Silicone Grease, K-Y Jelly, Vaseline |
| 4. Harris (4) | Polyethylene Glycol 600, Apiezon L, Apiezon H |
| 5. SRI (31) | Vaseline, Molykote III Compound, Stopcock Grease, Dow Corning II Compound, Polyethylene Glycol 600, High Vacuum Grease, UCW:98, Apiezon L, Kiln Bearing Grease, 200 Fluid, Fluorolube GR-362, Fluorolube GR-544, Fluorolube GR-470, Fluorolube GR-290, Fluorolube GR-660, Carbowax 1000, Carbowax 4000, Carbowax 20M, STP Oil Treatment, Reeve Angel 934 AH, Gelman AE, Gelman Spectro Glass, Whatman GF/A |

reported with the $Dp_{50}$ method of data reduction previously described, preferably based upon calibrated cut-points. The resulting particle size distribution can then be defined by the mass median diameter and the geometrical standard deviation, assuming the distribution is log-normal.

A more involved method of data reduction has been proposed by Picknett (32). This method calculates the mass contributions of a set of particle size intervals which would result in the actual collection efficiencies measured and is based upon a previous knowledge of the stage collection efficiencies for the chosen size intervals. A comparison of the Picknett and $Dp_{50}$ methods for a test aerosol size distribution show that while the indicated mmd's are approximately the same, the Picknett method gives a better approximation of the true distribution (4).

SRI has also conducted a number of field tests with various models of in-stack impactors (5,7). Results show that the mass loadings obtained from cascade impactors commonly differ as much as three times that of EPA Method 5 loadings.

## SECTION 4

## EXPERIMENTAL APPARATUS, METHODS AND PROCEDURES

### A. INTRODUCTION

Initial information was gained concerning the effects of various operating parameters for in-stack cascade impactors based upon extensive use of the MK III University of Washington source test cascade impactor. After establishing a general test procedure with the MK III, other commercially available in-stack cascade impactor units were tested. They were: a Sierra Model 226 source cascade impactor; an Andersen Mark III stack sampler; and a modified Brink Model B cascade impactor. Basic differences between models are the impactor nozzle design and the unit's compatability with alternative collection surfaces. Each individual device is described in later sections.

### B. GENERAL EXPERIMENTAL SETUP

The basic experimental arrangement involved equipment for generating a reproducible (monodisperse or polydisperse) test aerosol of a variety of materials; means of determining collection efficiency and interstage losses; pumps, valves and metering devices for controlling and measuring flow; a variable temperature environment; and an air supply. The general arrangement of this test equipment is shown in Figure 8. The building compressed air system was filtered and used to operate the aerosol generator and as a source of dilution air. Monodisperse test aerosols were generated with a vibrating orifice type aerosol generator, similar to the one described by Berglund and Liu (33), while polydisperse test aerosols were generated with a three jet Collison atomizer (34). The conditioned, neutralized and diluted aerosol stream was then sampled using an in-stack impactor assembly operated at a predetermined set of conditions (flow rate, impactor collection surface coating and sampling time). Flow rate was monitored by rotameters and the sampled volume measured with dry gas meters. A parallel control filter was tun to determine the mass output of the aerosol generator and serve as a comparison for the total mass collected by the impactor. An oven was used to run impactor tests at elevated temperatures. Collection efficiencies were determined by gravimetric or fluorescent techniques. Major components are further discussed in the following section.

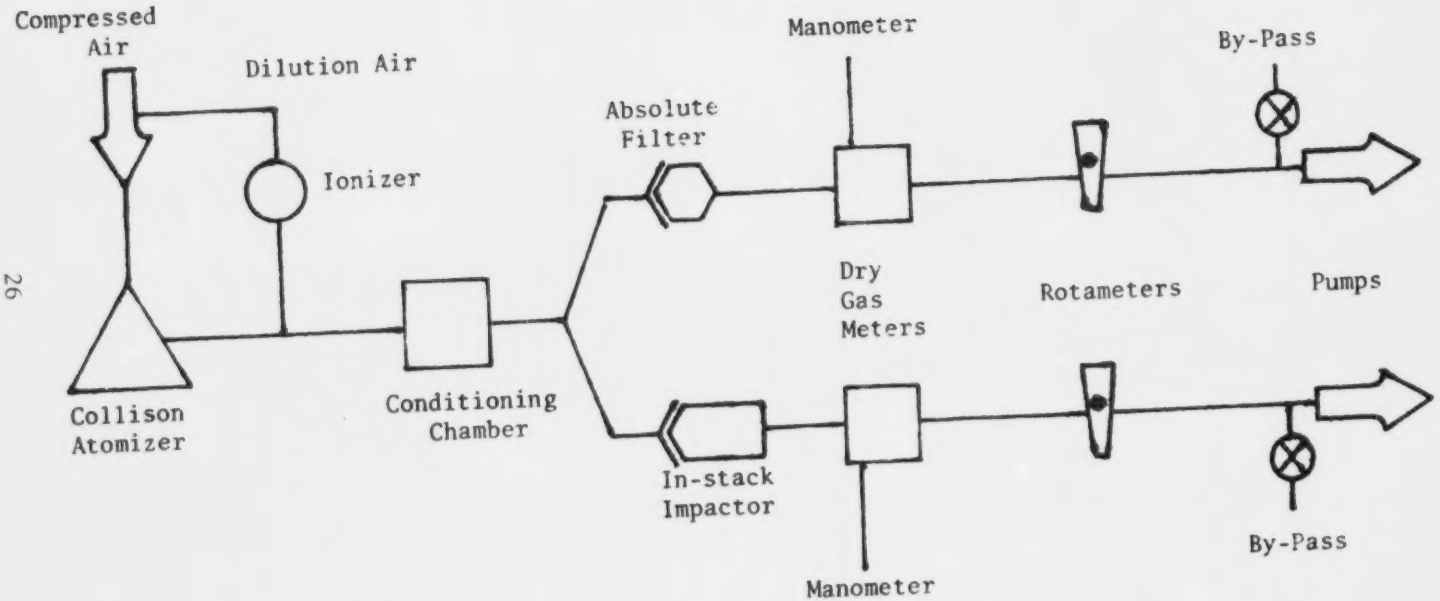


Figure 8. General arrangement of test equipment.

## C. DESCRIPTION OF THE IN-STACK IMPACTORS

### 1. MK III University of Washington Source Test Cascade Impactor (Model D)

The MK III University of Washington source test cascade impactor is a round jet impactor consisting of seven stages plus a final filter. It is designed to be inserted directly into the ducting or stack to obtain particle size distributions. Construction is of machined stainless steel throughout, with both the alternating nozzles and collection plates and the final filter assembly enclosed by a threaded cylindrical casing (Figure 9). A variety of isokinetic sampling nozzles are provided which thread into the inlet section. All of the isokinetic nozzles taper to form the first stage nozzles of approximately 1.865 cm (Table 6). Viton o-rings are fitted about each of the nozzle stages and the final filter collar, as well as onto the threaded outlet section to prevent leakage. These o-rings are recommended for use at temperatures up to 500°F. For operating temperatures in excess of 500°F the manufacturer suggests that the o-rings be removed and an extra collection plate be used as a spacer after stage seven.

The collection plates accommodate aluminum foil, stainless steel foil, polymer films and glass fiber collection surfaces which are easy to cut due to the simple design of the collection plates. The final filter assembly accepts a 47 mm glass fiber filter which is supported by a mesh screen and perforated plates, and held in place by a collar.

Table 6 compares the reported geometrical dimensions of each of the seven stages with the measured values of the impactor purchased for this study. The reported ratios of jet-to-plate/jet diameter (S/W) varies from 0.78 to 12.50, while the jet depth/jet diameter (T/W) varies from 0.55 to 4.03 for the seven stages of the impactor. The measured pressure drop through the complete impactor is presented for flow rates of 0.25, 0.5 and 1.0 scfm in Table 7.

The manufacturer supplies a nomograph which relates calculated $Dp_{50}$ cut-points for each impactor stage to volumetric flow rates over a range from 0.25 to 2.5 scfm for three given temperatures of the process gas stream. It is stated that the particle density for the calculated values is assumed to be 1.0 g/cm$^3$; however, further basis for the calculations are not presented (Figure 10). Table 8 lists other published $Dp_{50}$ values, both calibrated and calculated, for various flow rates. The basis for the calculated values is seldom given.

### 2. Sierra Model 226 Source Cascade Impactor

The Sierra Model 226 cascade impactor is an in-stack, multi-stage cascade impactor of radial slot design. It consists of six common nozzle-collection plates and a final filter assembly (Figure 11). A selection of isokinetic nozzles can be attached to a cylindrical inlet section with a 5/8 inch Swaglock fitting; this inlet section and the six nozzle-collection plates are held together by means of two studs and thumb nuts protruding from the final filter stage. The backside of the final filter stage has 1/2"NPT pipe threads which accommodate the sampling probe. All construction is of stainless steel

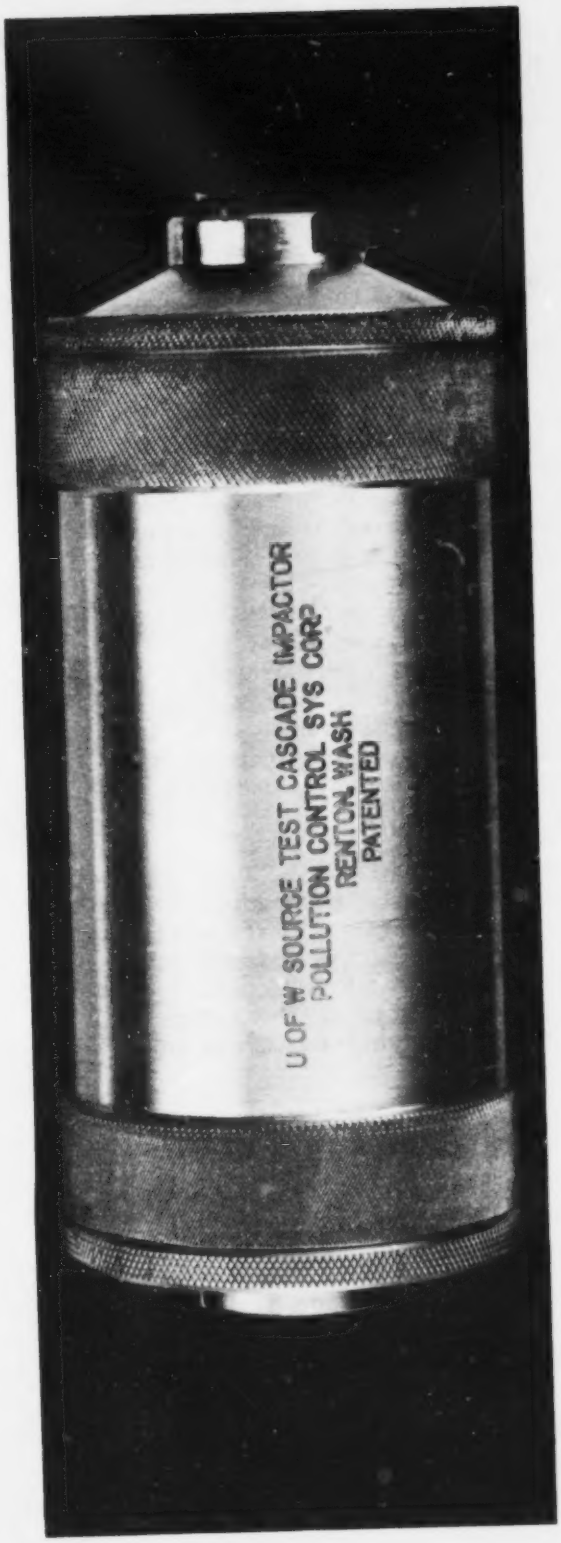


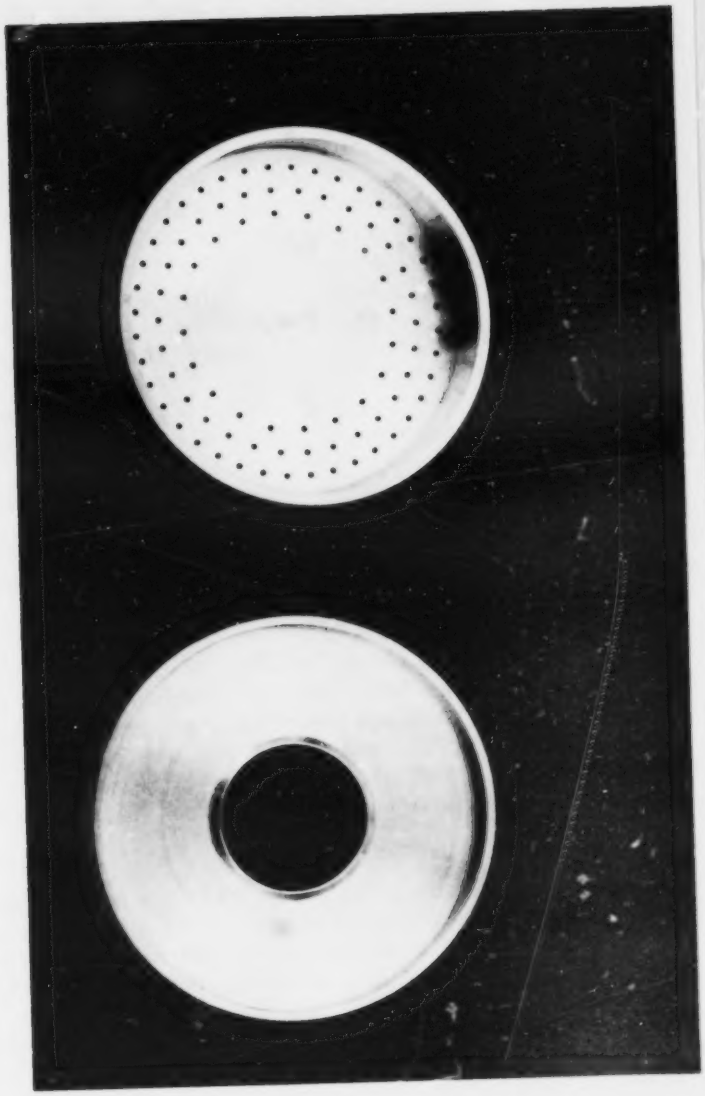

Figure 9. MK III University of Washington source test cascade impactor. Complete unit and individual nozzle and impaction plates.

TABLE 6. MK III UNIVERSITY OF WASHINGTON SOURCE TEST CASCADE IMPACTOR CRITICAL DIMENSIONS

| Stage No. | No. of Jets | Jet Width (in.) | Jet-to-Plate Distance (in.) | S/W | T/W | Reynolds Number @ 0.5 cfm |
|---|---|---|---|---|---|---|
| 1 | 1 | 0.7180<br>(0.7340) | 0.56<br>(0.568) | 0.78<br>(0.77) | 2.09<br>(1.70) | -----<br>(1070) |
| 2 | 6 | 0.2280<br>(0.2240) | 0.255<br>(0.226) | 1.80<br>(1.01) | 1.60<br>(0.58) | -----<br>(584) |
| 3 | 12 | 0.0960<br>(0.0910) | 0.125<br>(0.125) | 1.97<br>(1.37) | 1.97<br>(1.38) | ----<br>(719) |
| 4 | 90 | 0.0310<br>(0.0292) | 0.125<br>(0.127) | 4.03<br>(4.35) | 4.03<br>(4.32) | ----<br>(299) |
| 5 | 110 | 0.0200<br>(0.0200) | 0.125<br>(0.126) | 6.25<br>(6.30) | 3.15<br>(3.03) | ----<br>(357) |
| 6 | 110 | 0.0135<br>(0.0133) | 0.125<br>(0.123) | 9.26<br>(9.25) | 2.22<br>(1.92) | ----<br>(536) |
| 7 | 90 | 0.0100<br>(0.0099) | 0.125<br>(0.125) | 12.50<br>(12.63) | 3.00<br>(2.32) | ----<br>(883) |

Note: Manufacturer's reported values listed with measured values in parentheses.

TABLE 7. MK III UNIVERSITY OF WASHINGTON SOURCE TEST CASCADE IMPACTOR MEASURED PRESSURE DROP AT VARIOUS FLOW RATES

| Flow rate (acfm) | Pressure Drop ("Hg) |
|---|---|
| 1.0 | 5.6" |
| 0.5 | 1.6" |
| 0.25 | 0.45" |

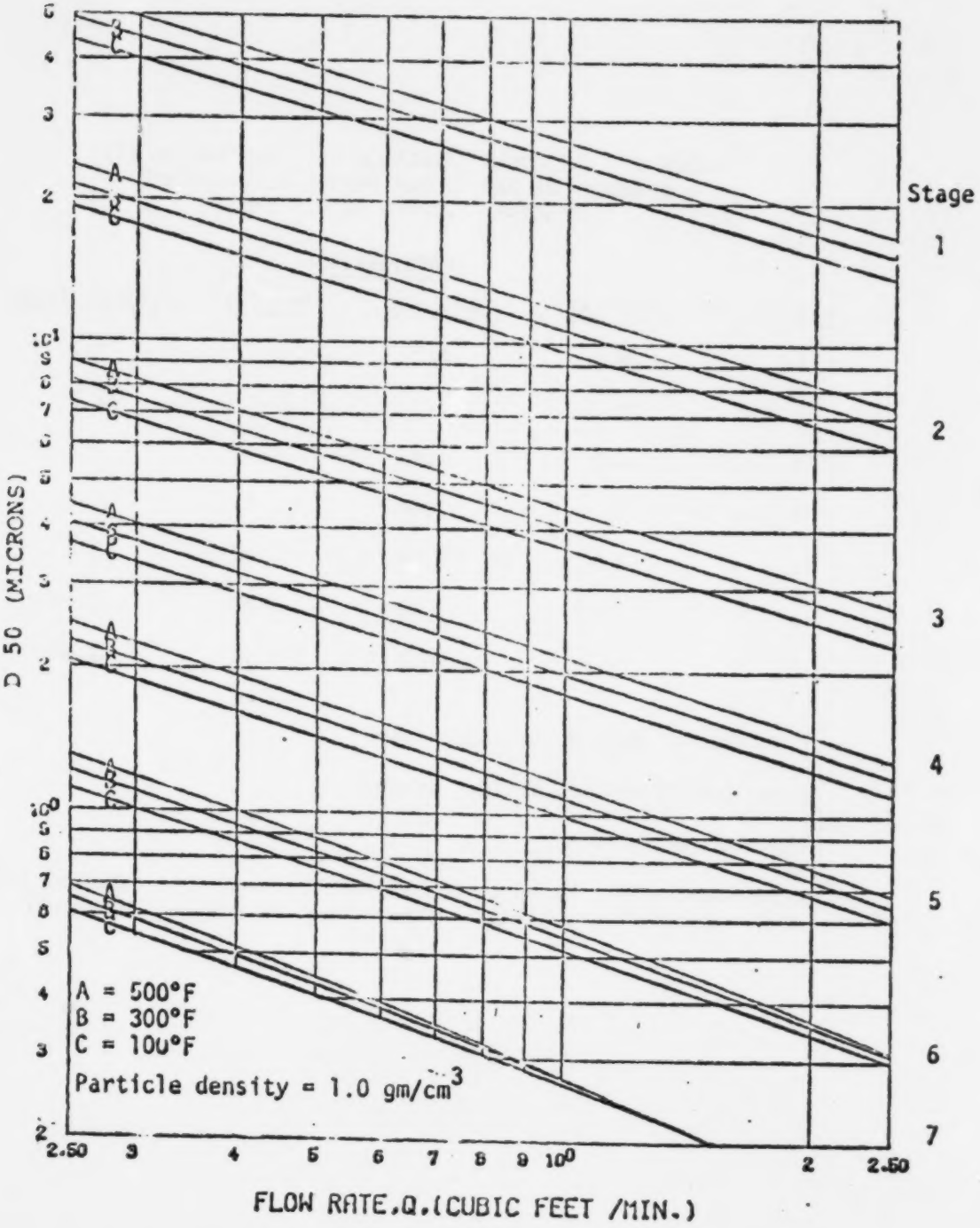


Figure 10. MK III University of Washington source test cascade impactor nomograph for determining $D_{P_{50}}$ cut-points (supplied by the manufacturer).

TABLE 8. REPORTED VALUES OF $D_{p_{50}}$ FOR THE MK III UNIVERSITY OF WASHINGTON SOURCE TEST CASCADE IMPACTOR OPERATED AT 0.5 CFM

| | References | | | |
|---|---|---|---|---|
| Stage # | SRI (3)* | SRI (3)+ | APT (2)** | Present Study++ |
| 1 | 14.0 | 10.5 | --- | 28.3 |
| 2 | 11.2 | 10.0 | --- | 11.5 |
| 3 | 4.1 | 4.4 | --- | 4.2 |
| 4 | 1.86 | 1.86 | 1.85 | 2.1 |
| 5 | 1.57 | 1.60 | 1.22 | 1.3 |
| 6 | 0.67 | 0.66 | 0.60 | 0.65 |
| 7 | --- | 0.30 | 0.35 | 0.35 |

* experimental values, exclude losses

\+ experimental values, include losses

** experimental values

++ calculated values based upon a $\sqrt{STK_{50}}$ value of 0.44 obtained based upon the impactor's critical dimensions and Marple's curves (12).

and the manufacturer claims the unit is capable of operation in corrosive environments at temperatures of up to 1500°F.

Slotted glass fiber collection surfaces are sandwiched between stages and double as pressure seals. For operation at temperatures in excess of 500°F, stainless steel collection plates are available or the impactor stage itself may be used. The final filter assembly accepts a 47 mm glass fiber filter supported by a screen and held in place by the collection plate for stage 6.

Table 9 compares the measured geometrical dimensions of the Sierra Model 226 obtained in this study with the values reported by the manufacturer. Pressure drop across the complete impactor is reported by the manufacturer as about 33 inches of water at 0.75 cfm, 25°C and 760 mm Hg, and measured values are listed in Table 10.

The reported $Dp_{50}$ for unit density spheres at 0.75 scfm are given in Table 11 along with other published cut-points. The impactor is designed to operate at flow rates below 0.5 scfm.

3. Andersen MK III Stack Sampler

The Andersen MK III stack sampler consists of eight stages plus a final filter. Each stage has a number of concentric round nozzles, offset on each succeeding stage such that the one plate serves both as nozzle and collection surface. The impactor stages accept precut glass fiber collection surface coatings which are held in place by cross bars. Stainless steel rings serve both as spacers between stages and as gaskets. The assembled stages and final filter are held in a plate holder which is enclosed in a stainless steel housing with a 1/2 inch female pipe fitting to allow attachment to the sampling probe (Figure 12). Both straight and "gooseneck" isokinetic sampling nozzles are available to allow for operation with a variety of stacks. With stainless steel plates the unit is reported to operate at temperatures up to 1500°F under corrosive conditions.

Table 12 lists the measured dimensions of the unit used in this study and compares it to manufacturer's values. The measured pressure drops across the unit at flow rates of 0.25 cfm, 0.5 cfm and 1.0 cfm are reported in Table 13. The manufacturer provides a nomograph and set of correction factor figures for obtaining the stage cut-points ($Dp_{50}$), reportedly based upon calibration with unit density spheres. These and other reported values of $Dp_{50}$ are listed in Table 14.

4. Modified Brink Model B Cascade Impactor

The Brink impactor is designed for operation at low flow rates (0.04 to 0.07 cfm) and is therefore well suited for sampling gas streams with high mass loadings. Each stage has a single round nozzle and separate collection surface. The impactor obtained for this study had been previously modified to include both a 0 and 6th stage and a final filter, providing a total of seven impactor stages. The unit is shown in Figure 13. The collection surfaces are suited for use with either foil or glass fiber inserts.

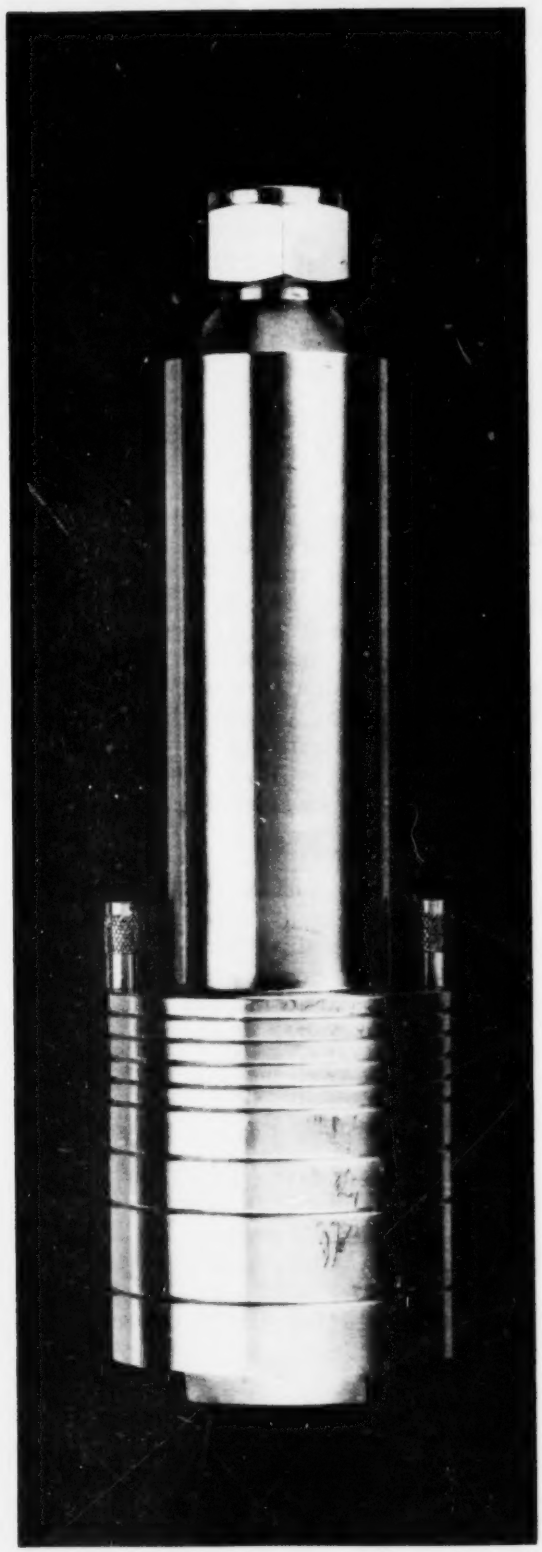

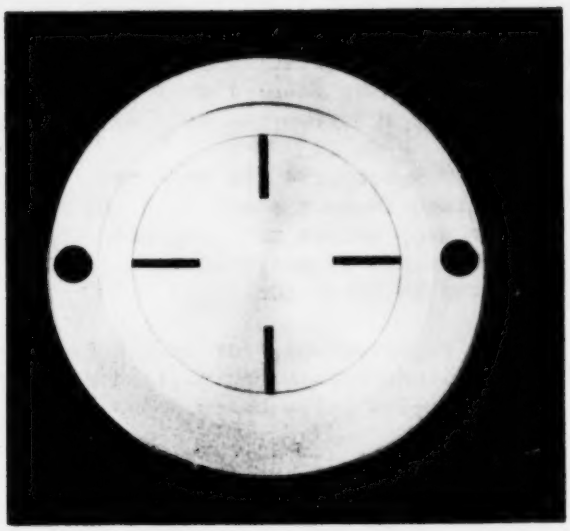

Figure 11. Sierra Model 226 source cascade impactor. Complete unit and combination nozzle impaction plate.

TABLE 9 . SIERRA MODEL 226 SOURCE CASCADE IMPACTOR CRITICAL DIMENSIONS

| Stage No. | No. of Jets | Jet Width (in.) | Jet-to-Plate Distance (in.) | S/W | T/W | Reynolds Number @ 0.25 cfm |
|---|---|---|---|---|---|---|
| 1 | 4 | 0.141<br>(0.137) | 0.250<br>(0.252) | 1.78<br>(1.8) | 2.59<br>(2.7) | ----<br>(308) |
| 2 | 4 | 0.0782<br>(0.074) | 0.125<br>(0.124) | 1.60<br>(1.7) | 3.04<br>(3.4) | ----<br>(308) |
| 3 | 4 | 0.045<br>(0.042) | 0.094<br>(0.103) | 2.08<br>(2.5) | 5.30<br>(5.7) | ----<br>(409) |
| 4 | 4 | 0.025<br>(0.024) | 0.094<br>(0.105) | 3.75<br>(4.4) | 2.04<br>(2.3) | ----<br>(412) |
| 5 | 4 | 0.014<br>(0.012) | 0.094<br>(0.104) | 6.67<br>(8.7) | 3.64<br>(4.25) | ----<br>(404) |
| 6 | 4 | 0.010<br>(0.011) | 0.094<br>(0.104) | 9.40<br>(9.5) | 5.10<br>(5.0) | ----<br>(685) |

Note: Manufacturer's reported values listed with measured values in parentheses.

TABLE 10. SIERRA MODEL 226 SOURCE CASCADE IMPACTOR MEASURED PRESSURE DROP AT VARIOUS FLOW RATES

| Flow Rate (scfm) | Pressure Drop ("Hg) |
|---|---|
| 1.0 | 5.3" |
| 0.5 | 2.25" |
| 0.25 | 0.95" |
| 0.125 | 0.3" |

TABLE 11. REPORTED VALUES OF $D_{p_{50}}$ FOR THE SIERRA MODEL 226 SOURCE CASCADE IMPACTOR

| | Reference | | | |
|---|---|---|---|---|
| Stage # | SRI (3)* | SRI (3)+ | Sierra Instruments** | Present Study++ |
| 1 | 18.0 | 14.5 | 16.0 | 20.3 |
| 2 | 11.0 | 12.0 | 8.6 | 11.0 |
| 3 | 4.4 | 4.2 | 3.9 | 5.25 |
| 4 | 2.65 | 2.55 | 2.4 | 3.0 |
| 5 | 1.70 | 1.65 | 1.2 | 1.5 |
| 6 | 0.95 | 0.95 | 0.61 | 1.0 |

* experimental values, exclude wall losses at 0.25 cfm

\+ experimental values, include wall losses at 0.25 cfm

** reported values at 0.75 scfm

\++ calculated values at 0.25 cfm based upon a $\sqrt{STK}_{50}$ value of 0.7 obtained based upon impactor's critical dimensions and Marple's curves (12).

Figure 12. Andersen MK III stack sampler. Complete unit and combination nozzle impaction plate.

TABLE 12 . ANDERSEN MK III STACK SAMPLER CRITICAL DIMENSIONS

| Stage No. | No. of Jets | Jet Width (in.) | Jet-to-Plate Distance (in.) | S/W | T/W | Reynolds Number @ 0.5 cfm |
|---|---|---|---|---|---|---|
| 1 | 264 | 0.065<br>(0.057) | 0.102<br>(0.101) | 1.57<br>(1.75) | ----<br>(1.09) | -----<br>(52) |
| 2 | 264 | 0.049<br>(0.044) | 0.102<br>(0.100) | 2.08<br>(2.27) | ----<br>(0.82) | -----<br>(68) |
| 3 | 264 | 0.037<br>(0.036) | 0.102<br>(0.101) | 2.76<br>(2.81) | ----<br>(0.97) | -----<br>(83) |
| 4 | 264 | 0.0295<br>(0.0292) | 0.102<br>(0.102) | 3.46<br>(3.49) | ----<br>(1.16) | -----<br>(102) |
| 5 | 264 | 0.021<br>(0.021) | 0.102<br>(0.101) | 4.86<br>(4.81) | ----<br>(1.71) | -----<br>(142) |
| 6 | 264 | 0.0146<br>(0.0135) | 0.102<br>(0.099) | 6.99<br>(7.3) | ----<br>(1.41) | -----<br>(221) |
| 7 | 264 | 0.0107<br>(0.0095) | 0.102<br>(0.100) | 9.53<br>(10.5) | ----<br>(1.89) | -----<br>(313) |
| 8 | 156 | 0.0096<br>(0.0095) | 0.102<br>(0.100) | 10.6<br>(10.5) | ----<br>(1.89) | -----<br>(530) |

Note: Manufacturer's reported values listed with measured values in parentheses.

TABLE 13. ANDERSEN MK III STACK SAMPLER MEASURED PRESSURE DROP AT VARIOUS FLOW RATES

| Flow Rate (scfm) | Pressure Drop ("Hg) |
|---|---|
| 1.0 | 3.55" |
| 0.5 | 1.15" |
| 0.25 | 0.4" |

TABLE 14. REPORTED VALUES OF $D_{p_{50}}$ FOR THE ANDERSEN MK III STACK SAMPLER

| | References | | | |
|---|---|---|---|---|
| Stage # | SRI (3)* | SRI (3)+ | Andersen 2000, Inc** | Present Study++ |
| 1 | 14.0 | 10.5 | 13.0 | 13.4 |
| 2 | 10.4 | 9.4 | 8.6 | 8.8 |
| 3 | 6.1 | 5.8 | 5.7 | 5.5 |
| 4 | 4.0 | 4.4 | 4.0 | 3.8 |
| 5 | 2.35 | 2.20 | 2.55 | 2.15 |
| 6 | 1.20 | 1.20 | 1.25 | 1.24 |
| 7 | 0.76 | 0.70 | 0.80 | 0.75 |
| 8 | 0.46 | 0.43 | 0.54 | 0.47 |

* experimental values, exclude losses at 0.5 cfm

+ experimental values, include losses at 0.5 cfm

** manufacturers reported values from nomograph at 0.5 cfm

++ calculated values at 0.5 cfm based upon a $\sqrt{STK}_{50}$ value of 0.52 obtained based upon the impactor's critical dimensions and Marple's curves (12).

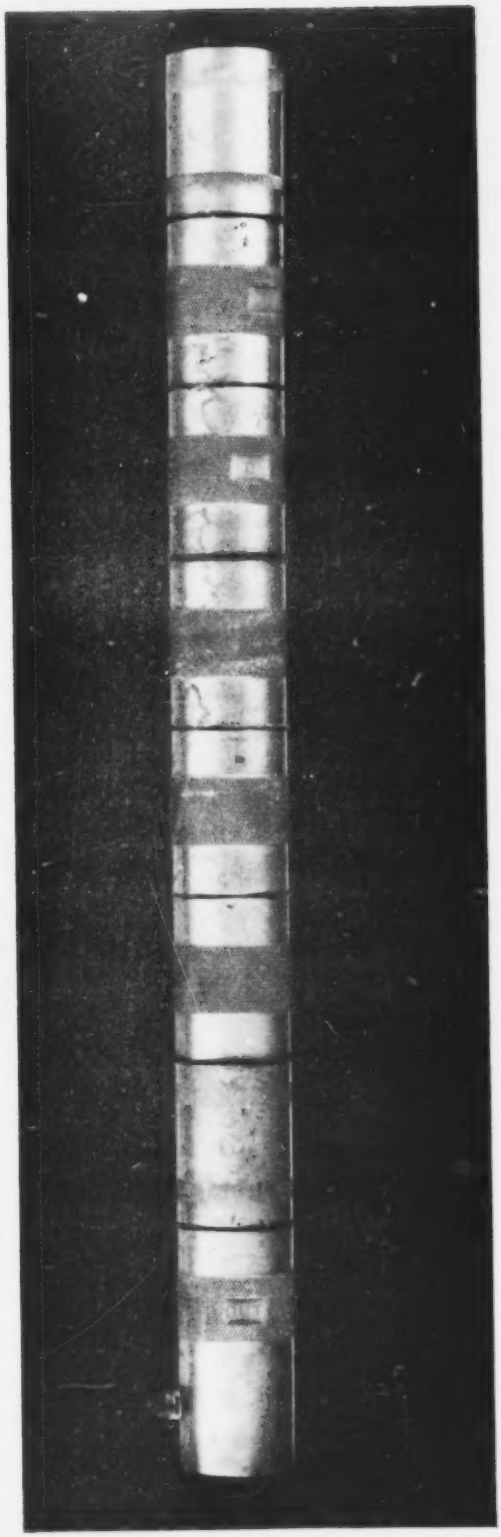

Figure 13. Modified Brink Model B cascade impactor. Complete unit and individual nozzle and impaction plate.

The impactor's measured dimensions are listed in Table 15 and are compared with the manufacturer's values. Measured pressure drops through the unit for flow rates of 0.025, 0.05 and 0.1 cfm are reported in Table 16. Table 17 lists the various $Dp_{50}$ values found in the literature and those used for this study.

## D. IMPACTOR COLLECTION SURFACE COATINGS

A variety of collection surface coatings (Table 2) were assessed as to: 1) their suitability for use at various operating temperatures and flow rates, and 2) their collection efficiency for several types of aerosols. Although the commercial impactors did not necessarily come with either aluminum and/or glass fiber collection plate inserts, it was entirely feasible to make them for use with most of the impactors tested.

Before applying any coating substrate to the aluminum inserts, they were first rinsed in chloroform to remove any residual coatings, then washed in warm soapy water, rinsed in distilled water, and allowed to dry. Several application methods were tried for the Dow Corning 200 fluid, all involving a volatile solvent to make possible a thin coating of the highly viscous substrate. Applications of both the 1% and 10% (by weight) solutions in benzene resulted in a nonuniform coating upon drying. One ml of a solution of 1% Dow Corning 200 fluid in hexane resulted in a uniform coating of approximately 2-4 μm thickness (calculated from coating weight). The resulting lowered viscosity made it possible to spread the substrate easily. Solutions of 10% in hexane were much more viscous, making it impossible to achieve uniform 2-4 μm thickness coatings. However, for applications of coatings of 10-20 μm thickness it was found that the 10% solution was easier to work with due to the excessive amount of 1% solution required to achieve the desired thickness. It is best to keep the volatile fraction to a minimum since incomplete drying could lead to weight loss during testing.

Application of the Dow Corning High Vacuum grease, the Apiezon grease and the White Petroleum jelly was accomplished by initially spreading the grease manually onto the aluminum surface, followed by wiping it smooth with a tissue. After several trials the proper amount for the desired thickness could be easily duplicated, making the application a simple matter.

The high viscosity industrial silicone spray was sprayed directly onto the aluminum inserts. Three passes with the spray at arm's length resulted in a 3-5 μm thickness coating (calculated from coating weight). This method of application was very easy and reproducible. Initially the surface appeared uneven; however, within five minutes the surface coating obtained a uniform thickness.

## E. AEROSOL GENERATION

### 1. Description of Test Aerosols

Laboratory test aerosols generated for use in this study (Table 18) were broadly classified as to three basic types, including: 1) liquid aerosols,

TABLE 15. MODIFIED BRINK MODEL B CASCADE IMPACTOR CRITICAL DIMENSIONS

| Stage No. | No. of Jets | Jet Diameter (in.) | Jet-to-Plate Distance (in.) | S/W | Reynolds Number @ .03 cfm |
|---|---|---|---|---|---|
| 0 | 1 | ----- (0.134) | ----- (0.395) | ----- (2.95) | --- (353) |
| 1 | 1 | 0.098 (0.091) | ----- (0.299) | ----- (3.29) | --- (483) |
| 2 | 1 | 0.070 (0.065) | ----- (0.200) | ----- (3.08) | --- (728) |
| 3 | 1 | 0.055 (0.050) | ----- (0.168) | ----- (3.36) | --- (860) |
| 4 | 1 | 0.037 (0.033) | ----- (0.103) | ----- (3.12) | --- (1279) |
| 5 | 1 | 0.029 (0.028) | ----- (0.079) | ----- (2.82) | --- (1632) |
| 6 | 1 | ----- (0.021) | ----- (0.078) | ----- (3.71) | --- (2253) |

Note: Manufacturer's reported values listed with measured values in parentheses.

TABLE 16. MODIFIED BRINK MODEL B CASCADE IMPACTOR MEASURED PRESSURE DROP AT VARIOUS FLOW RATES

| Flow Rate (scfm) | Pressure Drop ("Hg) |
|---|---|
| 0.1 | 17.4" |
| 0.05 | 2.2" |
| 0.025 | 0.9" |

TABLE 17. REPORTED VALUES OF $D_{p50}$ FOR THE MODIFIED BRINK MODEL B CASCADE IMPACTOR

| Stage # | SRI (3)* | SRI (3)+ | Present Study** |
|---|---|---|---|
| 0 | 9.3 | 9.3 | 9.1 |
| 1 | 5.8 | 5.4 | 5.6 |
| 2 | 3.7 | 3.7 | 3.35 |
| 3 | 2.30 | 2.35 | 2.32 |
| 4 | 1.05 | 1.10 | 1.24 |
| 5 | 0.78 | 0.76 | .84 |
| 6 | 0.46 | 0.46 | .49 |

* Experimental values, excludes losses at 0.03 cfm

\+ Experimental values, includes losses at 0.03 cfm

** Calculated values at .03 cfm based upon a $\sqrt{STK}_{50}$ value of 0.46 obtained based upon the impactor's critical dimensions and Marple's curves (12).

TABLE 18. TEST AEROSOLS

1. Oil (liquid)
   A. 1% and 2% solutions of DOP in ethanol
   B. 100% DNP

2. Soft "hygroscopic" Aerosol
   A. 1% solution of uranine-methylene blue (90:10) in water - ethanol (50:50)
   B. 30% solution of sodium chloride in water

3. Hard (solid) Aerosol
   A. Polystyrene Latex Spheres dispersed in water

2) relatively "soft" hygroscopic aerosols, and 3) "hard" solid aerosols. The liquid aerosols can be characterized as "sticky", being generated from both dioctyl phthalate (DOP) and dinonyl phthalate (DNP). Such an aerosol would be characteristic of the condensation aerosol stream produced by processes which involve petroleum products and resins. The "soft" hygroscopic aerosols are characterized as having a low to medium potential for bounce, and were generated from solutions of both a uranine-methylene blue mixture and sodium chloride (NaCl). These "soft" hygroscopic aerosols reflect the properties of many aerosol streams. The "hard" solid aerosols can be considered as having a high potential for bounce; these aerosols were generated from a suspension of polystyrene latex spheres (PSL) and served to characterize mineral dust aerosol streams.

All of the above aerosols were generated with a three-jet Collison atomizer (34). They were chosen based on the fact that they are accepted as standard test aerosols which result in a consistent, reproducible aerosol stream. Through the use of test aerosols with such a variety of surface characteristics it was possible to assess the degree to which the type of aerosol defines the optimum operating parameters for an in-stack impactor.

2. Vibrating Orifice Aerosol Generator

A vibrating orifice type aerosol generator similar to that described by Berglund and Liu (33) was used to generate monodisperse particles from 2 to 13 μm diameter. The generator consisted of a constant rate liquid feed system, an orifice-piezoelectric crystal assembly, a signal generator and an aerosol flow system incorporating dispersion air and dilution air for drying and neutralization of the aerosol stream.

A solution of a nonvolatile solute in a volatile solvent was delivered at a constant rate by a syringe pump to the orifice assembly. By applying a periodic disturbance of an appropriate frequency, the liquid jet formed at the orifice-piezoelectric crystal assembly was broken into uniform droplets. The volume of each droplet was calculated by liquid feed rate and the frequency of the disturbance. The droplets were dispersed to prevent coagulation, and upon evaporation of the volatile solvent, an aerosol of the nonvolatile fraction was formed. The final diameter of the aerosol particle formed was defined by the nonvolatile volume concentration of the solution as:

$$D_p = D_d(\text{Conc})^{1/3} \qquad (3)$$

where:

$D_p$ = particle diameter

$D_d$ = droplet diameter

Conc = volumetric concentration of the solution

Thus, a range of particle sizes was obtained simply by varying the solute concentration. The electrical charge of the aerosol stream was brought to a Boltzman's Equilibrium through the use of a 10 mc Kr-85 radioactive source.

Monodisperse particles of uranine, a fluorescent dye, were generated having an average geometrical standard deviation of 1.02 as determined by optical sizing from a light microscope equipped with a filar eyepiece. A 50:50 solvent mixture of distilled water and ethanol was found upon drying to produce the most spherical particles. Concentrations of uranine ranged from 10 ppm to 1%. A 20 μm diameter orifice gave trouble-free operation over the range of particle sizes desired with the mass output of the generator being stable throughout periods of up to 3 hours.

3. Three Jet Collison Atomizer

A three jet Collison atomizer as described by Green and Lane (34) was used to generate polydisperse test aerosols over a range from 0.35 μm mmd to 1.8 μm mmd. The atomizer was operated at 30 psig, resulting in an 11 ℓ/min aerosol flow rate. The aerosol stream was then increased to 76 ℓ/min upon dilution by the charge neutralizing airstream.

The ionizer used with the Collison atomizer was similar to that previously described by Whitby (35). The ion generator was operated at a 3,000 volt A.C. potential with a constant air flow of 61 ℓ/min. A 69 ℓ capacity conditioning chamber provided adequate time for both the evaporation of the solvent and contact with the stream of bipolar ions to insure achievement of an equilibrium change distribution.

Test aerosols were generated from a variety of materials, including uranine, DOP, DNP, sodium chloride and polystyrene latex spheres. In all cases samples of the aerosol were viewed with an optical microscope to further characterize the particles. The mass output of the atomizer was found to be constant over the periods of time required to achieve the desired loading.

F. TECHNIQUES FOR MASS DETERMINATION

1. Fluorometric Technique

Fluorometric analysis was employed for collection efficiency measurements (when applicable) because of the method's excellent sensitivity and ease of use. The uranine dye was detectable within ±0.0001 μg for most applications and thus was suited for detection with low mass loadings and measurement of wall losses.

Initial background fluorescence was determined for all the collection surface coatings used and this correction factor was applied to obtain the final mass values. After a given impactor run, collection surfaces and both nozzles and collection plates were individually washed with 20 mℓ of distilled water and allowed to set for 12 hours to insure that all the uranine had gone into solution. The samples were then diluted (if necessary) with distilled water and the fluorescence measured with a Turner Model 110 fluorometer. The mass concentration (μg/ℓ) of uranine was determined from a prepared standard calibration of measured fluorescence vs. uranine mass concentration and multiplied by the appropriate dilution factor (ℓ) to obtain the collected mass (μg).

2. Gravimetric Technique

Gravimetric measurement of mass was achieved with a Cahn Model 4700 automatic electrobalance. Weighings were made to the nearest .001 mg with a typical 95% confidence interval of ±.005 mg. Prior tests showed that if initial and final weighings were made within several hours of each other, preliminary desiccation was not required to obtain stable weighings.

## G. DETERMINATION OF COLLECTION EFFICIENCY

As previously stated, the term collection efficiency will be used in this study to characterize the mass fraction collected by each of the impactor stages. The mass collected upon individual collection plates was determined by either fluorometric or gravimetric techniques (see Section F) and reported as the mass collected for that stage. The total mass collected by all seven stages plus the final filter was reported as the total impactor catch. Thus, the collection efficiency for any given impactor stage can be defined as:

$$C.E._{s-i} = \frac{M_i}{\sum_{i=1}^{i=F} M_i} \qquad (4)$$

where:

$C.E._{s-i}$ = collection efficiency for stage desired

$M_i$ = mass collected upon desired stage

$\sum_{i=1}^{i=F} M_i$ = total impactor stage catch

The cumulative stage collection efficiencies were then plotted against the corresponding $Dp_{50}$ for the given stage on log-normal probability paper to obtain a graphical representation of the measured particle size distribution.

Deposition onto surfaces other than the impactor collection surface coating was considered interstage loss and not included as mass collected by a given stage unless otherwise noted. Both interstage loss per stage and the total interstage losses are reported as a percent of the total impactor catch.

## H. MEASUREMENT OF FLOW RATE, TEMPERATURE, AND RELATIVE HUMIDITY

For laboratory testing, the impactor and parallel filter were followed directly by calibrated dry gas meters used to record the sampled volume of the aerosol stream. The flow rate was monitored by calibrated rotameters and maintained throughout the sampling period by means of a bypass valve in line with the pump. The pressure drops at the dry gas meters were measured directly by mercury manometers. The temperature of the gas stream was

measured by bimetal dial thermometers. The volume of gas sampled at laboratory conditions was then calculated as:

$$V_{acf} = V_m \times \frac{T_a}{T_m} \times \frac{P_a - \Delta P_m}{P_a} \qquad (5)$$

where:

$V_{acf}$ = actual cubic feet of aerosol stream sampled

$V_m$ = cubic feet of sampled aerosol stream measured by the dry gas meter

$T_a$ = actual temperature of the sampled aerosol stream (°K)

$T_m$ = temperature of the sampled aerosol stream at the dry gas meter (°K)

$P_a$ = actual pressure of the sampled aerosol stream ("Hg)

$\Delta P_m$ = pressure drop at the dry gas meter ("Hg)

This volume over the elapsed sampling time resulted in the volumetric sampling rate (flow rate) reported. The relative humidity of the gas stream was determined by the wet-bulb-dry-bulb technique.

## SECTION 5

## EXPERIMENTAL RESULTS

### A. INTRODUCTION

Results of the impactor testing are presented in sections corresponding to the parameter evaluated; i.e., collection surface coatings, flow rate, stage loading and interstage losses. Results of the in-depth testing performed with the MK III University of Washington source test cascade impactor were followed by results of tests from the Andersen MK III stack sampler, the Sierra Model 226 source cascade impactor and a modified Brink Model B cascade impactor for each section. A discussion of these results and comparison with prior findings is detailed in Chapter II.

### B. ANALYSIS OF ERRORS

The size distributions were calculated (Chapter IV, Section G) based upon $D_{p50}$ cut-points which were derived from the impactor's critical dimensions and the impactor efficiency curves of Marple (12). The intent of this study was not to calibrate the impactors, but rather to observe relative changes in the measured distributions due to the varied parameters. The mass output of the Collison atomizer has been previously characterized as log-normal, therefore, the apparent distributions should approximate straight line plots. The fact that the calculated cut-points do provide such apparent distributions suggests that they are accurate relative to themselves, although their absolute values may vary.

The errors associated with the individual mass measurements are outlined in Table 19. It was noted that handling losses and variability were different for the various types of collection surfaces used. The resulting confidence intervals corresponding to the individual size distributions are represented on the plots as percent mass by the use of error bands. Thus, the magnitude of the error band is inversely proportional to the amount of mass collected on the given stage. Nominal error bands ranged from ± 1% to ± 10%. The relative magnitudes of the error bands may appear to be distorted due to the probability function on which they were plotted. Significant differences between size distributions were defined by the above confidence intervals, and reproducibility of experimental results.

TABLE 19. ERRORS ASSOCIATED WITH MASS MEASUREMENT

1. Fluorometric Analysis
   reproducibility ± 0.68%
   impactor surfaces ± 0.0001 µg
   spray silicone ± 0.0017 µg
   glass fiber ± 0.0202 µg
   uncoated aluminum ± 0.0001 µg

2. Gravimetric Analysis
   reproducibility ± 0.005 mg
   spray silicone ± 0.02 mg
   glass fiber ± 0.04 mg
   uncoated aluminum ± 0.05 mg

Values shown are for 95% confidence interval.

## C. COLLECTION SURFACE COATINGS

### 1. Suitability of Use at Elevated Temperatures and High Jet Velocities

Collection surface coatings (Table 2) were subjected to various elevated temperatures for periods of one hour. The collection surfaces were weighed before and after exposure, allowing a measure of weight loss of the coating due to volatilization at the elevated temperature. After an initial one-hour exposure period, the identical coatings were re-exposed at the same temperature for an additional one hour in order to evaluate the extent to which preconditioning of the coatings would decrease weight loss during a testing period.

Results of this testing are summarized in Table 20. The values shown for weight losses and their corresponding variations were based upon two separate trials of three or more samples. In most cases, the measured weight losses during the second hour of exposure to the elevated temperature were decreased by a factor of ten (10) or more, and were accompanied by decreased variance between samples. Whereas the Dow Corning 200 Fluid, Apiezon grease and White petroleum jelly all were suitable at temperatures of 200°F, at 300°F and above, these coatings were observed to decompose (color change, splotchy appearance and running) and have highly variable weight losses, even after the initial one-hour exposure period. Exposure of both the Dow Corning High Vacuum grease and the industrial spray silicone after the initial one-hour period resulted in low weight losses and variability at test temperatures of 200°F, 300°F and 400°F, but were found to be unsatisfactory at 500°F, as evident by the greatly increased weight losses (Table 20). At temperatures of 500°F only the uncoated aluminum and glass fiber filter were found to have stable mass. No further tests were made at higher temperatures.

The above testing was conducted in an oven in still air and could be classified as a static test. Dynamic testing was performed by directing a jet of hot air at the coatings. The jet velocities of the final stages for the impactors fell within the range from 18 m/sec (Sierra at 0.25 cfm) to 100 m/sec (modified Brink at 0.05 cfm) when the units were operated at their design sampling rate (Table 21). Thus, the coatings were subjected to a similar range of incident velocities in order to evaluate their suitability. The test setup is shown in Figure 14. The nozzle diameter was 0.0368 cm and the jet-to-plate distance was 0.318 cm. These dimensions are approximately those of stage 6 of the MK III University of Washington source test cascade impactor. Both jet velocity and temperature were varied and the coatings checked as to their tendency to be blown off the collection surface to which they were applied. Each coating was exposed to an equal volume of air for varying velocities. Results are summarized in Table 22.

The Dow Corning 200 fluid was blown off under all the test conditions, resulting in a crater-like appearance. The thicker coating (≈15 μm) of Dow Corning High Vacuum silicone grease also proved unacceptable at all conditions tested; however, the end result was less drastic than for the Dow Corning 200 fluid. At room temperature and a velocity of 120 m/sec, the thinner coating of Dow Corning High Vacuum grease began showing signs of blow-off, with a slight build-up of coating around the perimeter of the area covered by the

TABLE 20. COLLECTION SURFACE COATING WEIGHT LOSS FOR 1-HOUR EXPOSURES TO TEMPERATURES OF 200°F & 500°F

| Collection Surface Coating | Initial Depth of Coating | (mg) Weight Loss @ 200°F | | (mg) Weight Loss @ 500°F | |
|---|---|---|---|---|---|
| | | 1st Hour | 2nd Hour | 1st Hour | 2nd Hour |
| Uncoated Aluminum | ----- | .09 | .03 ± .01 | .13 | .01 ± .01 |
| Dow Corning High *Vacuum Silicone* Grease | 4 µm | .12 | .01 ± .01 | .46 | .27 ± .05 |
| | 15 µm | .27 | .04 ± .02 | 1.18 | .55 ± .10 |
| Industrial Spray Silicone | 4 µm | .11 | .01 ± .01 | .44 | .30 ± .10 |
| | 15 µm | .37 | .03 ± .01 | .76 | 1.00 ± .30 |
| Gelman Type A Glass Fiber Filter | ----- | .28 | .02 ± .02 | .35 | .09 ± .05 |

Note:

1) Initial Depth of coating estimated according to coating weight

2) All weights are "dry" (after desiccation) weights

3) Dow Corning 200 fluid, Apeizon Grease and White Petroleum jelly all showed signs of decomposition and highly variable weight loss at temperatures above 300°F

TABLE 21. MAXIMUM JET VELOCITIES FOR IMPACTORS OPERATED AT DESIGN FLOW RATE

| Impactor | Maximum Jet Velocity |
|---|---|
| MK III University of Washington Source Test Cascade Impactor (0.5 cfm) | 53 m/sec |
| Andersen MK III Stack Sampler (0.5 cfm) | 33 m/sec |
| Sierra Model 2?6 Cascade Impactor (0.25 cfm) | 18 m/sec |
| Modified Brink Model B Cascade Impactor (0.05 cfm) | 107 m/sec |

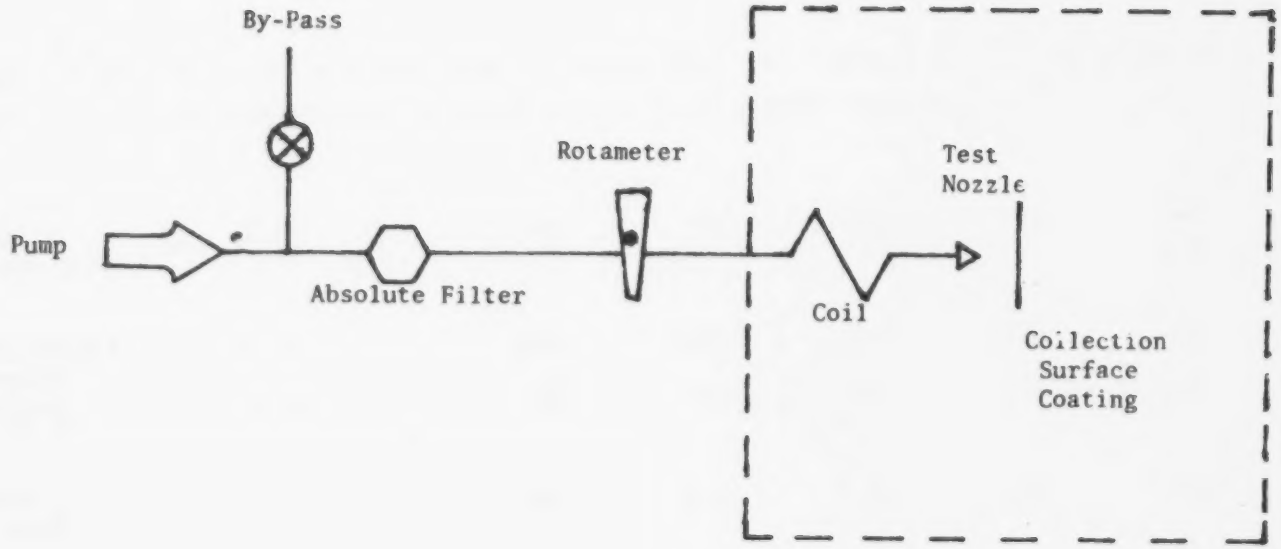


Figure 14. Test set-up for dynamic testing of collection surface coatings.

TABLE 22. OBSERVED TENDENCY OF COLLECTION SURFACE COATING TO BE BLOWN OFF BY AN IMPINGING JET OF VARYING VELOCITY AND TEMPERATURE

| Coating Substrate | Initial Depth Of Coating | Observed Blow Off of Coating Substrate | | | | |
|---|---|---|---|---|---|---|
| | | Room Temperature | | | 200°F | 500°F |
| | | 26 m/sec | 50 m/sec | 120 m/sec | 50 m/sec | 50 m/sec |
| Dow Corning 200 Fluid | 15 μm | Yes | Yes | Yes | Yes | Yes |
| Dow Corning High Vacuum Silicone Grease | 4 μm | No | No | Yes | No | Yes |
| | 15 μm | Yes | Yes | Yes | Yes | Yes |
| Industrial Spray Silicone | 4 μm | No | No | No | No | Yes |
| | 15 μm | No | No | No | No | Yes |

Note:

1) initial depth of coating estimated according to coating weight

2) a 0.0368 cm nozzle was used with a corresponding jet-to-plate distance of 0.318 cm (S/W = 8.64)

impinging jet. Both thicknesses of the industrial spray silicone showed only slight signs of the impinging jet at room temperature and 120 m/sec incident velocity, with the majority of the coating undisturbed. At 200°F and an incident velocity of 50 m/sec, both the Dow Corning High Vacuum grease and the industrial spray silicone proved suitable, with little or no visible sign of the impinging jet. When the temperature was raised to 500°F, all coatings exhibited areas from 0.5 to 2.0 cm in diameter over which the coatings were blown off, and some showed signs of decomposition, as previously noted. From these series of tests the industrial spray silicone was chosen as the most suitable representative of a "grease" type coating. Further testing of collection surface coatings involved only the spray silicone, glass fiber and uncoated aluminum.

2. Effect of Collection Surface Coating on the Measured Size Distribution

The MK III University of Washington source test cascade impactor was operated at 0.5 cfm during the testing of the following collection surfaces: 1) spray silicone, 2) glass fiber, and 3) uncoated aluminum. Various types of polydisperse test aerosols were sampled with each of these collection surfaces. Total impactor loadings were held constant for all tests compared. A comparison of the collection characteristics of each of the surface coatings was made based upon the observed differences in the resulting cumulative particle size distributions.

The effect of the collection surface coating on the measured size distribution for a polydisperse uranine aerosol is shown in Figure 15. The apparent measured size distribution obtained using the uncoated aluminum and the spray silicone collection surface coatings is not significantly different. However, when the glass fiber collection surfaces were employed, the apparent measured distribution shifted to an increased mmd and a slightly increased $\delta_g$.

When a similar sized aerosol of dioctyl phthalate (DOP) was tested, once again the apparent measured size distribution obtained with glass fiber collection surfaces was shifted toward an increased mmd relative to the distribution obtained for the spray silicone coatings (Figure 16). The geometric standard deviations ($\delta g$) for the surface coatings were observed to be approximately the same, with the distribution for the uncoated aluminum surface appearing to "tail off" with increased particle size. Such an effect may be attributed to several factors; however, since in this case it involved only 2% of the total mass collected, the data points were not weighted heavily when interpreting the apparent distribution.

Dinonyl phthalate (DNP), another oil aerosol having a larger size distribution, was also sampled. Again, the distribution obtained with the glass fiber collection surfaces was observed to have an increased mmd relative to the distributions for both the uncoated aluminum and the spray silicone (Figure 17). In the case of all the aerosols sampled (uranine, DOP and DNP), increased deposition of particles on the upper stages of the impactor was visually observed when glass fiber collection surfaces were used. This deposition was not confined just to the areas of the primary deposit beneath the impinging jet, but encompassed the entire collection surface as

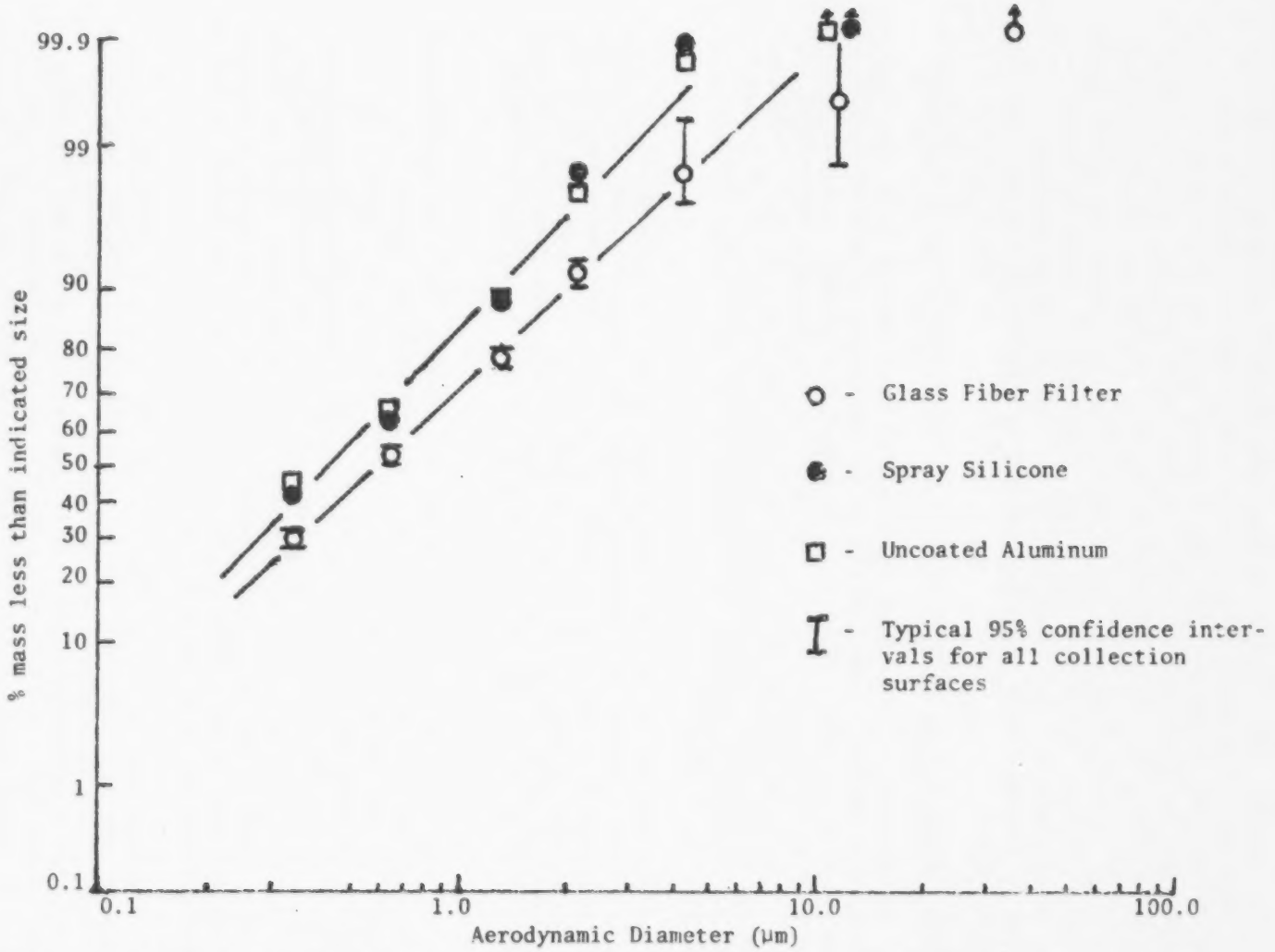


Figure 15. Effect of collection surface on measured size distribution for polydisperse uranine aerosol. (MK III University of Washington source test cascade impactor, 0.5 cfm, 70°F, 30.19 "Hg, 10.0 mg total loading, fluorometric analysis).

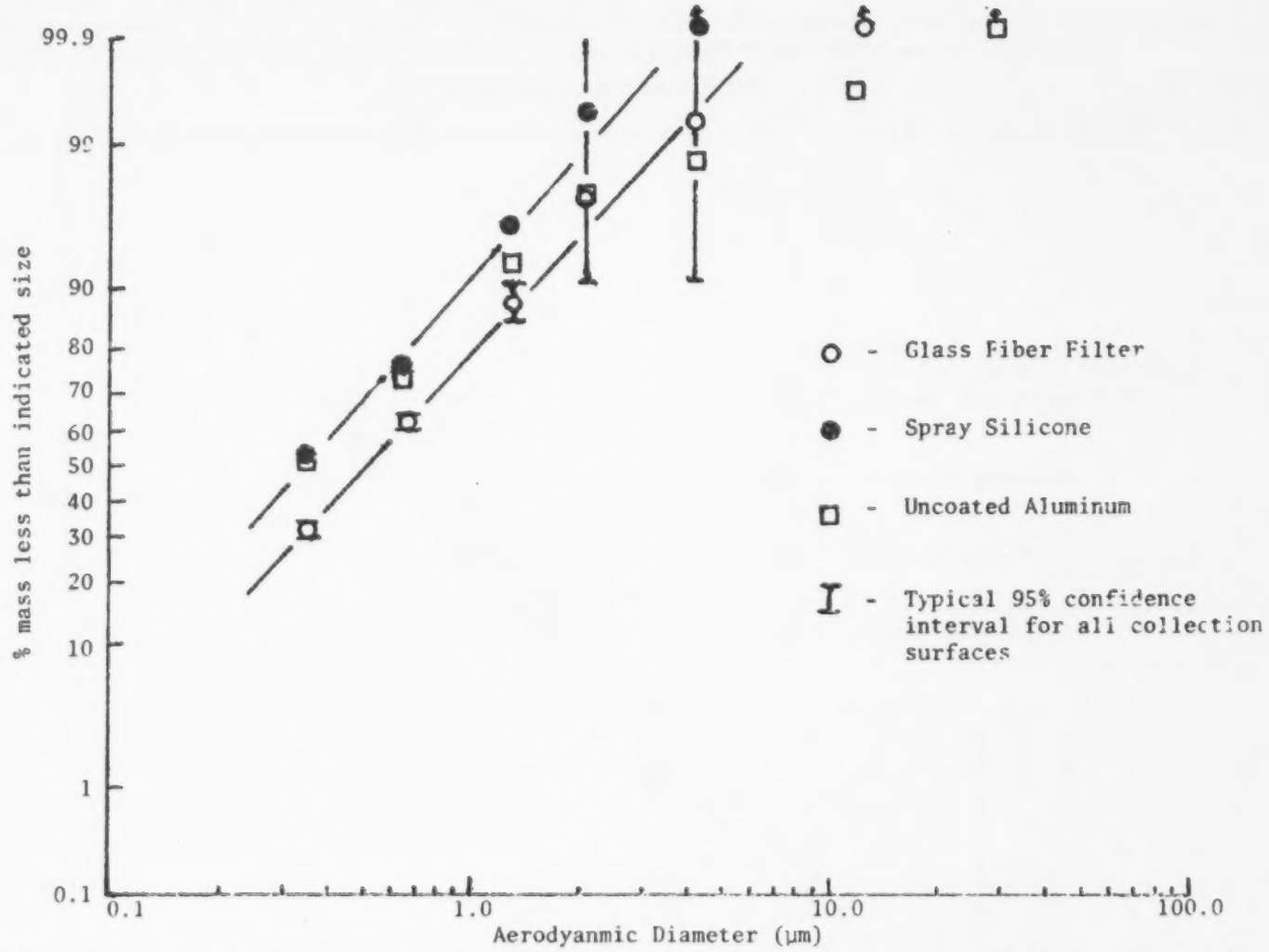


Figure 16. Effect of collection surface on measured size distribution for polydisperse oil aerosol (MK III University of Washington source test cascade impactor, 0.5 cfm, 70°F, 30.20 "Hg, 5.0 mg total loading, gravimetric analysis).

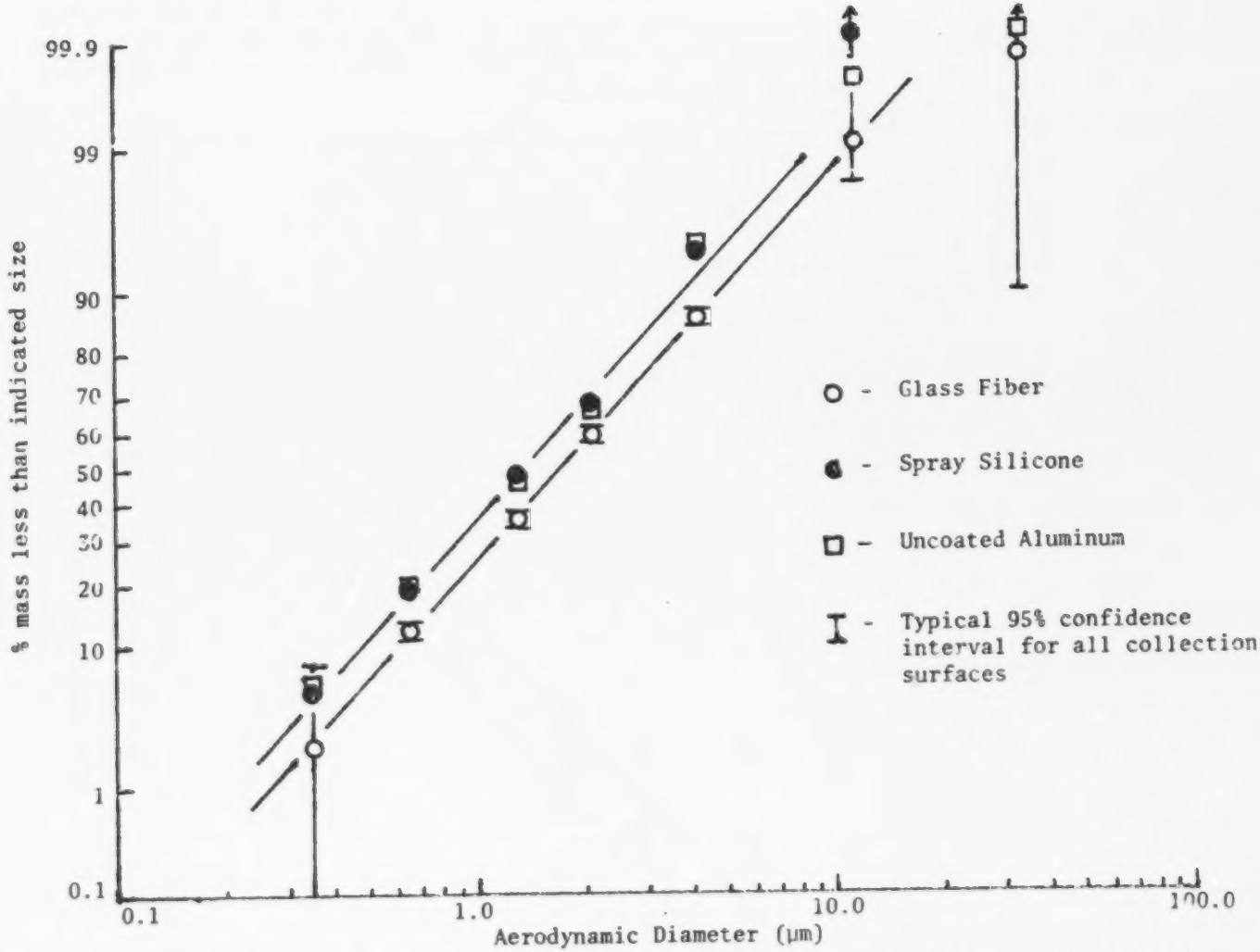


Figure 17. Effect of collection surface on measured size distribution for polydisperse oil aerosol (increased mmd) (MK III University of Washington source test cascade impactor, 0.5 cfm, 70°F, 30.06 "Hg, 30 mg total loading, gravimetric analysis).

seen in Figure 18. Similar secondary deposition was not apparent for either the uncoated aluminum or the spray silicone collection surface coatings.

As a result of these observations and in an attempt to determine if the glass fiber collection surfaces were selectively filtering out submicron particles, it was decided to sample an aerosol of such a size distribution that greater than 95% of the total mass should penetrate through to the final filter. A polydisperse uranine aerosol was sampled resulting in the data presented in Table 23. As shown, approximately 98% of the total collected mass penetrated through to the final filter when employing either uncoated aluminum or spray silicone collection surface coatings. When the impactor was operated with the glass fiber collection surfaces, only 79% of the total mass penetrated through to the final filter, thus significant increases in deposited mass were detected for all but the initial stage of the impactor.

The modified Brink was operated at 0.05 cfm with both spray silicone and glass fiber collection surface coatings. A polydisperse uranine aerosol was sampled and resulted in the apparent measured size distributions shown in Figure 19. As seen with the MK III University of Washington source test cascade impactor, when glass fiber collection surfaces were used, an increased size distribution was observed. Similar tests were not run with the Andersen and Sierra samplers. However, when these impactors were each operated at their nominal flow rates with the pre-cut glass fiber collection surfaces and sampling the same polydisperse uranine aerosol, the apparent measured size distributions obtained were all very similar, as shown in Figure 20. Thus, it is suspect that the size distributions obtained with any impactor would exhibit an increased mmd due to the use of a glass fiber (or a filter media) collection surface as opposed to use of an uncoated or grease coated surface.

## D. EFFECT OF FLOW RATE ON THE MEASURED SIZE DISTRIBUTION

The MK III University of Washington source test cascade impactor was operated at flow rates of 0.25 cfm, 0.5 cfm, and 1.0 cfm, with 0.5 cfm reported as the design flow rate. Both spray silicone and glass fiber collection surface coatings were used over the complete range of test flow rates. Various types of polydisperse test aerosols were sampled in an attempt to determine: 1) if the operational flow rate had any effect upon the resulting particle size distribution, and 2) an upper and lower limit of the operational flow rate with respect to both the aerosol being sampled and the collection surface coating being used.

Figure 21 presents the measured size distributions obtained when sampling a polydisperse uranine aerosol at various flow rates onto spray silicone collection surfaces. Sizing data obtained at the three different flow rates (0.25 cfm, 0.5 cfm and 1.0 cfm) resulted in virtually the same cumulative distribution, although specific observations were made associated with each flow rate. At the lower end of the distribution there was evidence of mass carry-over onto the final filter when the impactor was operated at 1.0 cfm. This was reflected on the plot as a displaced data point. Visual observation of the 7th stage collection surface deposition (Figure 22) revealed halo-like deposits which have been previously associated with particle bounce. Such

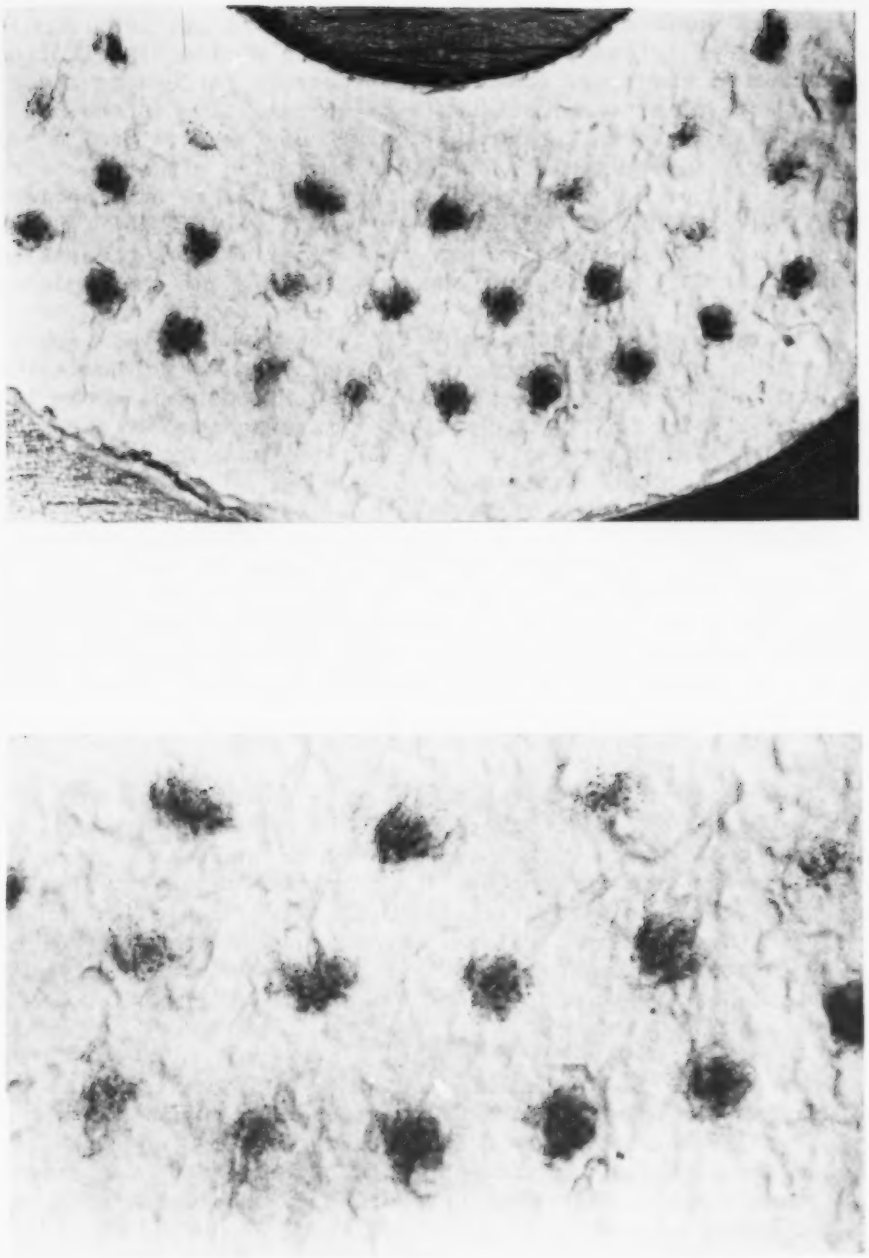

Figure 18. MK III University of Washington source test cascade impactor stage 4 deposition of uranine aerosol onto glass fiber collection surface at 0.5 cfm.

TABLE 23 PERCENT OF TOTAL COLLECTED MASS PER STAGE FOR A POLYDISPERSE URANINE AEROSOL (MK III UNIVERSITY OF WASHINGTON SOURCE TEST CASCADE IMPACTOR, 0.5 CFM, 70°F, 30.18"Hg, 1.0 mg TOTAL LOADING, FLUOROMETRIC ANALYSIS)

| Collection Surface | S-1 | S-2 | S-3 | S-4 | S-5 | S-6 | S-7 | S-F |
|---|---|---|---|---|---|---|---|---|
| Uncoated Aluminum | 0.03 | 0.07 | 0.15 | 0.21 | 0.23 | 0.53 | 1.22 | 97.56 |
| Glass Fiber | 0.05 | 0.21 | 0.53 | 1.17 | 1.75 | 5.22 | 11.87 | 79.28 |
| Spray Silicone | 0.03 | 0.04 | 0.09 | 0.14 | 0.20 | 0.43 | 1.35 | 97.71 |

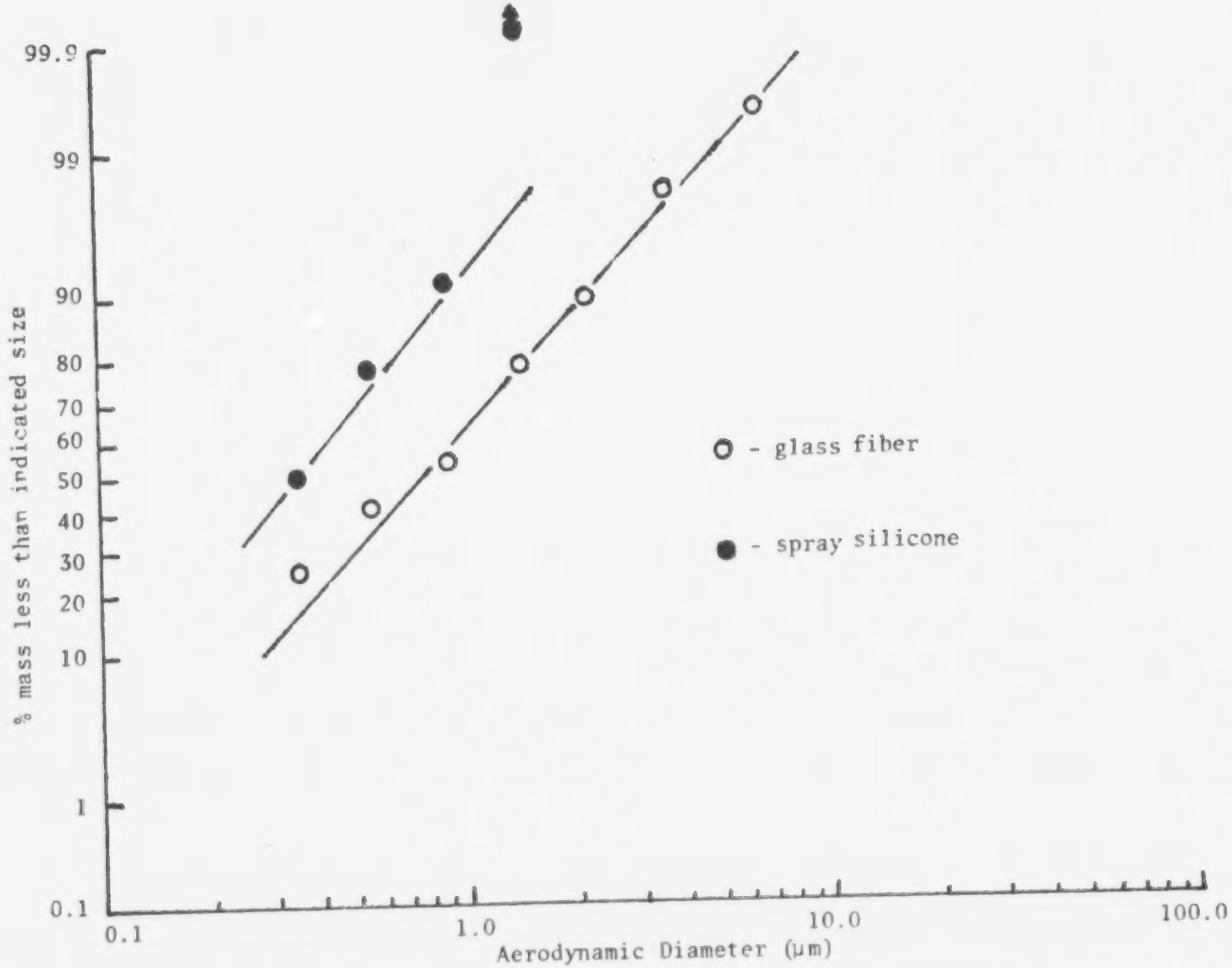


Figure 19. Effect of collection surface coating on measured size distribution for polydisperse uranine aerosol (Modified Brink Model B cascade impactor, 0.05 cfm, 70°F, 30.06 "Hg, 15.0 mg total loading, gravimetric analysis).

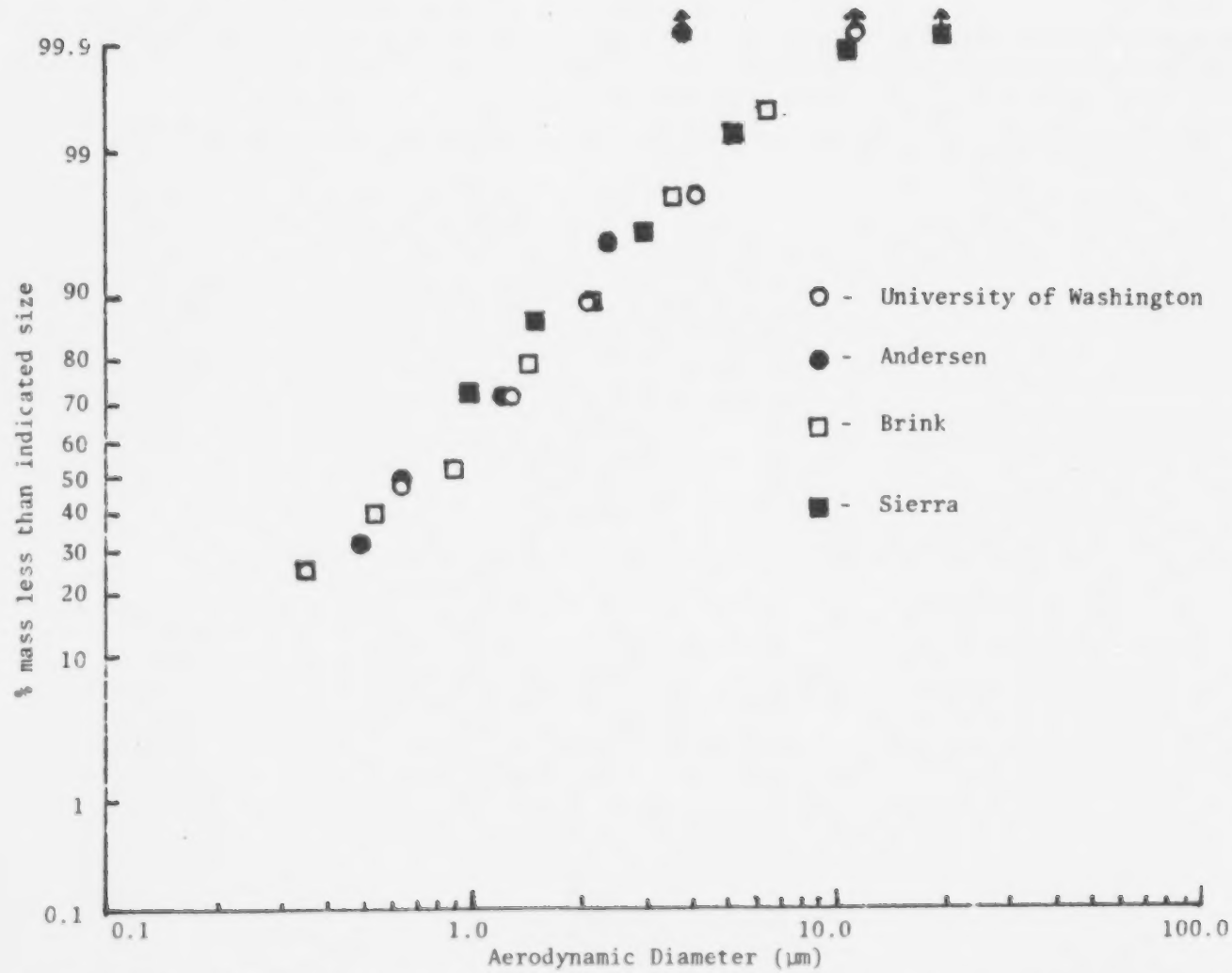


Figure 20. Measured size distributions for a polydisperse uranine aerosol, using glass fiber collection surfaces obtained with the MK III University of Washington source test cascade impactor, Andersen MK IV stack sampler, modified Brink Model B cascade impactor and Sierra Model 226 source cascade impactor (design flow rates, 70°F, 30.10 "Hg, 15.0 mg total loading, gravimetric analysis).

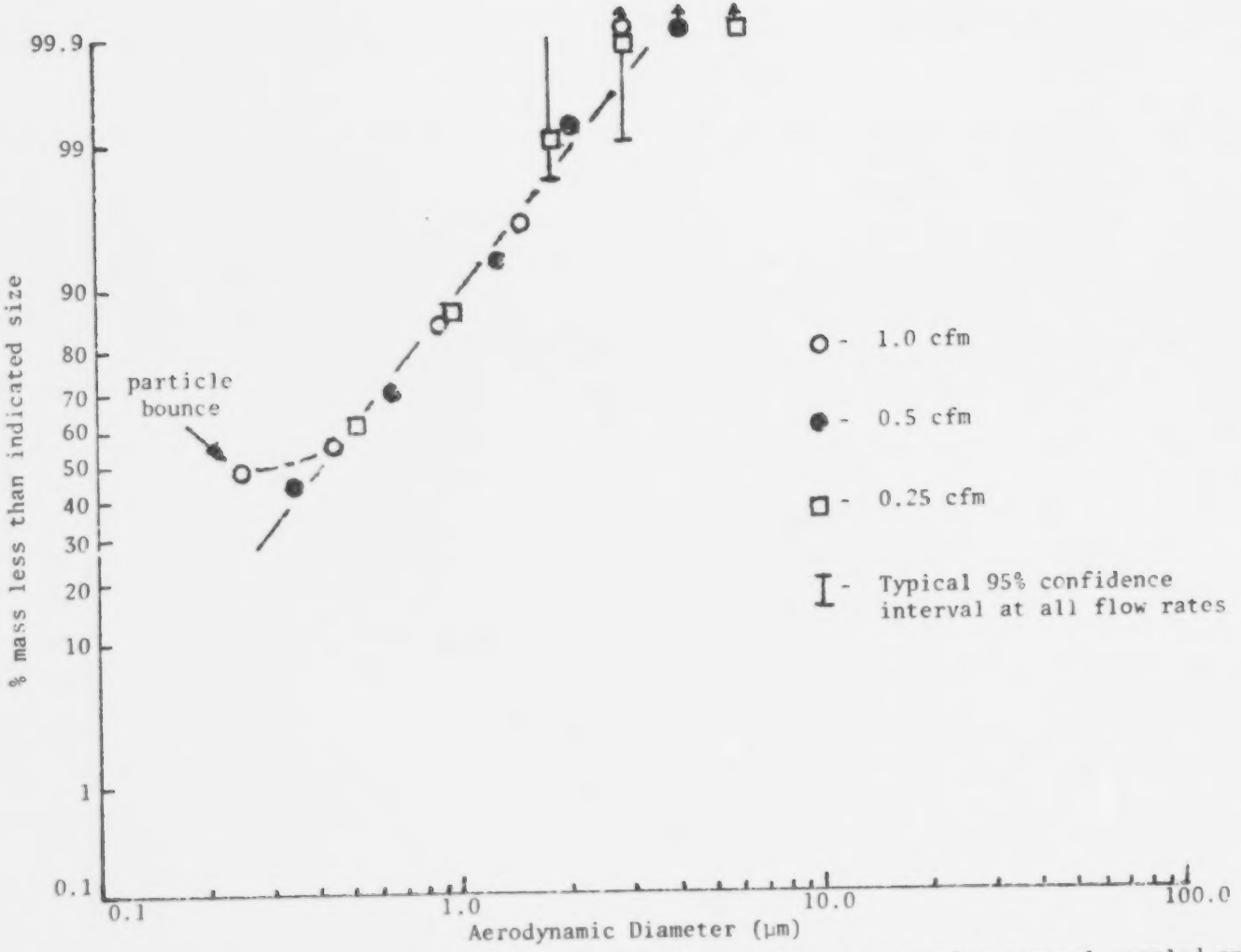


Figure 21. Effect of flow rate on measured size distribution for polydisperse uranine aerosol sampled onto spray siiicone collection surfaces (MK III University of Washington source test cascade impactor, 70°F, 29.93 "Hg, 0.3 mg total loading, fluorometric analysis).

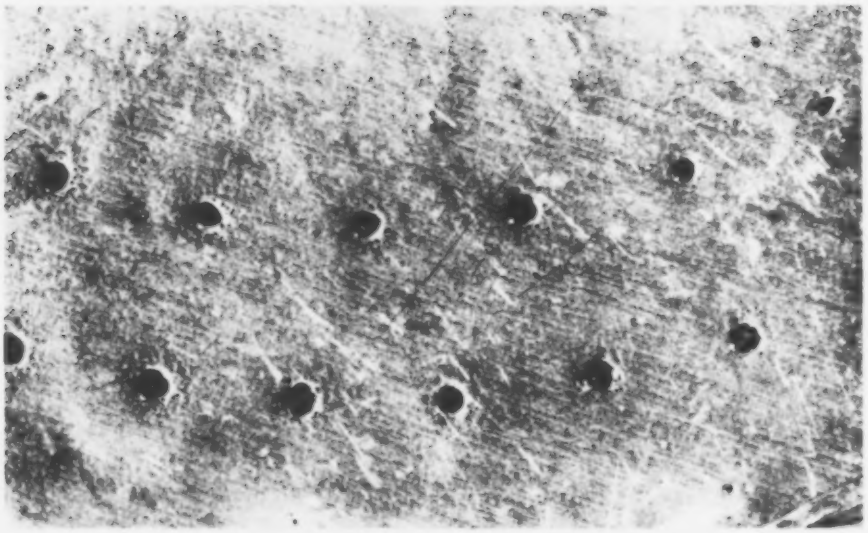

Figure 22. MK III University of Washington source test cascade impactor stage 7 deposition of uranine aerosol onto spray silicone collection surface at 1.0 cfm.

deposits were not observed when sampling at flow rates of 0.5 cfm or 0.25 cfm.

When this same aerosol was sampled onto glass fiber collection surfaces at these flow rates, the same effect was observed (Figure 23). Equivalent distributions were obtained when sampling at either of the three flow rates. Tailing was observed at the upper end of the distributions, however, only 1% of the total collected mass was involved. Once again, there was evidence of particle bounce off, resulting in an increase of mass associated with the final filter when the impactor was operated at 1.0 cfm.

A similarly sized liquid aerosol (DOP) sampled under the same conditions (flow rate, loading and collection surfaces) resulted in distributions having approximately the same mmd's but with apparently different $\delta_g$'s (Figures 24 and 25). Distributions derived from collection onto both spray silicone and glass fiber surfaces all showed the similar trend of increasing $\delta_g$ with increased sampling rate. This testing was repeated several times, always with the same results. The sizing data for the oil aerosol reflects particle bounce problems at the 1.0 cfm flow rate as previously seen with the uranine aerosol. Once again inspection of the collection surfaces themselves revealed evidence of this problem (Figure 26). As the photographs show, the well-defined deposits collected upon stage 6 at 0.5 cfm are quite different from the highly splattered stage 7 deposits collected at 1.0 cfm. At 0.5 cfm the stage 7 deposits exhibited only slight splattering, with no significant problem evident. Close inspection of the stage 7 DOP deposition (1.0 cfm) revealed primary deposits surrounded by rings of secondary deposits, similar to the halo-like effect previously noted with the uranine aerosol.

Sampling of liquid aerosol (DNP) having a distribution of somewhat larger mmd onto both glass fiber and spray silicone collection surface coatings did not show the above mentioned trend of increasing $\delta_g$ with increasing sampling rate (Figures 27 and 28). Distributions obtained from both the glass fiber and spray silicone collection surfaces at 1.0 cfm showed signs of increased mass penetration onto the final filter and visual observation revealed similar splattered deposits on the stage 7 collection surfaces (as previously cited).

Where there was no apparent problem with particle bounce off on stage 7 when operated at 0.5 cfm for either collection surfaces and sampling the uranine and oil aerosols, the polystyrene latex (PSL) spheres were observed to bounce excessively. The PSL spheres sampled were monodisperse and thus should have been predominantly collected on a single stage (stage 5). As determined from the collection efficiencies for the surface coatings tested, of the approximately 36% mass which penetrated past stage 5, 34% of this mass penetrated on through to the final filter when the spray silicone coatings were used, 42% when glass fiber surfaces were used, and 89% when the uncoated aluminum was used as a collection surface. Observation of the stage 6 spray silicone collection surface revealed uniform circular primary deposits (Figure 29). The stage 6 and 7 uncoated aluminum collection surfaces as well as the stage 7 spray silicone surface exhibited secondary deposition about the area of the primary deposit (Figure 29).

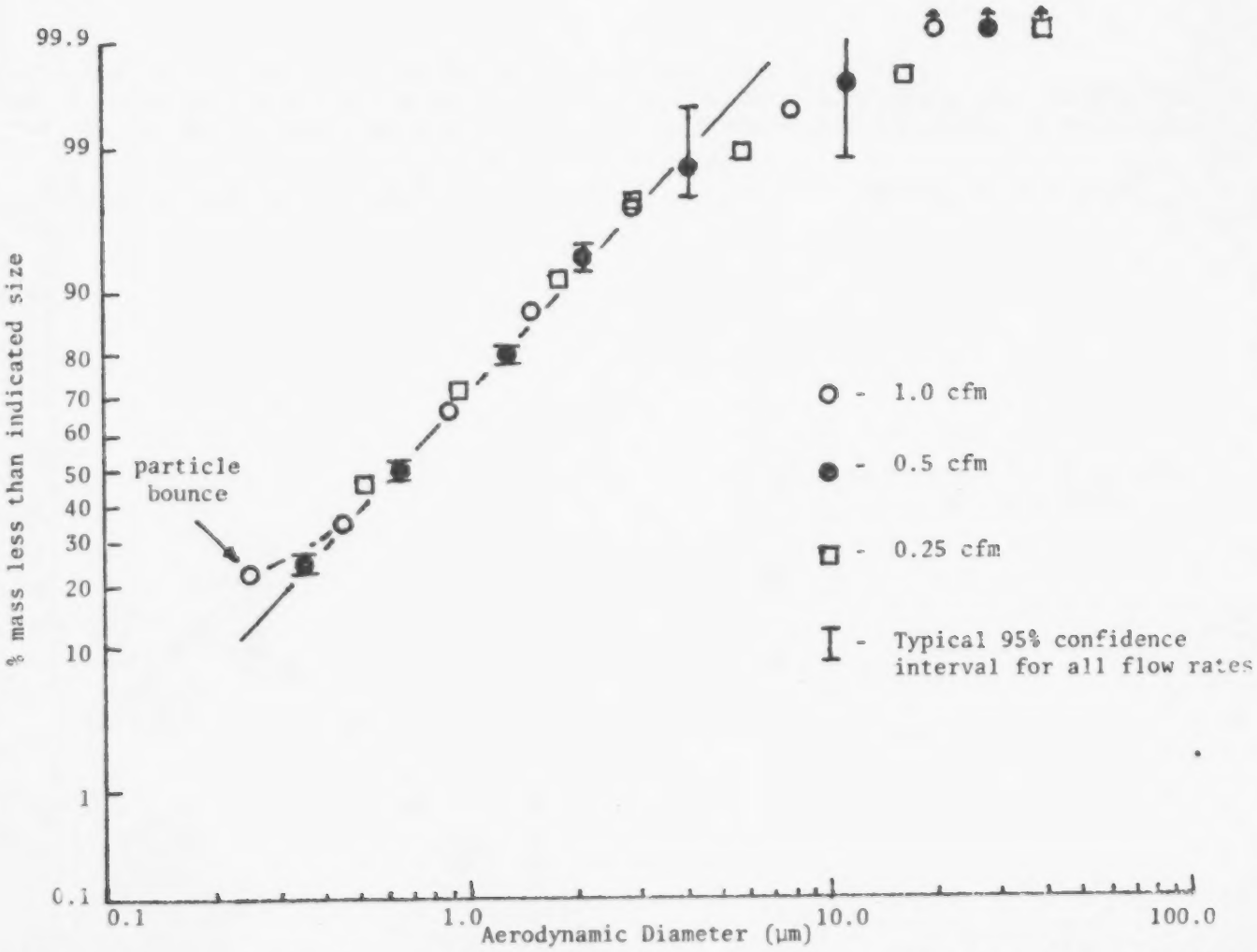


Figure 23. Effect of flow rate on measured size distribution for polydisperse uranine aerosol sampled onto glass fiber collection surfaces (MK III University of Washington source test cascade impactor, 70°F, 30.29 "Hg, 0.3 mg total loading, fluorometric analysis).

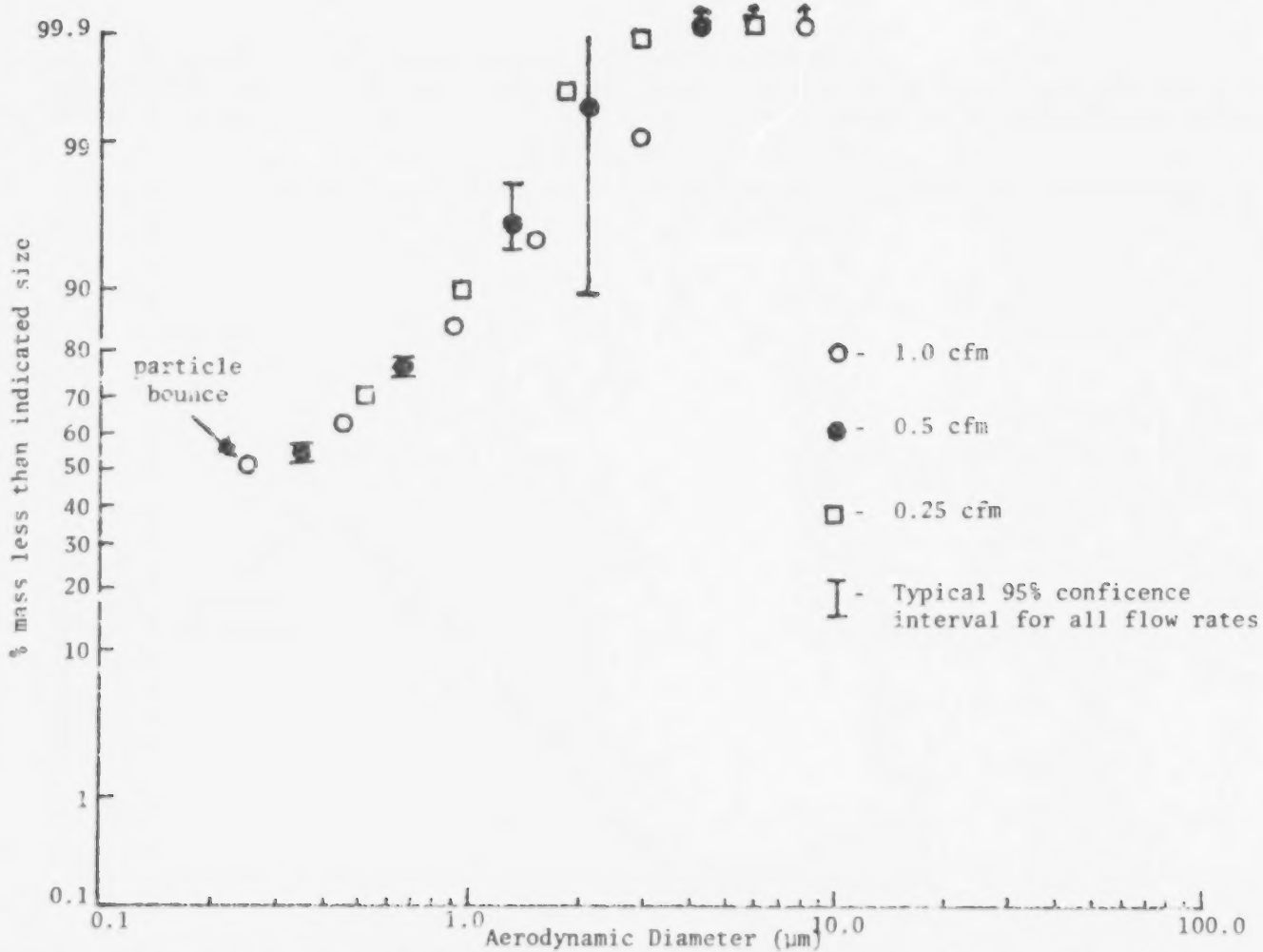


Figure 24. Effect of flow rate on measured size distribution for polydisperse oil aerosol sampled onto spray silicone collection surface (MK III University of Washington source test cascade impactor, 70°F, 30.04 "Hg, 5.0 mg total loading, gravimetric analysis).

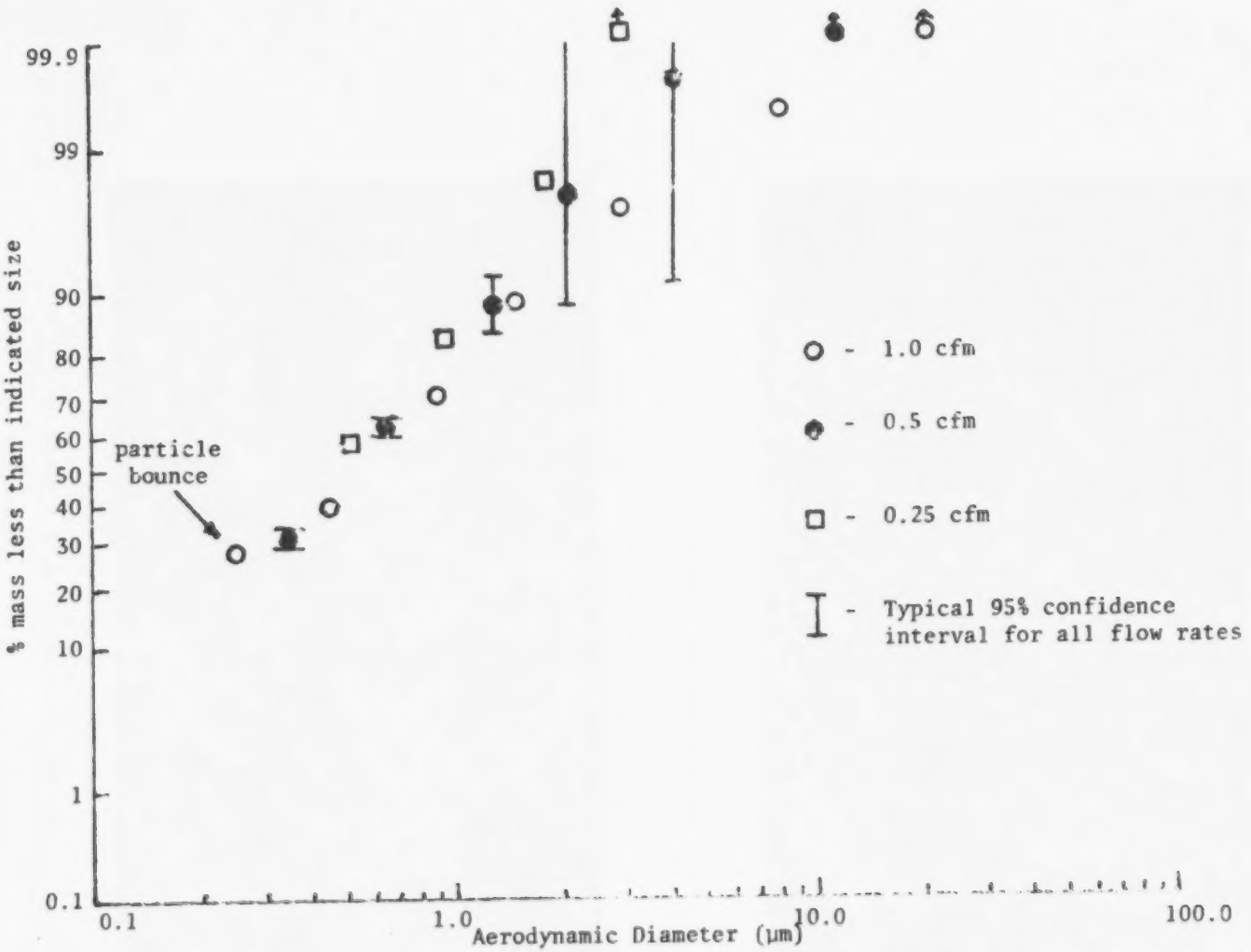


Figure 25. Effect of flow rate on measured size distributions for polydisperse oil aerosol sampled onto glass fiber collection surfaces (MK III University of Washington source test cascade impactor, 70°F, 29.85 "Hg, 5.0 mg total loading, gravimetric analysis).

a) Stage 6 onto spray silicone at 0.5 cfm.

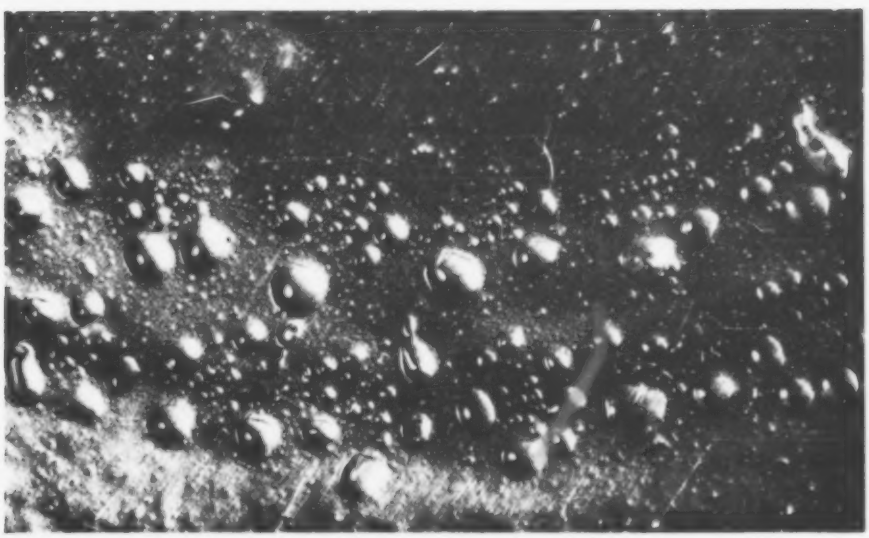

b) Stage 7 onto spray silicone at 1.0 cfm.

Figure 26. MK III University of Washington source test cascade impactor deposition of oil aerosol.

c) Stage 7 onto spray silicone at 0.5 cfm.

Figure 26. (cont.)

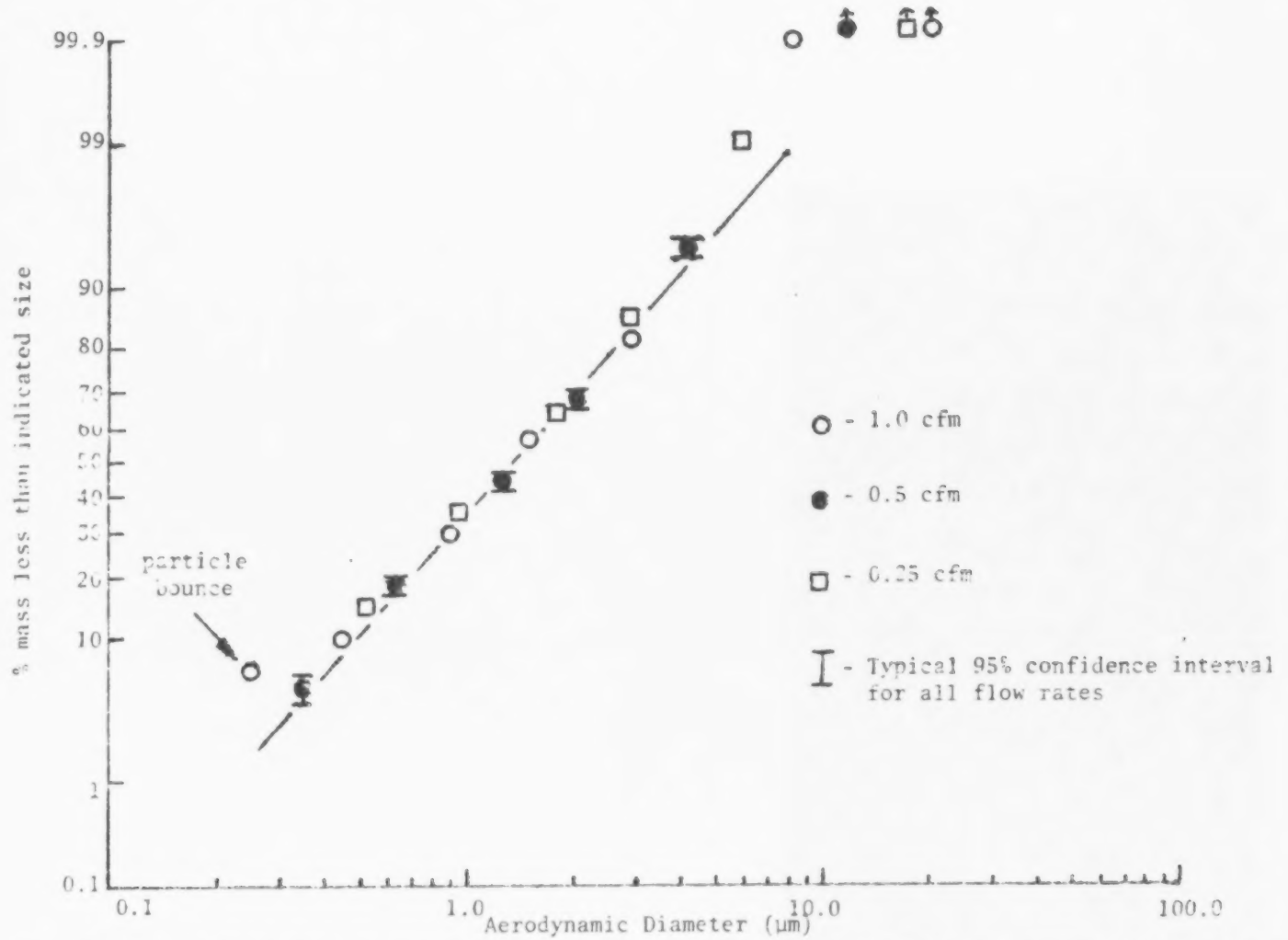


Figure 27. Effect of flow rate on measured size distribution for polydisperse oil aerosol (increased mmd) sampled onto spray silicone collection surfaces (MK III University of Washington source test cascade impactor, 70°F, 30.00 "Hg, 30.0 mg total loading, gravimetric analysis).

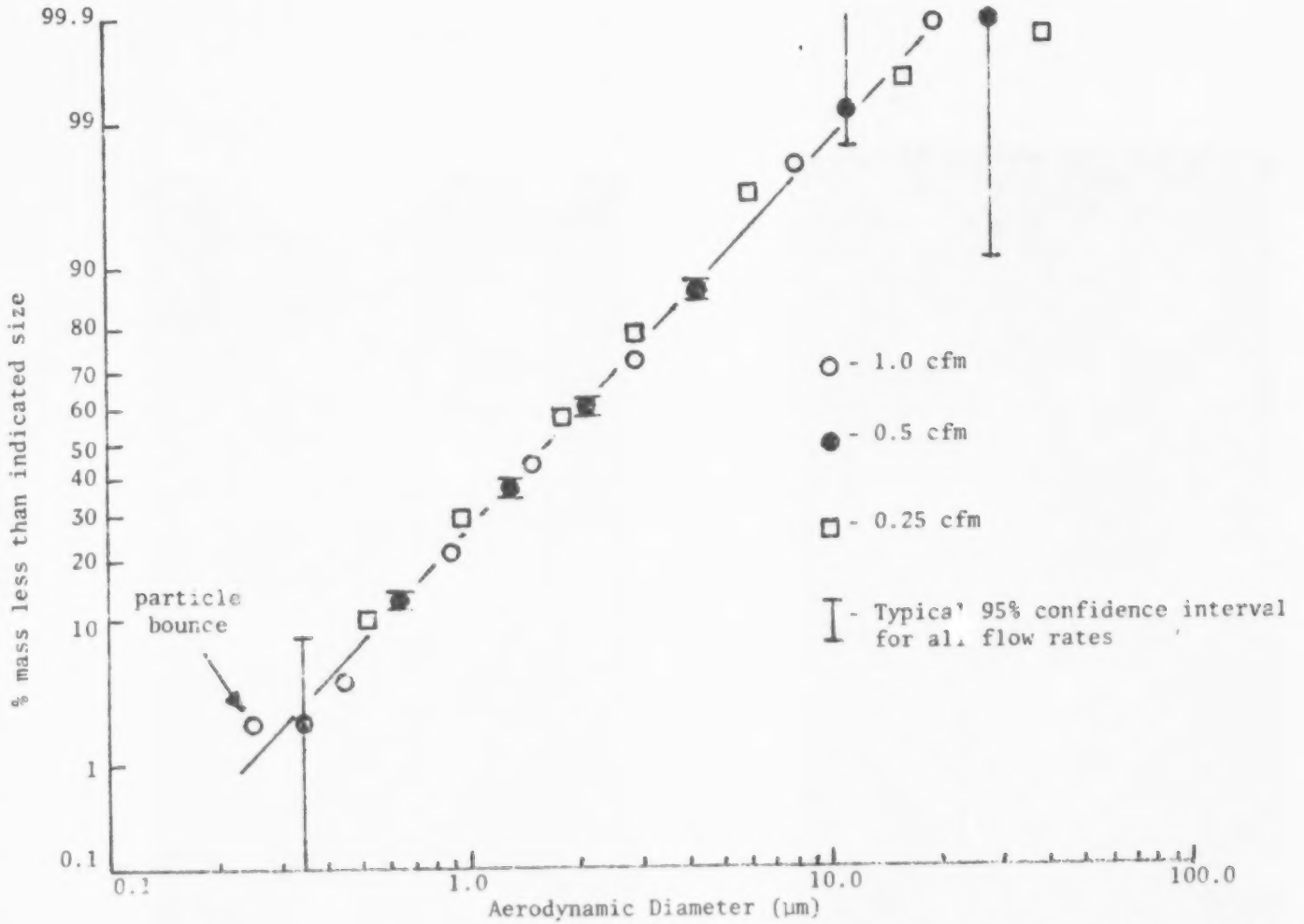


Figure 28. Effect of flow rate on measured size distribution for polydisperse oil aerosol (increased mmd) sampled onto glass fiber collection surfaces (MK III University of Washington source test cascade impactor, 70°F, 30.00 "Hg, 30.0 mg total loading, gravimetric analysis).

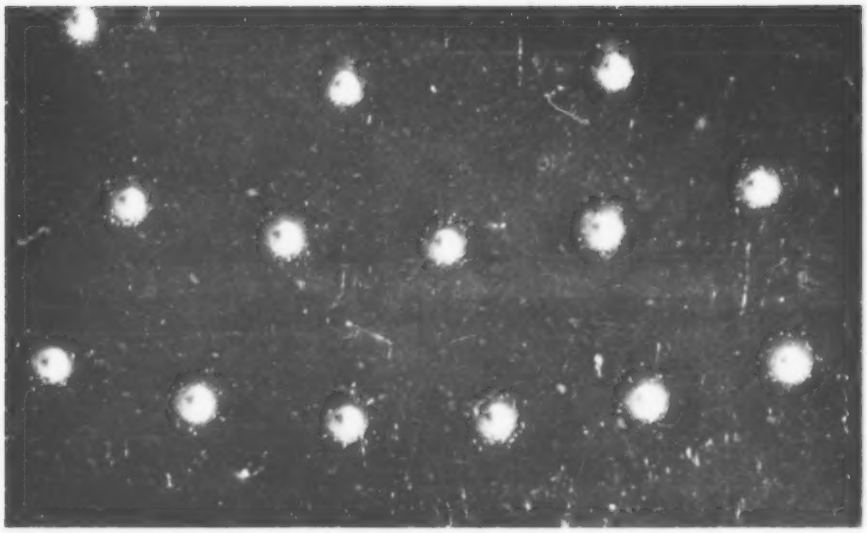

a) Stage 6 onto spray silicone at 0.5 cfm.

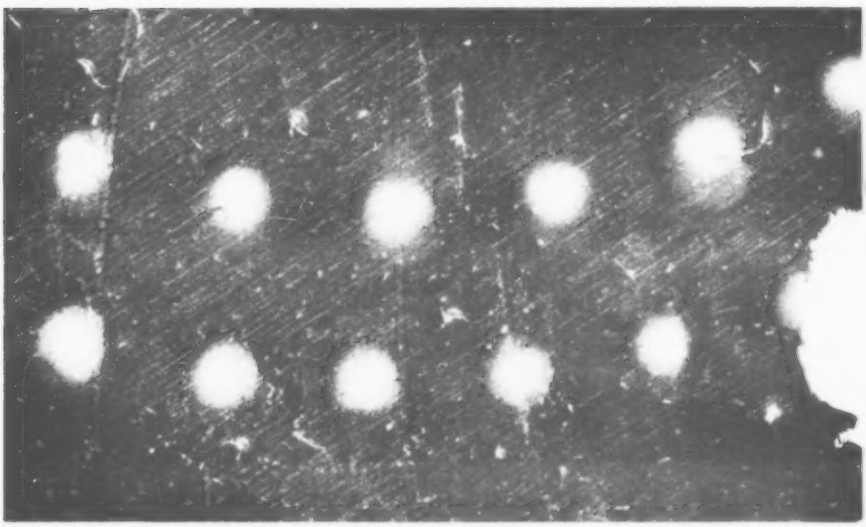

b) Stage 7 onto spray silicone at 0.5 cfm.

Figure 29. MK III University of Washington source test cascade impactor deposition of polystyrene latex spheres.

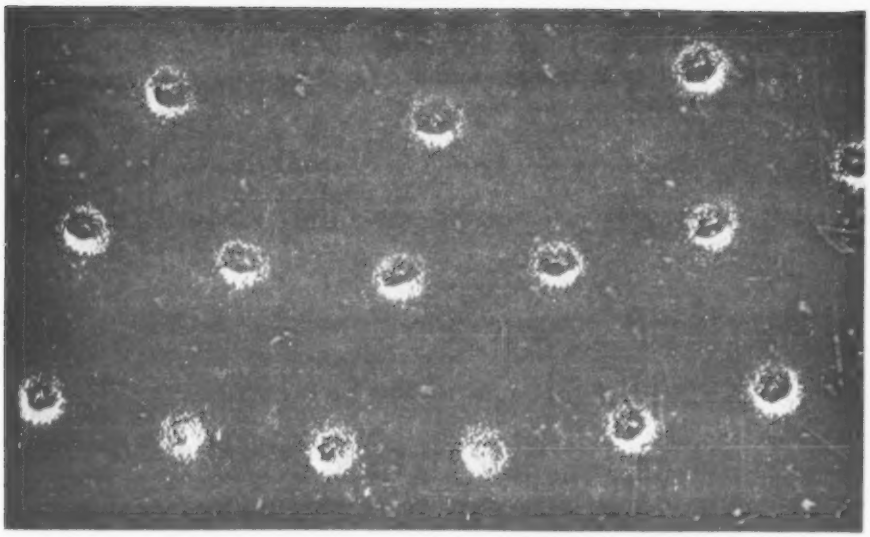

c) Stage 6 onto uncoated aluminum at 0.5 cfm.

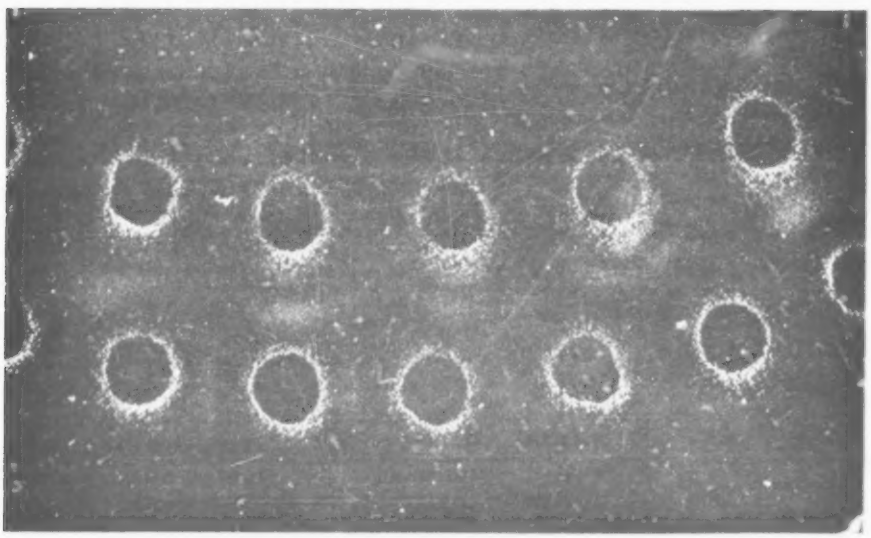

d) Stage 7 onto uncoated aluminum at 0.5 cfm.

Figure 29. (cont.)

A polydisperse uranine aerosol was also sampled at various flow rates with the Andersen, Sierra and modified Brink impactors. Figures 30, 31 and 32 are the cumulative distributions obtained from each of these impactors when employing glass fiber collection surfaces. In the case of both the Andersen and the Sierra, particle bounce was not observed at the upper flow rate. The Brink, however, showed visual signs of bounce off of the last stages at both 0.05 and 0.1 cfm flow rates.

As a point of interest, it was noted that the increase in mmd of the distribution observed when using glass fiber collection surfaces was also evident when sampling at higher or lower flow rates, as is evident in Figures 33 and 34.

## E. STAGE LOADING

### 1. Effect of Stage Loading on Stage Collection Efficiency

The effect of a given stage loading upon that stage's collection efficiency was observed using the MK III University of Washington source test cascade impactor. This was accomplished by varying the stage loading, through increased sampling times, and measuring the mass penetration past that stage. Measurements were made at the design flow rate of 0.5 cfm using spray silicone, glass fiber and uncoated aluminum collection surface coatings in an attempt to characterize the collection characteristics of each type of coating with increasing stage loadings.

Results are presented in Figure 35 for a polydisperse uranine aerosol. In the case of both uncoated aluminum and spray silicone collection surfaces, an initial effect was observed with the increased mass loading to stage 7. Penetration decreased with increased loading up to approximately 0.5 mg, at which time it leveled out. This effect corresponds to an increase in the collection efficiency after some deposit has occurred upon the collection surface. In contrast, the glass fiber collection surface showed a gradual increase in penetration with increased loading. Observation of the various stage 7 collection surfaces at 2 mg mass loading revealed heavy uniform depositions, with their peaks standing almost to the back side of the nozzle plate.

The results of a similar test using an oil aerosol (DOP) are presented in Figure 36. Collection characteristics of the glass fiber surfaces were observed to be relatively stable, with penetration gradually increasing with increased loading. Penetration past the spray silicone collection surfaces was also quite constant, as seen in the figure. Collection characteristics of the uncoated aluminum surfaces were found to be quite variable, with no trend evident.

Results of tests extending the stage loadings from 2-3 mg to 15-20 mg for oil polydisperse aerosols (DOP and DNP) suggest no drastic changes in collection efficiencies from the previously cited observations (Figure 37). When the glass fiber collection surfaces were loaded to greater than 15-20 mg with the oil aerosol (DNP and DOP), the oil was observed to penetrate through

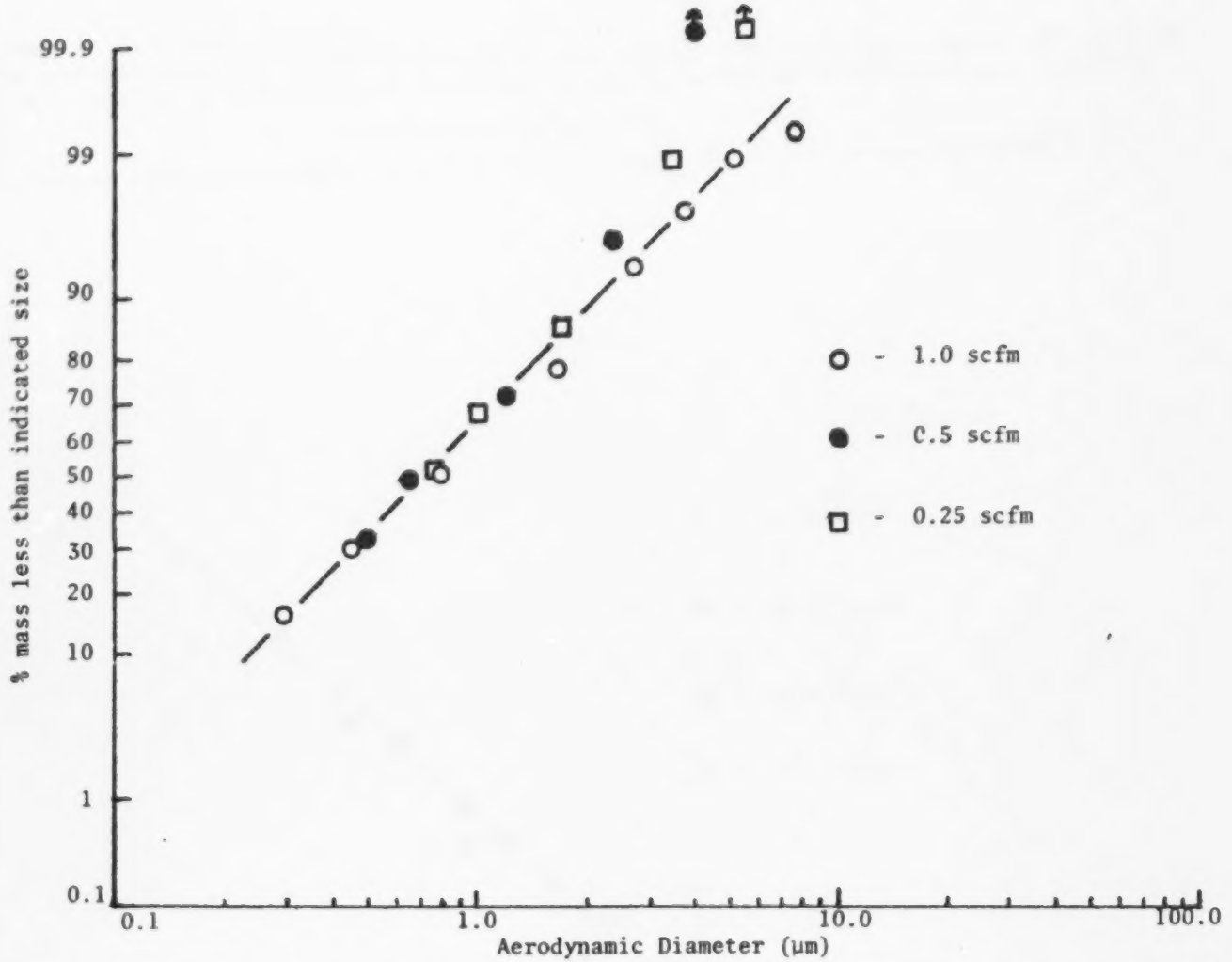


Figure 30 Effect of flow rate on measured size distribution for polydisperse uranine aerosol collected on glass fiber collection surface (Andersen MK III stack sampler, 70°F, 30.00 "Hg, 15.0 mg total loading, gravimetric analysis).

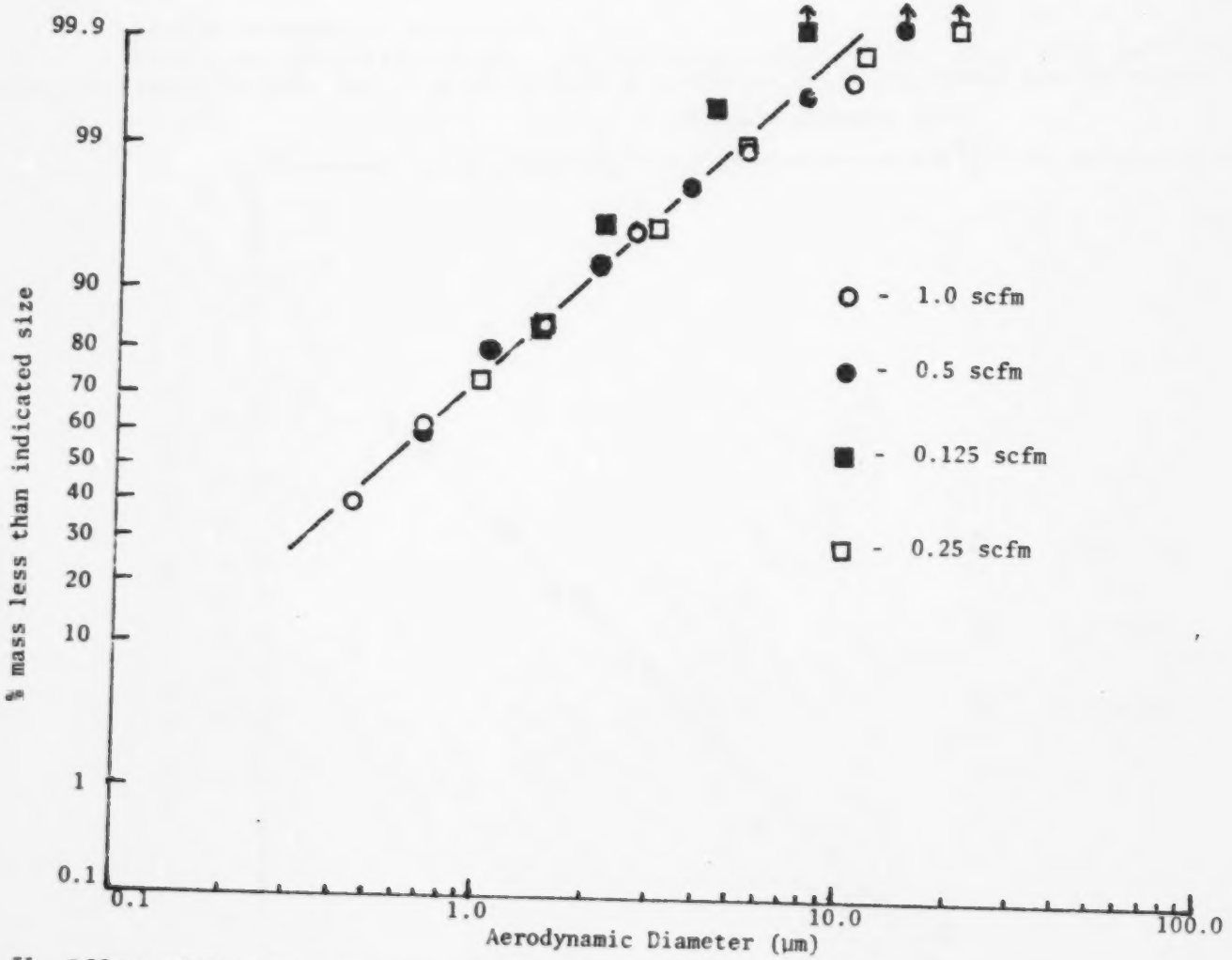


Figure 31. Effect of flow rate on measured size distribution for polydisperse uranine aerosol collected on glass fiber collection surface (Sierra Model 226 cascade impactor, 70°F, 30.04 "Hg, 15.0 mg total loading, gravimetric analysis).

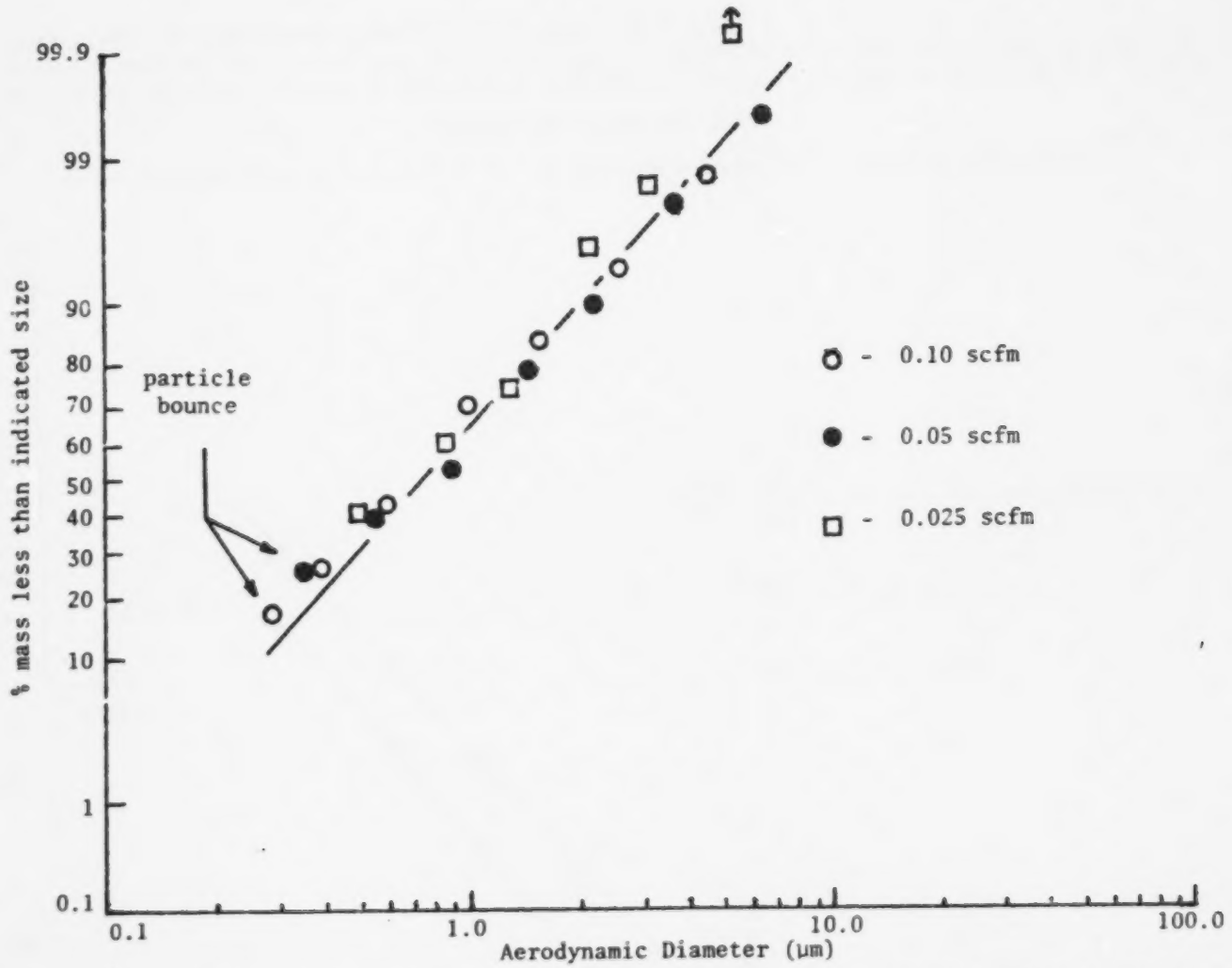


Figure 32 - Effect of flow rate on measured size distribution for polydisperse uranine aerosol collected on glass fiber collection surfaces (Modified Brink Model B cascade impactor, 70°F, 30.06 "Hg, 15.0 mg total loading, gravimetric analysis).

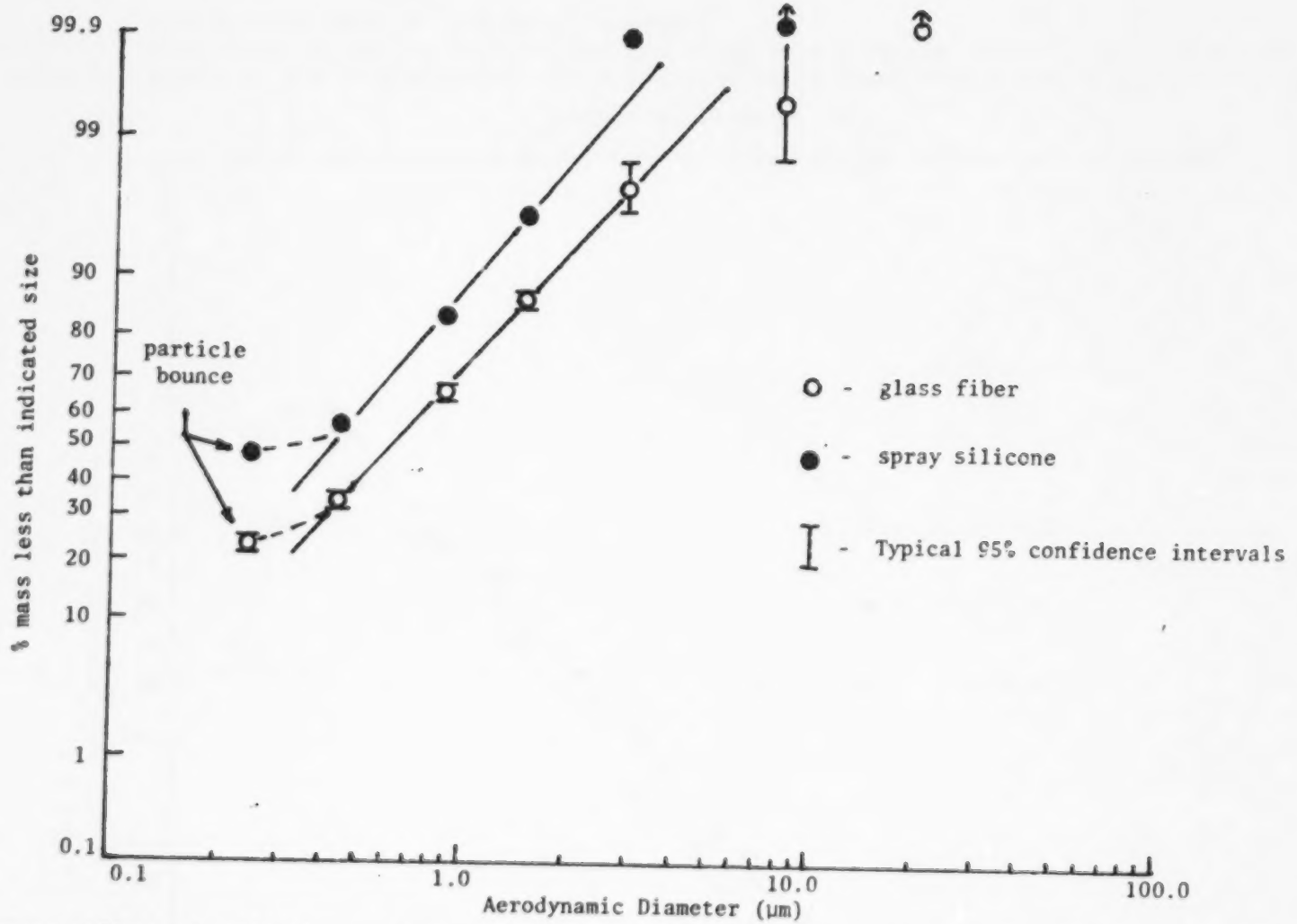


Figure 33. Effect of collection surface coating on measured size distribution of polydisperse uranine aerosol sampled at 1.0 cfm (MK III University of Washington source test cascade impactor, 70°F, 30.12 "Hg, 15.0 mg total loading, gravimetric analysis).

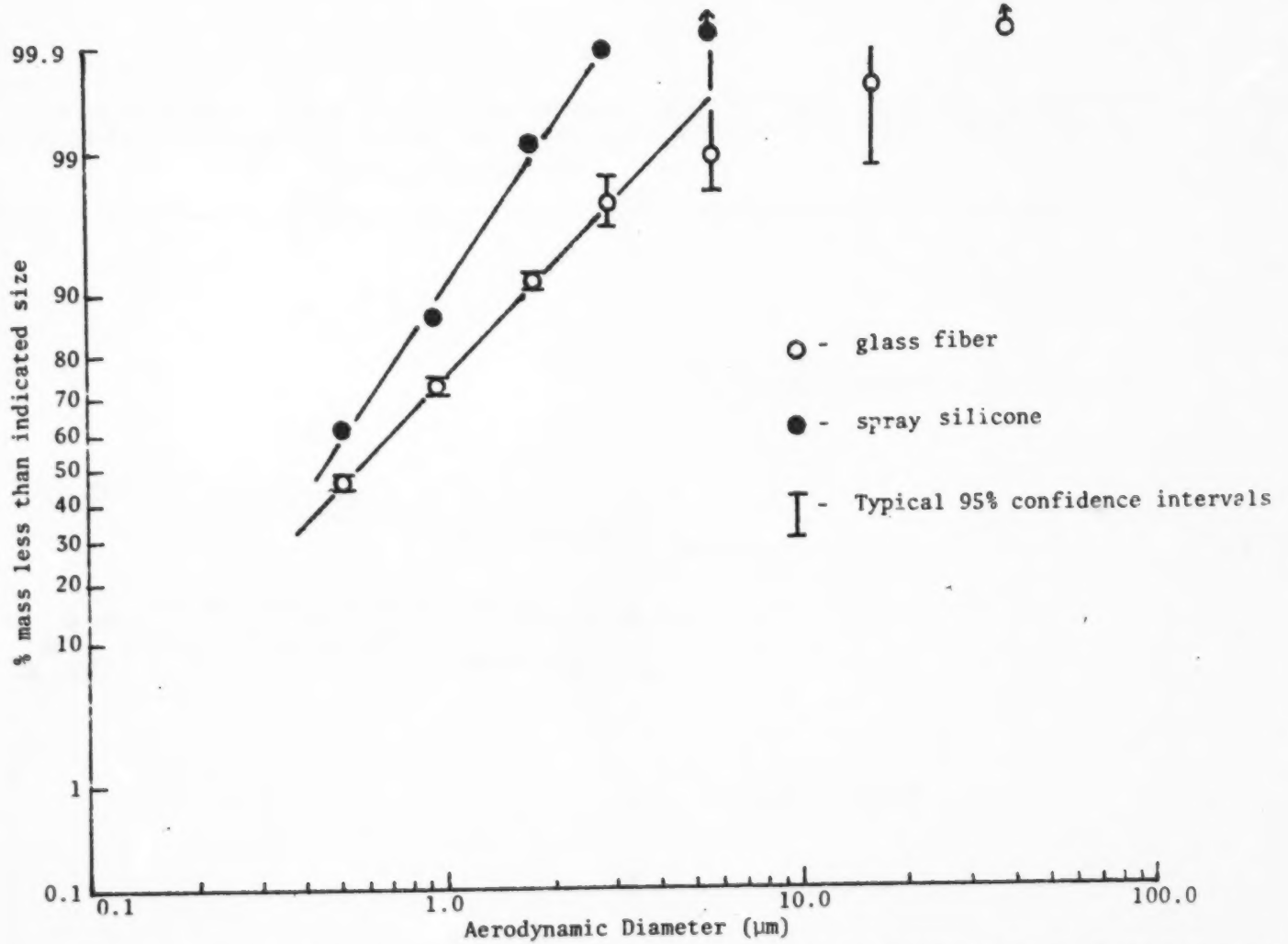


Figure 34. Effect of collection surface coating on measured size distribution of polydisperse uranine aerosol sampled at 0.25 cfm (MK III University of Washington source test cascade impactor, 70°F, 30.12 "Hg 15.0 mg total loading, gravimetric analysis).

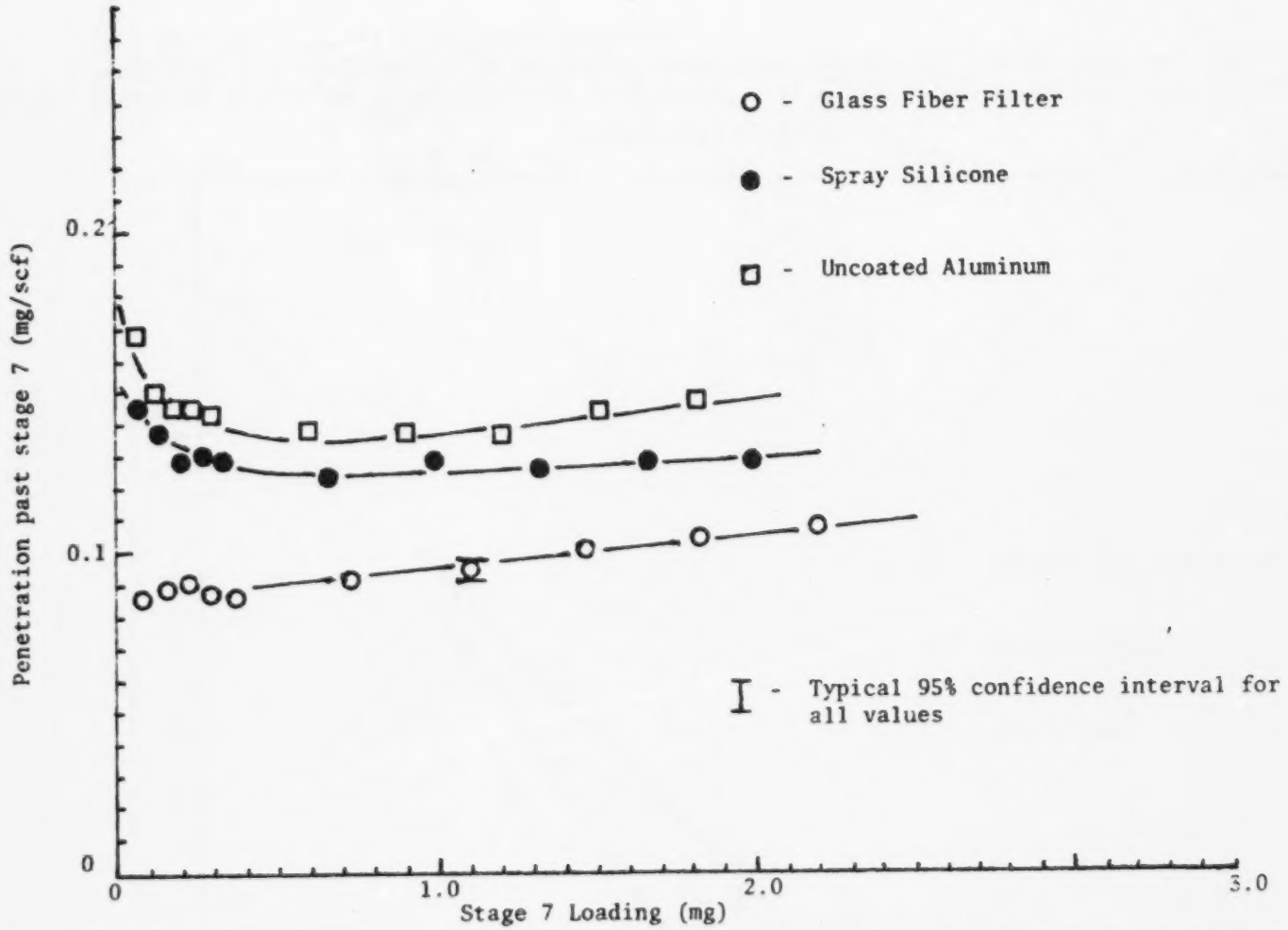


Figure 35. Effect of stage loading on penetration past stage 7 for polydisperse uranine aerosol (MK III University of Washington source test cascade impactor, 0.5 cfm, 70°F, 30.20 "Hg, fluorometric analysis).

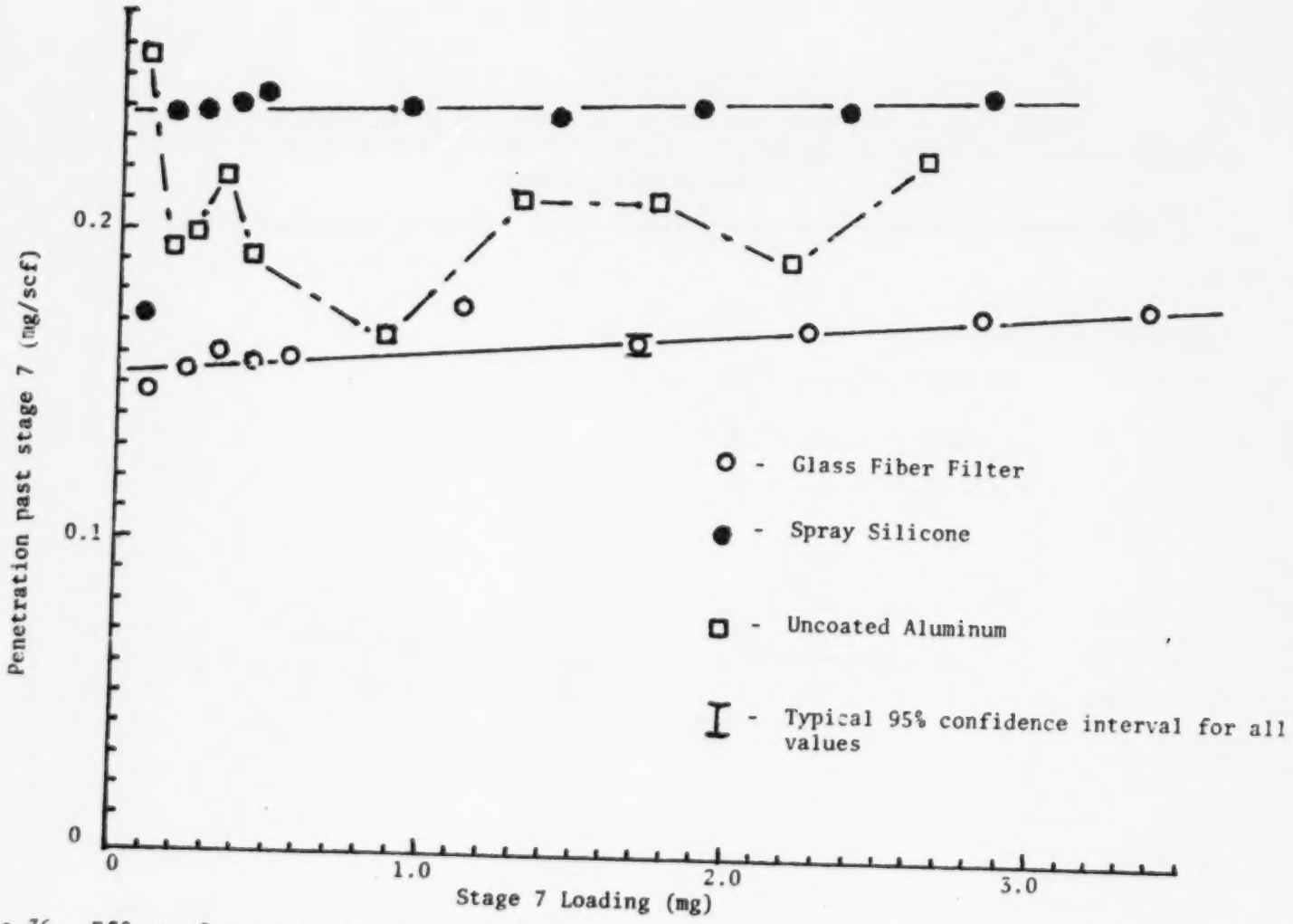


Figure 36. Effect of stage loading on penetration past stage 7 for polydisperse oil aerosol (MK III University of Washington source test cascade impactor, 0.5 cfm, 70°F, 30.02 "Hg, fluorometric analysis).

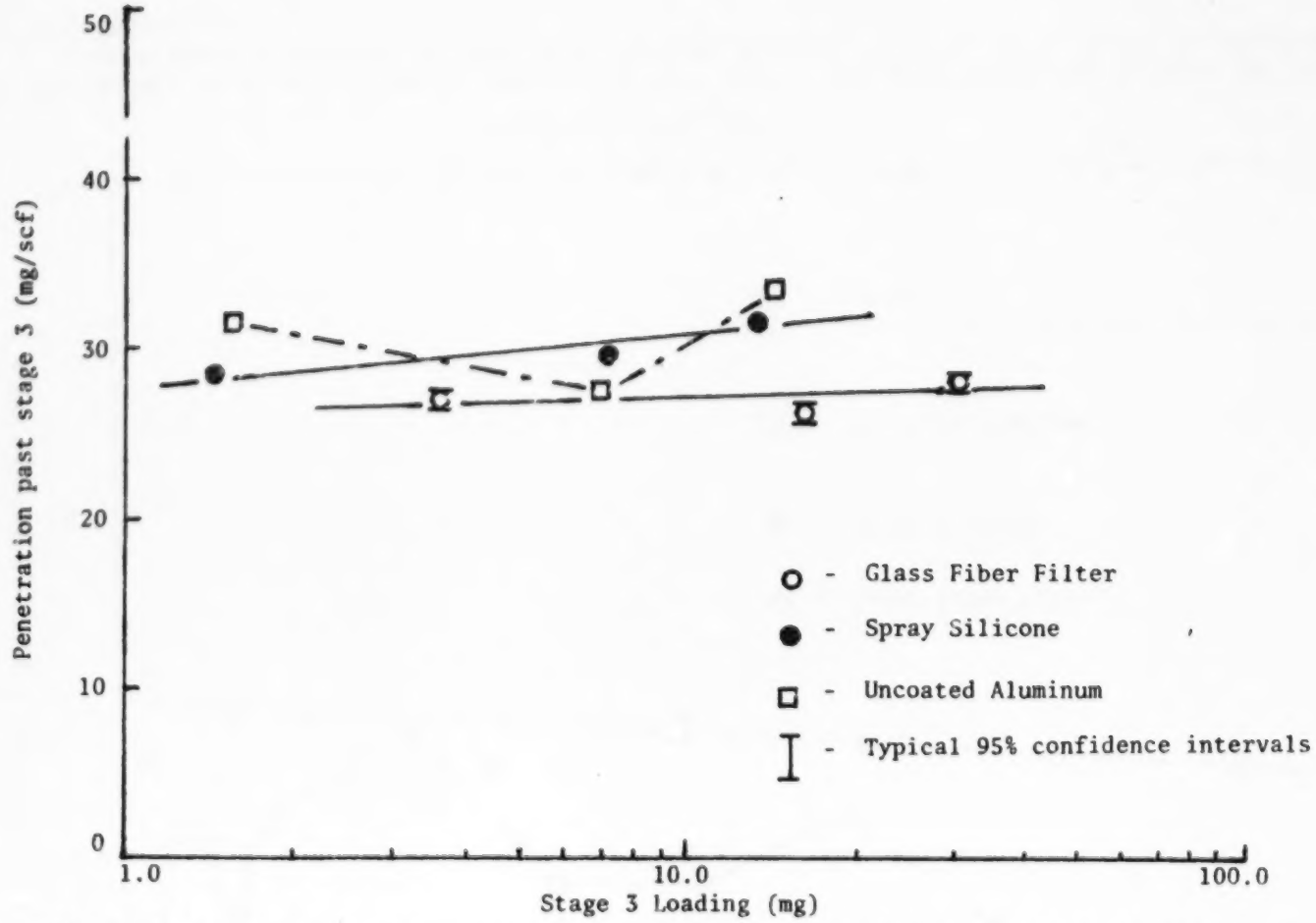


Figure 37. Effect of stage loading on penetration past stage 3 of the MK III University of Washington source test cascade impactor at 0.5 cfm (70°F, 30.36 "Hg, gravimetric analysis).

the glass fiber mats. This suggests the possibility of mass loss to the collection plate supporting the glass fiber filter and a subsequent error in sizing data. No tests were run to quantitate such mass loss. When the uncoated aluminum surfaces were loaded to greater than 10-15 mg with the oil aerosol (DNP and DOP), there were visible signs of the oil deposits running, due to the vertical alignment of the collection surface. This effect was not observed when spray silicone collection surfaces were used.

At 10-15 mg loadings of a hygroscopic solid (sodium chloride), all of the tested collection surfaces were observed to be overloaded. Individual deposits were observed to be overlapping. In addition, there was a significant increase in the visual losses to outer walls and undersides of the nozzle plates. The penetration for these heavy loadings was highly variable for all the surface coatings tested (Figure 38).

2. Effect of Stage Loading on the Measured Size Distribution

Further characterization of the surface coating's collection characteristics with increased mass loading was made based upon a comparison of cumulative particle size distributions obtained from impactor catches of increasing total mass. Such a comparison also indicated the effect of stage loading on the measured particle size distribution.

Figure 39 presents the measured size distributions of a polydisperse uranine aerosol collected on spray silicone at 0.5 cfm, obtained after sampling a total of: 1) 0.3 mg and 2) 10.0 mg mass. These total loadings corresponded to the initial and final stage loadings for which the penetration was measured past stage 7, as previously described (Figure 35). There is evidence that with increasing stage loadings (total loading) the distribution shifts toward a larger mmd and $\delta_g$, indicating decreased penetration. When glass fiber collection surfaces were employed, the size distributions obtained after total loadings of 0.3 mg and 10.0 mg were not significantly different (Figure 40). The data point corresponding to the stage 7 collection showed the only sign of any discrepancy, indicating a possible increase in penetration. Referring back to the plot of penetration versus stage loading for both spray silicone and glass fiber surfaces (Figure 35), it should be noted that the effect of stage loading on the measured size distribution was as expected from those results. In both tests, the glass fiber collection surface displayed stable collection characteristics over the range of stage loadings, while the spray silicone initially had relatively greater penetration (decreased collection efficiency) resulting in the observed difference in measured distributions.

Total loadings of 30 mg and 80 mg, corresponding to maximum stage loadings of 8 mg and 16 mg, were sampled of a polydispersed oil aerosol (DNP) at 0.5 cfm. As shown in Figure 41, the measured size distribution does not show any effect due to increased loading when collected on glass fiber surfaces. Similar results were obtained using spray silicone collection surfaces (Figure 42).

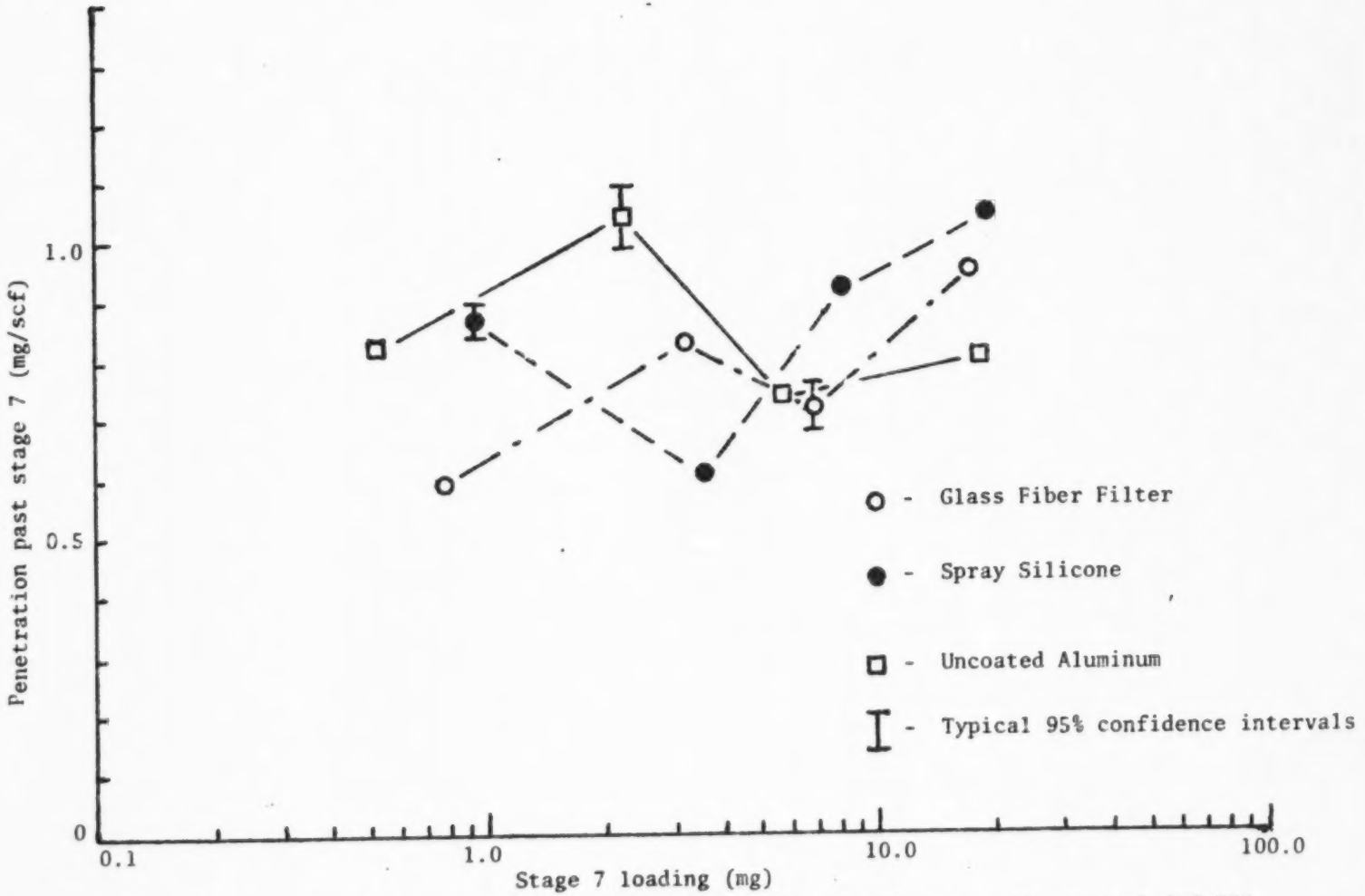


Figure 38. Effect of stage loading on penetration past stage 7 for polydisperse salt aerosol (MK III University of Washington source test cascade impactor, 0.5 cfm, 30.13 "Hg, gravimetric analysis).

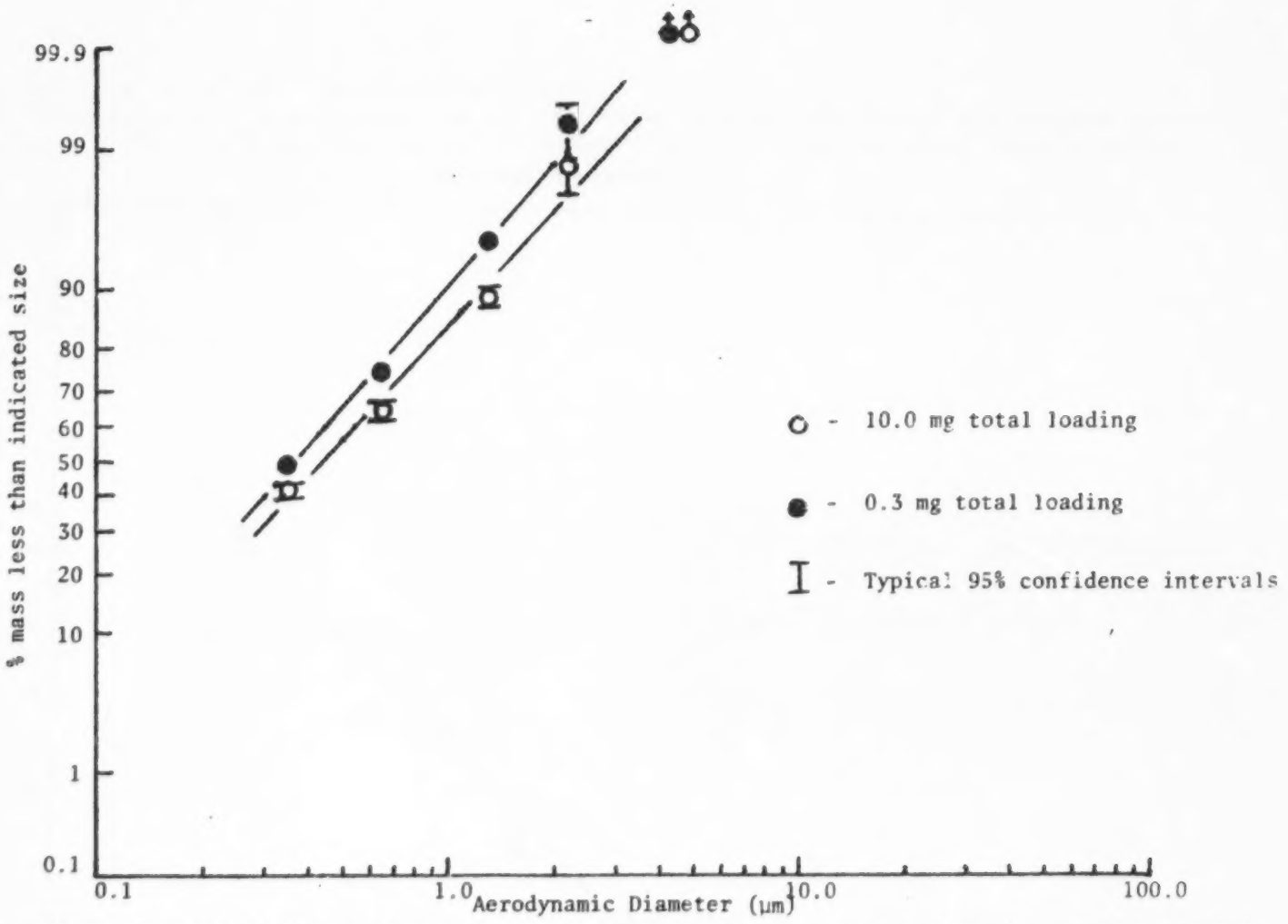


Figure 39. Effect of stage loading on measured size distribution for polydisperse uranine aerosol sampled onto spray silicone (MK III University of Washington source test cascade impactor, 0.5 cfm, 70°F, 30.12 "Hg, fluorometric analysis).

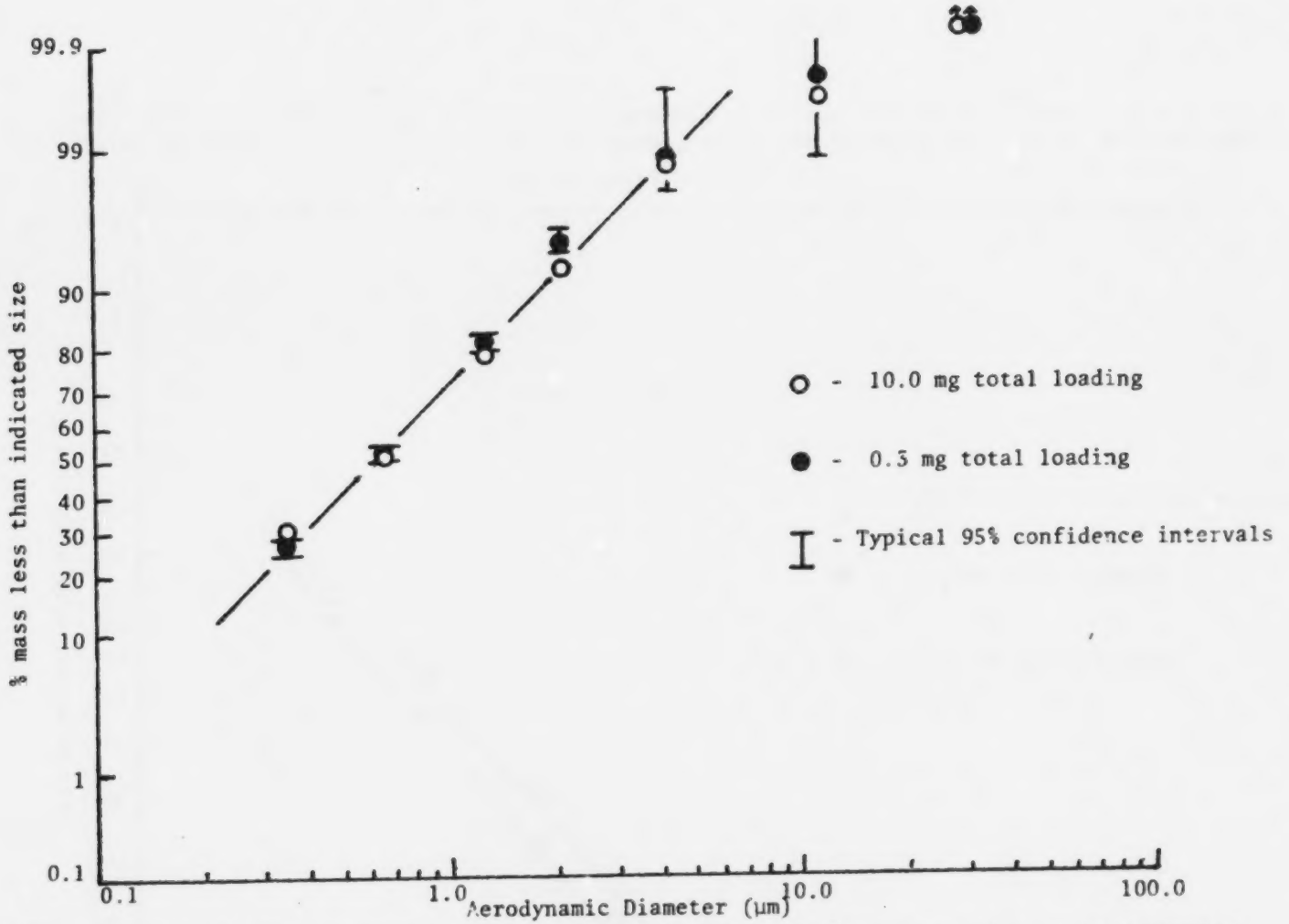


Figure 40. Effect of stage loading on measured size distribution for polydisperse uranine aerosol sampled onto glass fiber collection surface (MK III University of Washington source test cascade impactor, 0.5 cfm, 70°F, 30.13 "Hg, fluorometric analysis).

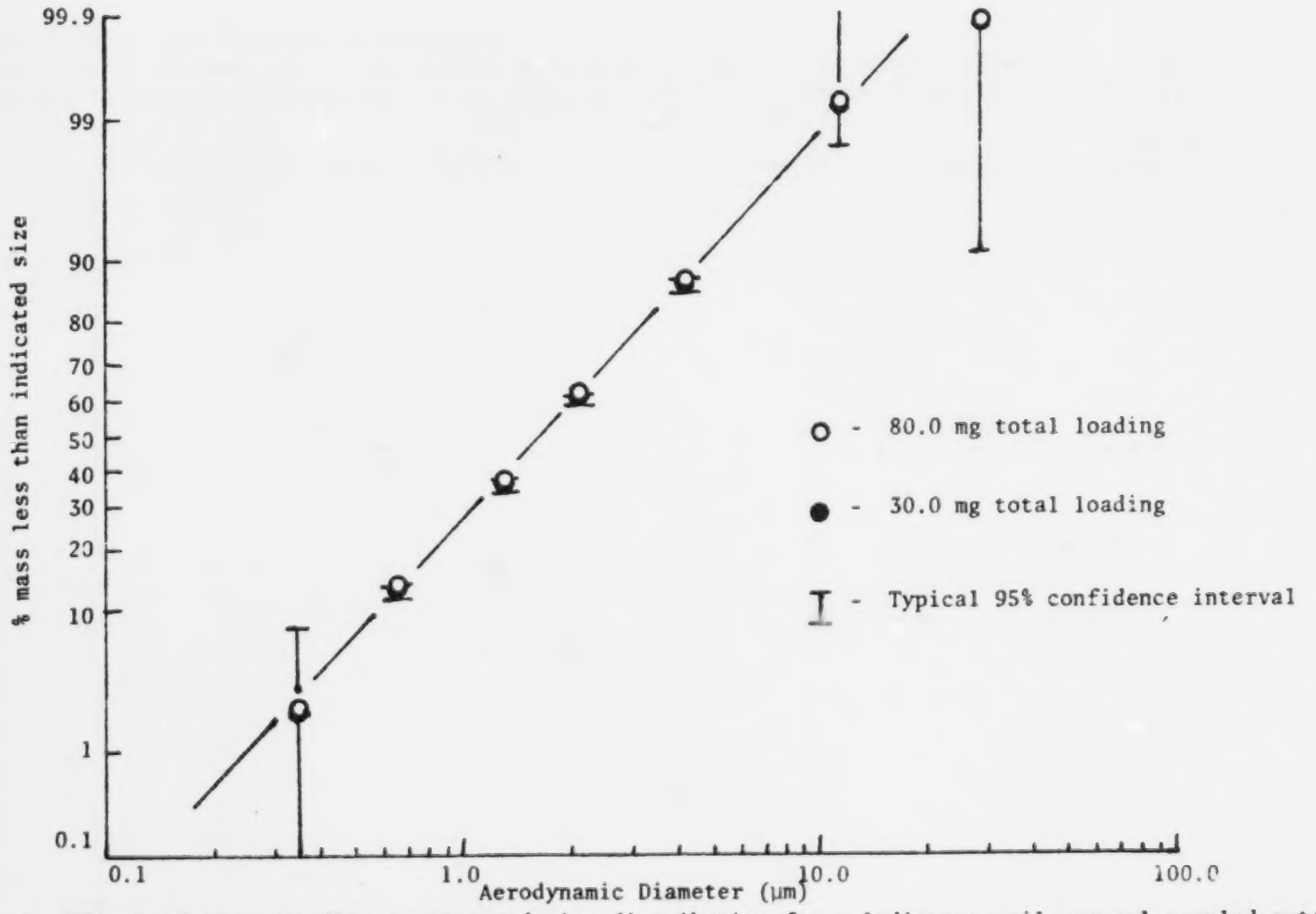


Figure 41. Effect of stage loading on measured size distribution for polydisperse oil aerosol sampled onto glass fiber collection surfaces (MK III University of Washington source test cascade impactor, 0.5 cfm, 70°F, 30.00 "Hg, gravimetric analysis).

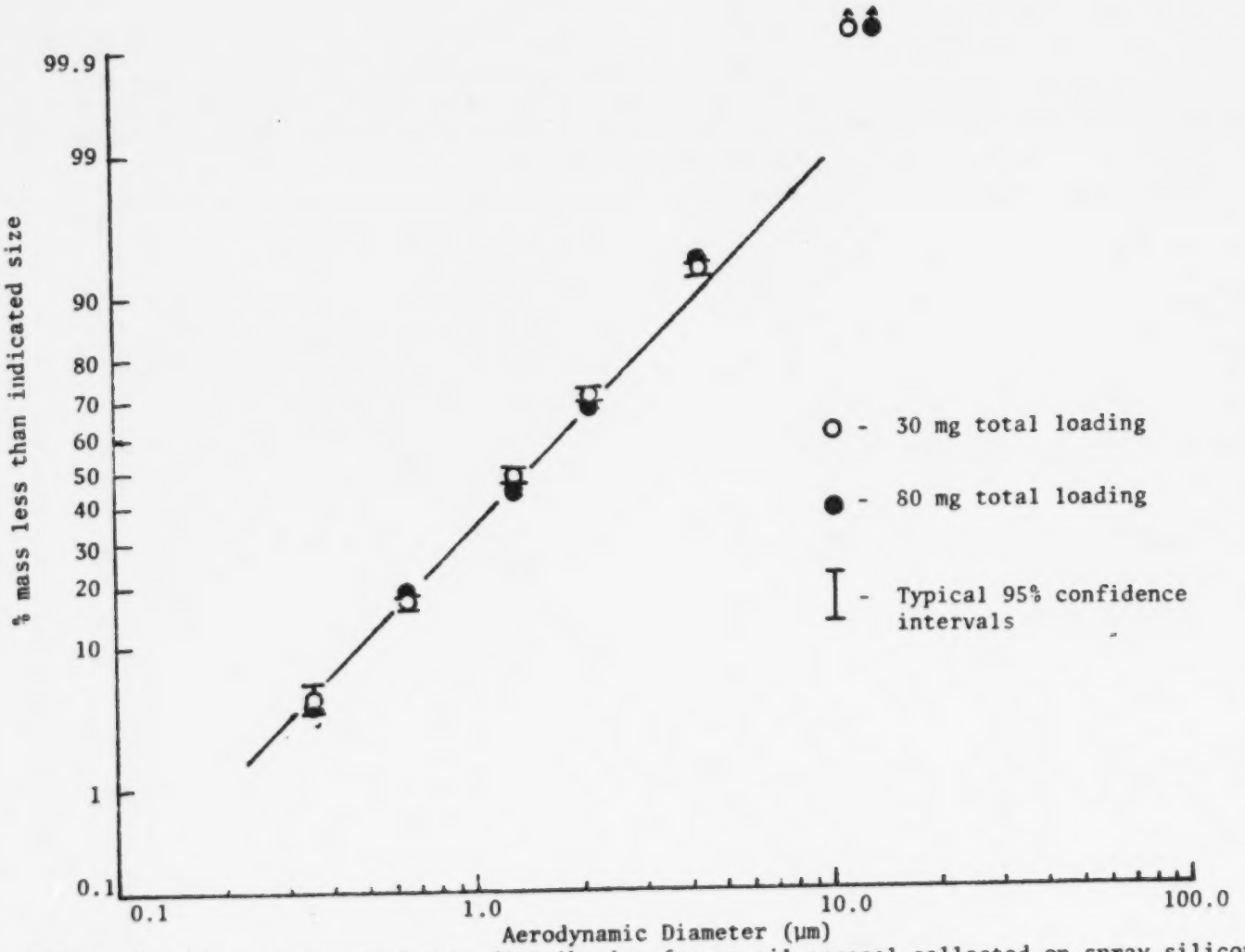


Figure 42 Effect of loading on measured size distribution for an oil aerosol collected on spray silicone collection surfaces (MK III University of Washington source test cascade impactor, 0.5 cfm, 70°F, 30.00 "Hg, gravimetric analysis).

## F. INTERSTAGE LOSSES

### 1. Interstage Losses as a Function of Particle Size

Monodisperse particles of uranine-methylene blue (90%:10% by weight) were generated over a size range from 2-13 μm diameter and sampled with the MK III University of Washington source test cascade impactor. The impactor was operated at 0.5 cfm and collection was onto spray silicone collection surface coatings. Total interstage losses were determined as previously described (Chapter IV, Sections F and G).

In Figure 43, results are plotted as total interstage losses versus particle diameter. Interstage losses accounted for as little as 2% of the total collected mass for 2 μm diameter particles, to as much as 45% for 13 μm diameter particles.

### 2. Effect of Interstage Losses on Size Distribution

Wall losses for the MK III University of Washington source test cascade impactor were also evaluated for a polydisperse uranine aerosol. The impactor was operated at its design flow rate of 0.5 cfm and equal volumes of the aerosol stream were sampled except where noted.

Histograms of the interstage losses incurred when sampling different total loadings of a polydisperse uranine aerosol collected onto both glass fiber and spray silicone collection surfaces are shown in Figures 44 and 45. At a total loading of 0.3 mg (Figure 44), the total interstage losses were 2% and 4% of the total collected mass for spray silicone and glass fiber collection surfaces, respectively. However, when the total loadings were increased to 10 mg (Figure 45), interstage losses increased to 13% and 12% for these same type collection surfaces. It was observed that at 10 mg total loading, interstage losses associated with the uncoated aluminum collection surfaces were significantly greater, at 20%. In all cases, the majority of the losses were to the nozzle plates rather than the collection plates. Observation of the nozzle plates revealed losses to: 1) the inside walls of the nozzles, 2) the top center of the plates, directly beneath the opening from the previous collection plate, and 3) the underside of the nozzle plates. Losses to the collection plates were predominantly in the area of the outer wall.

The effect of excluding these losses from the apparent measured size distribution is shown in Figures 46 through 49, for both glass fiber and spray silicone collection surfaces at total loadings of 0.3 mg and 10.0 mg. In all cases, there was little change in the apparent distribution when the recovered losses were excluded. Corresponding measured size distributions

Similar tests were conducted using the Andersen, Sierra and modified Brink impactors, all operated at their suggested flow rate. Equal volumes of the aerosol stream were sampled, resulting in total impactor catches of approximately 15 mg. Histograms of the measured interstage losses are shown in Figures 50 a through c. Table 3 summarizes the measured total interstage losses for each of the impactors used. Corresponding measured size distributions again show little effect when these losses are excluded (Figures 49-53).

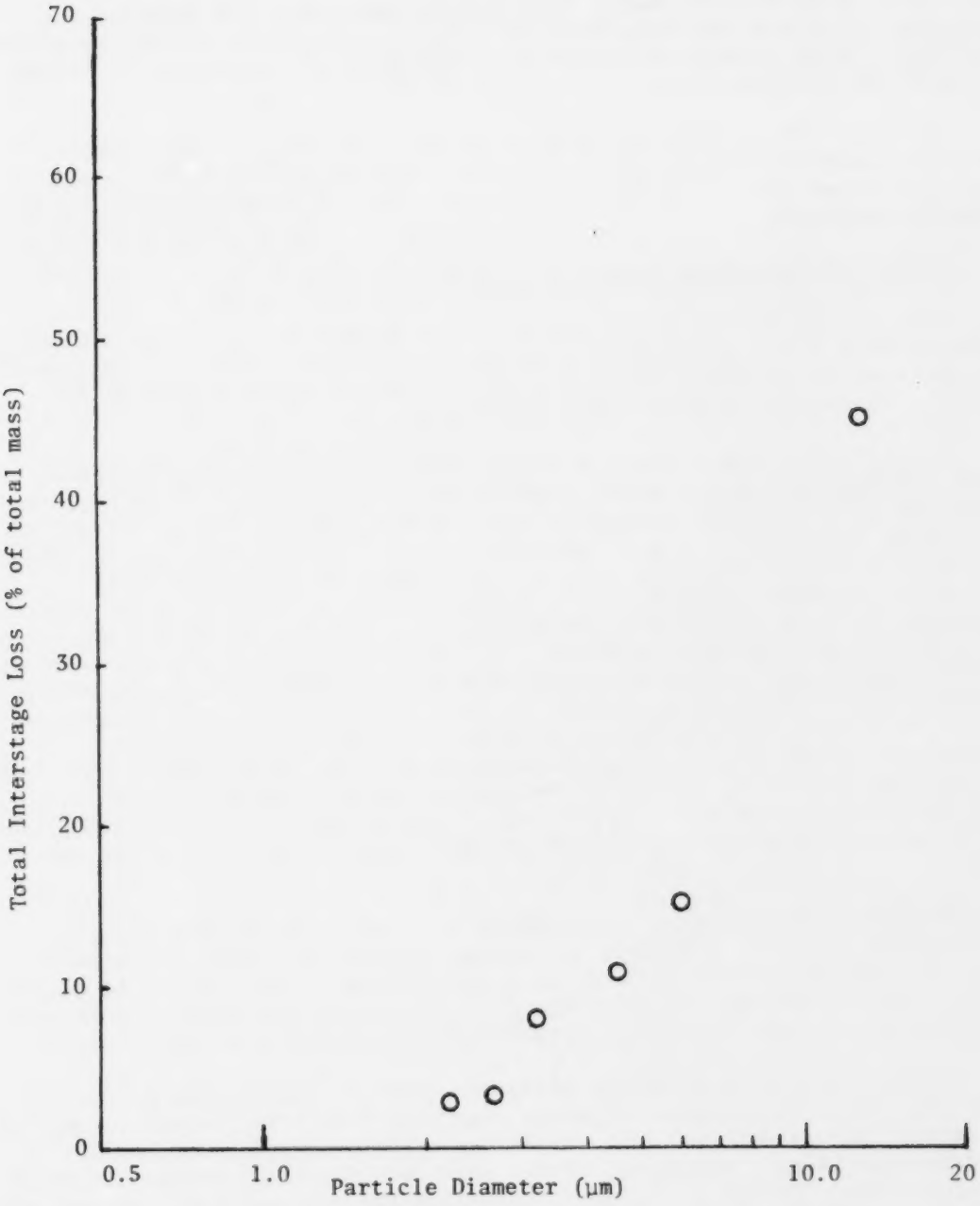


Figure 43. Total interstage loss versus particle diameter for the University of Washington MK III source test cascade impactor.

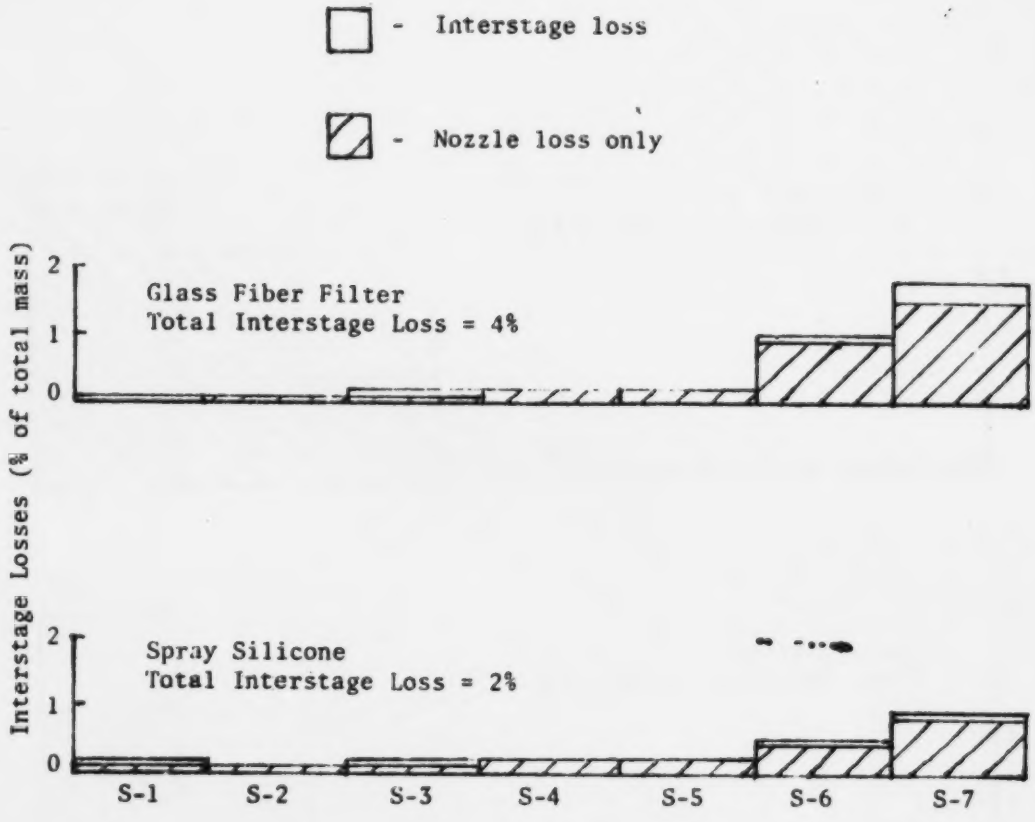


Figure 44. MK III University of Washington source test cascade impactor measured interstage losses for a polydisperse uranine aerosol of mmd = 0.45 μm, at a total loading of 0.3 mg.

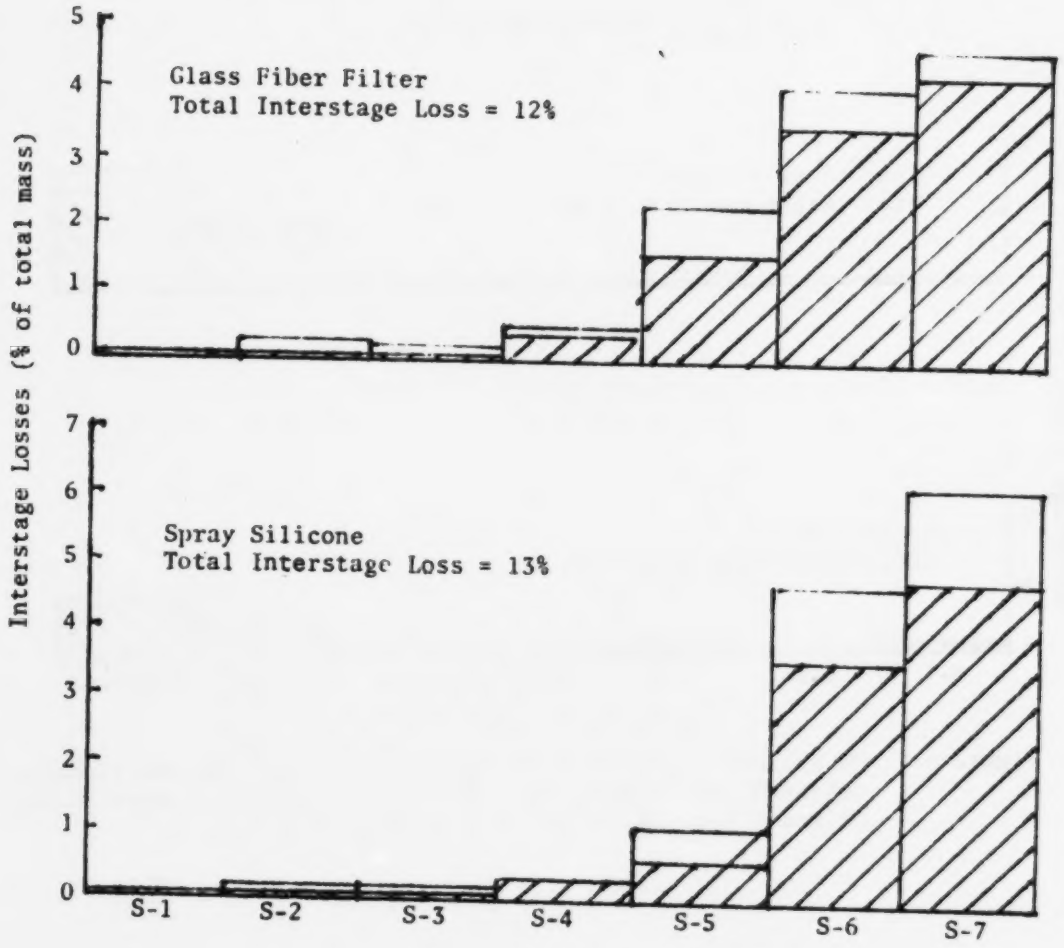


Figure 45. MK III University of Washington source test cascade impactor measured interstage losses for a polydisperse uranine aerosol of mmd = 0.45 μm, at a total loading of 10.0 mg.

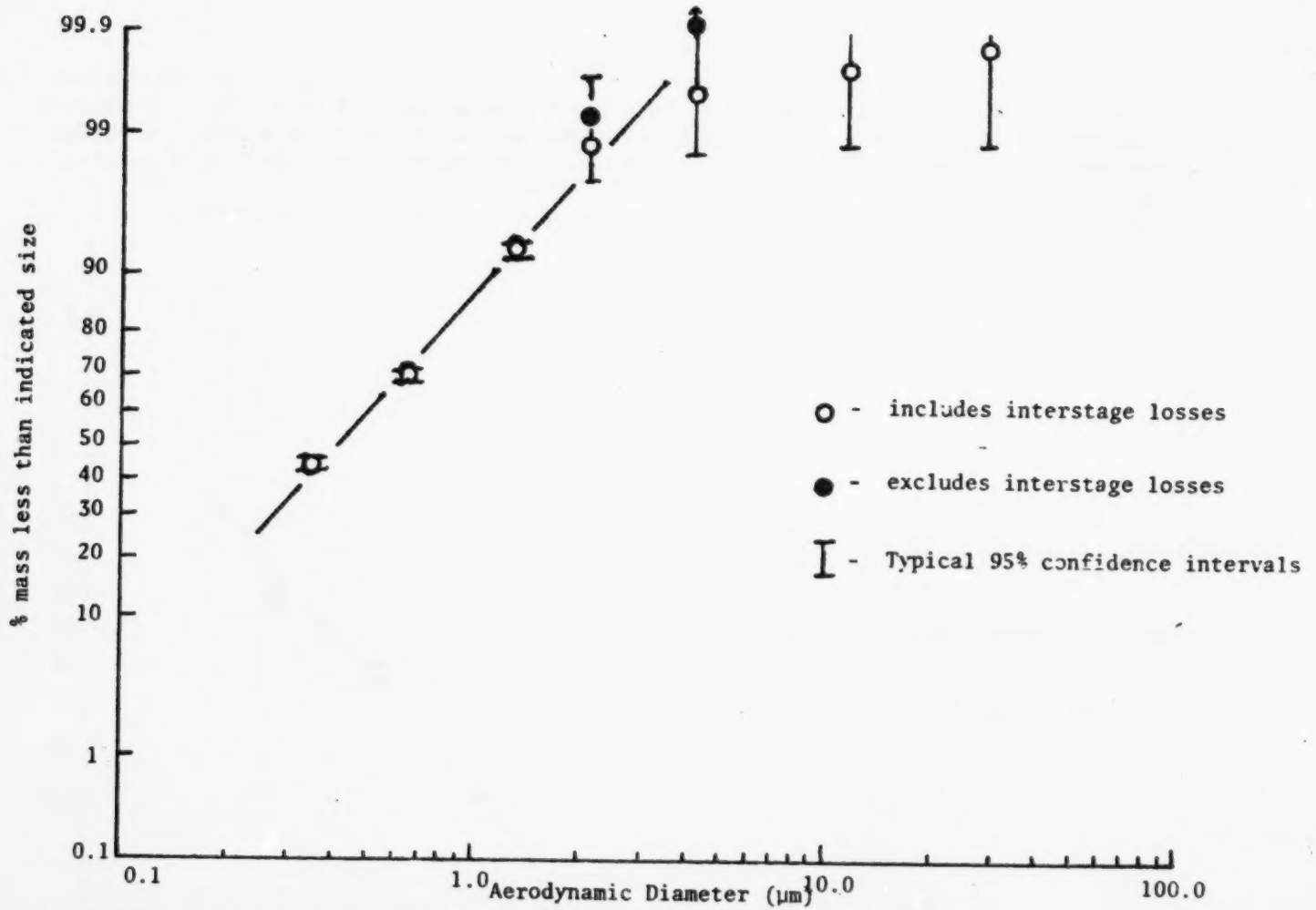


Figure 46. Effect of interstage losses on measured size distribution of polydisperse uranine aerosol sampled onto spray silicone at low stage loading (MK III University of Washington source test cascade impactor, 0.5 cfm, 70°F, 29.93 "Hg, 0.3 mg total loading, fluorometric analysis).

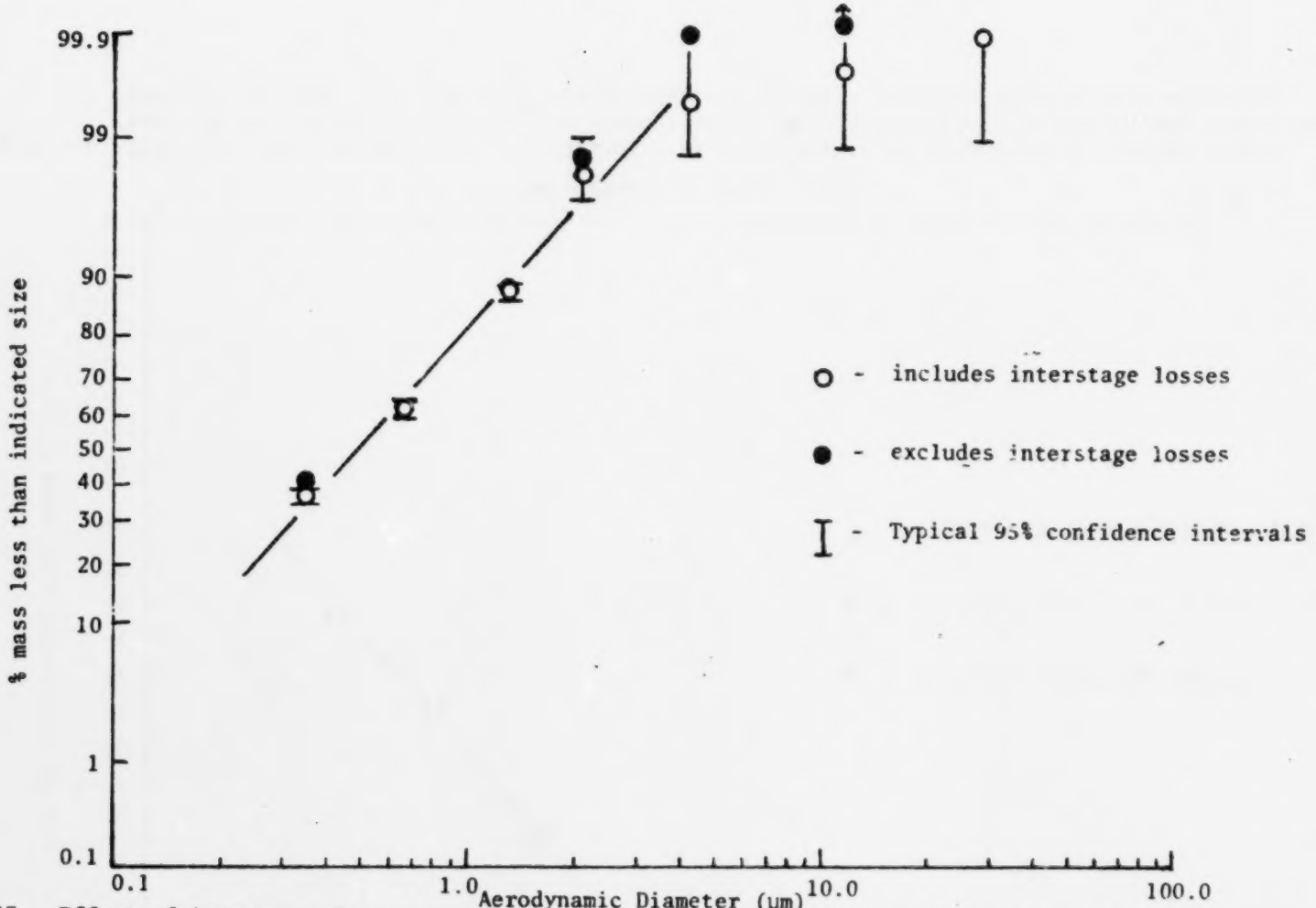


Figure 47. Effect of interstage losses on measured size distribution for polydisperse uranine aerosol sampled onto spray silicone collection surfaces at high stage loadings (MK III University of Washington source test cascade impactor, 0.5 cfm, 70°F, 30.20 "Hg, 10.0 mg total loading, fluorometric analysis).

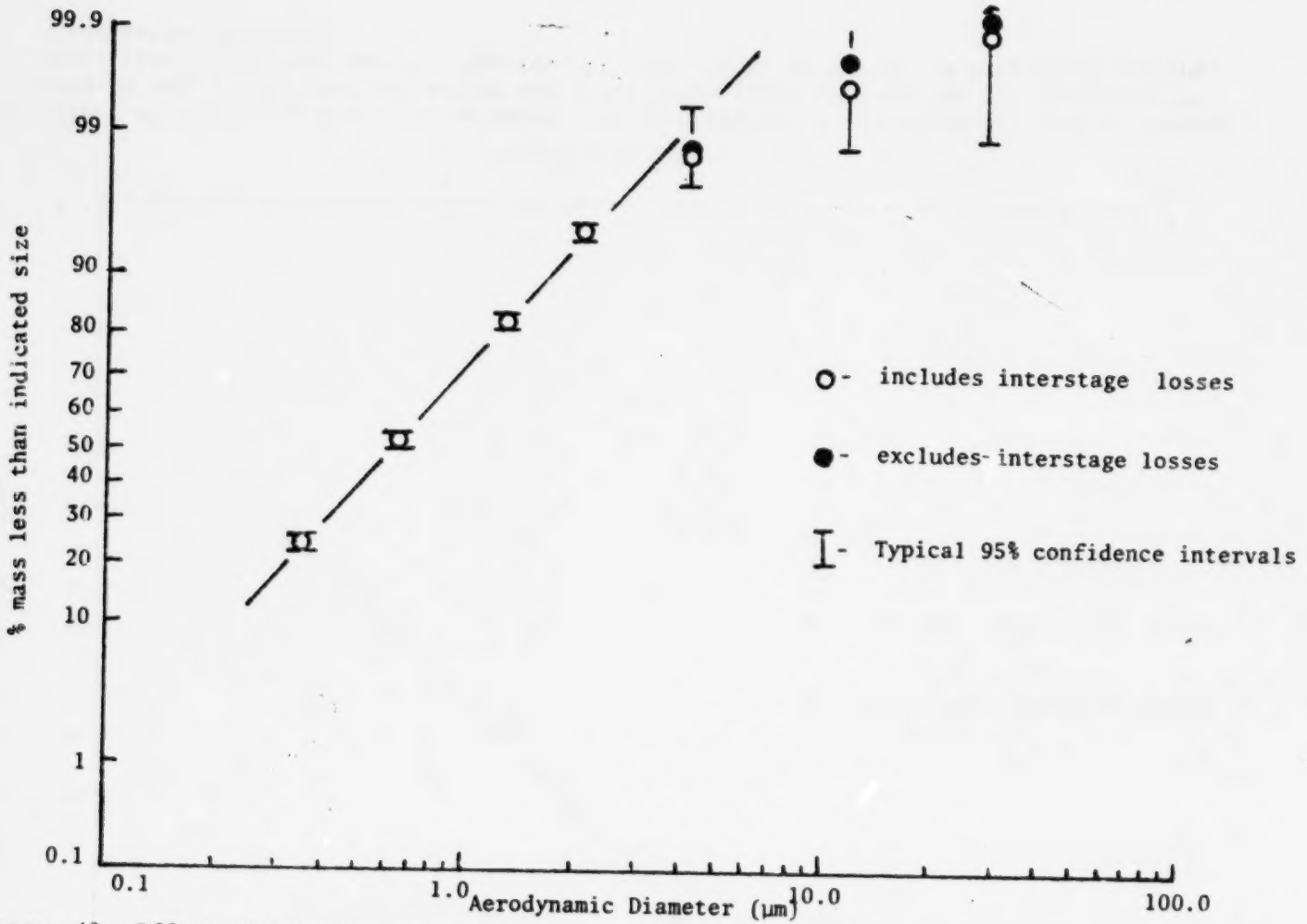


Figure 48. Effect of interstage losses on measured size distribution for polydisperse uranine aerosol sampled onto glass fiber collection surface at low stage loading (MK III University of Washington source test cascade impactor, 0.5 cfm, 70°F, 30.19 "Hg, 0.3 mg total loading, fluorometric analysis).

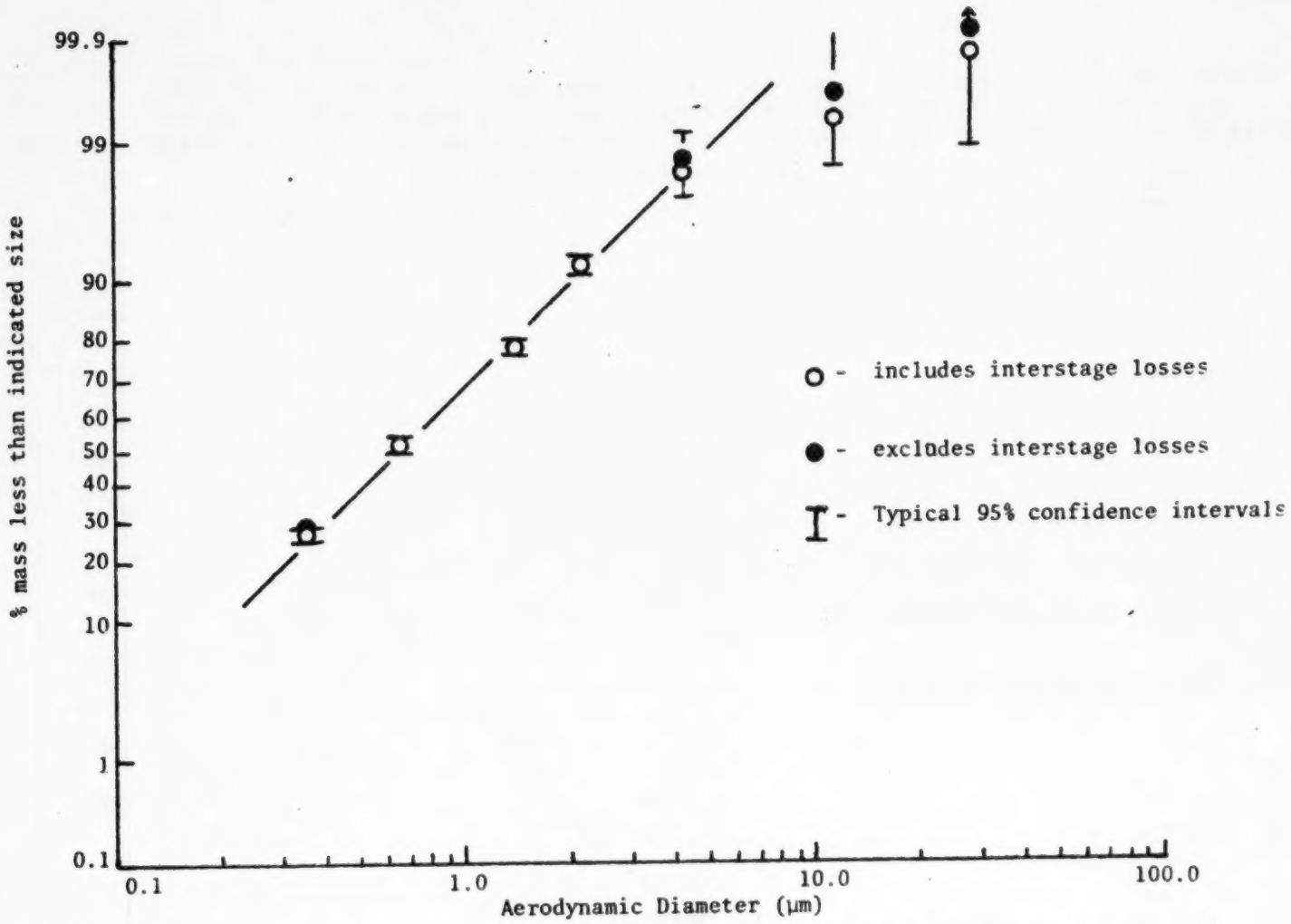


Figure 49. Effect of interstage losses on measured size distribution for polydisperse uranine aerosol sampled onto glass fiber collection surface at high stage loadings (MK III University of Washington source test cascade impactor, 0.5 cfm, 70°F, 30.20 "Hg, 10.0 mg total loading, fluorometric analysis).

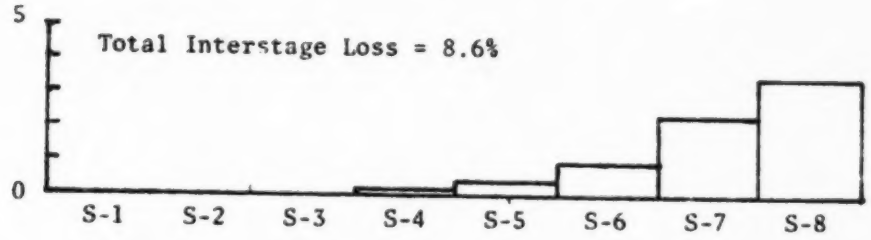


a. Andersen MK III stack sampler, 0.5 cfm, glass fiber collection surface, 15.0 mg total loading, fluorometric analysis.

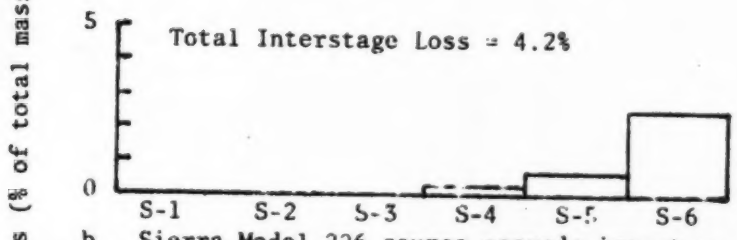


b. Sierra Model 226 source cascade impactor, 0.25 cfm, glass fiber collection surface, 15.0 mg total loaiding, fluorometric analysis.

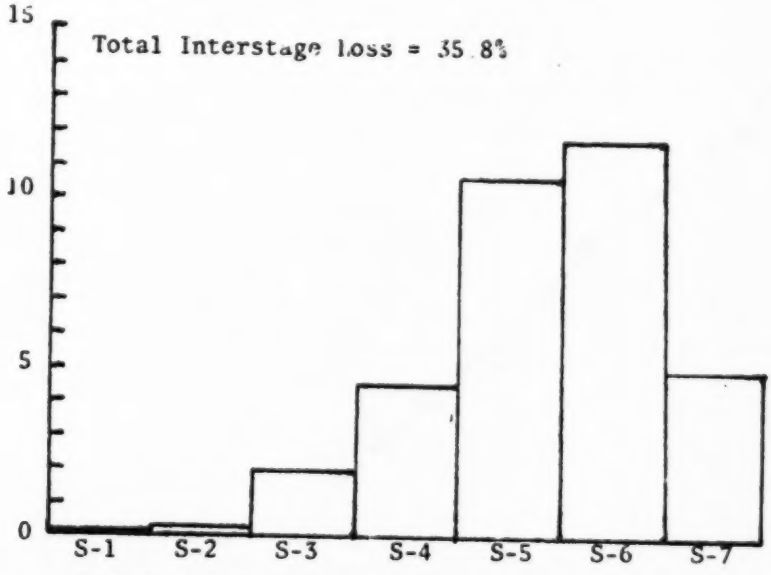


c. Modified Brink Model B cascade impactor, 0.05 cfm, glass fiber collection surface, 15.0 mg total loading, fluorometric analysis.

Figure 50. Histograms of measured interstage losses for the Andersen, Sierra and Brink impactors (polydisperse uranine aerosol of mmd = 0.72 μm).

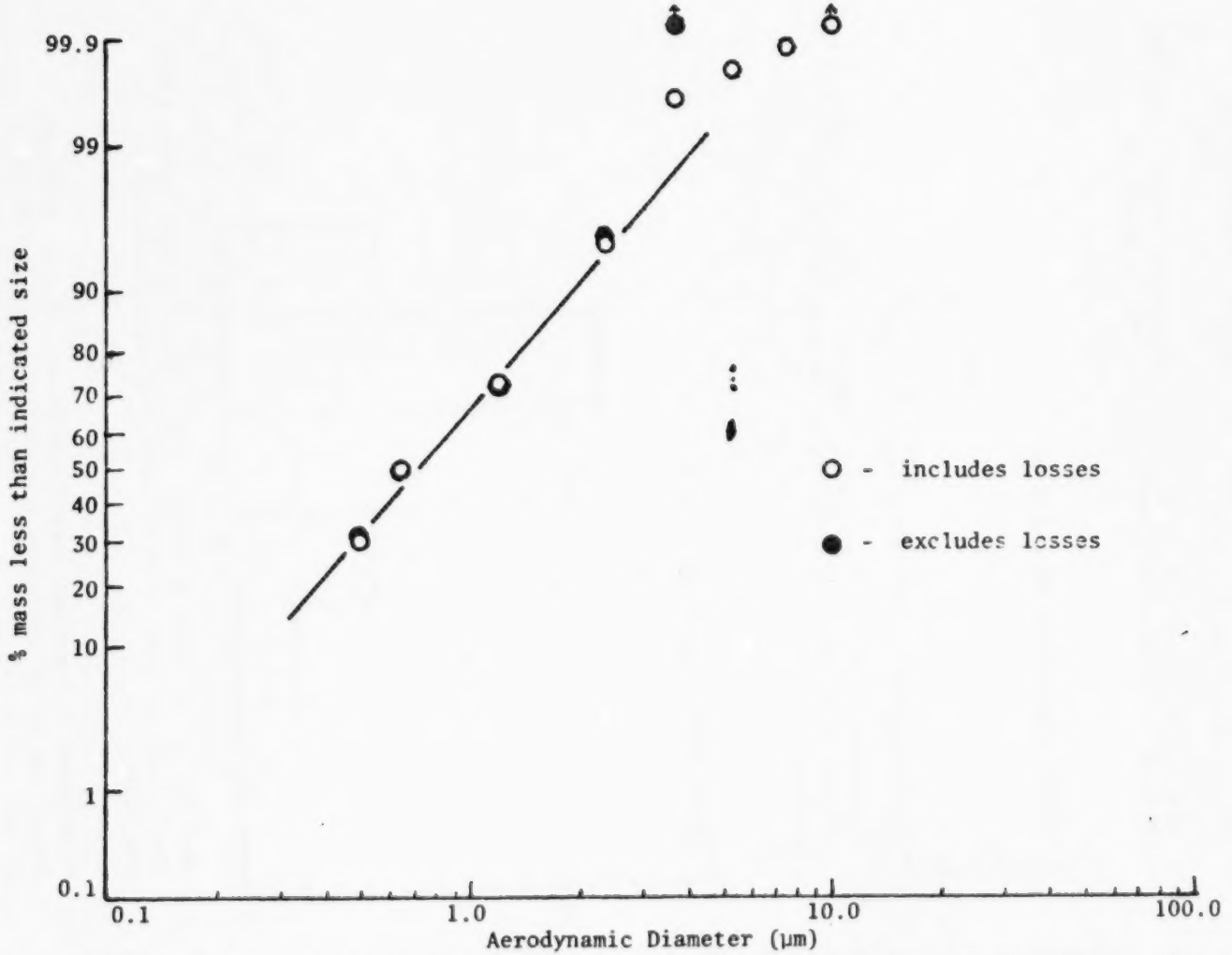


Figure 51. Effect of interstage losses on measured size distribution for a polydisperse uranine aerosol sampled using the Andersen MK III stack sampler (0.5 cfm, glass fiber collection surfaces, 70°F, 30.00 "Hg, 15.0 mg total loading, gravimetric analysis).

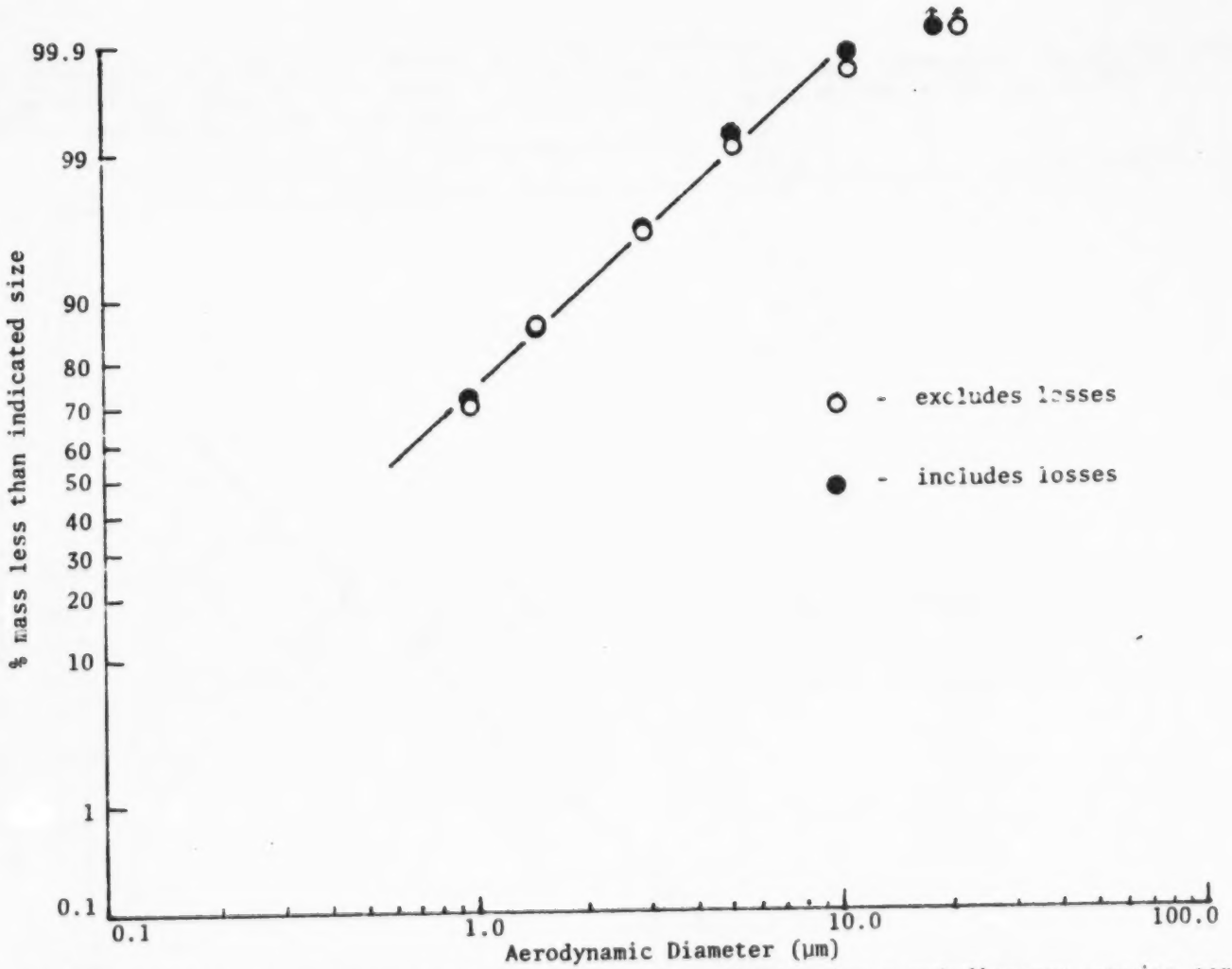


Figure 52. Effect of interstage losses on measured size distribution for a polydisperse uranine aerosol sampled using the Sierra Model 226 source cascade impactor (0.25 cfm, glass fiber collection surface, 70°F, 30.04 "Hg, 15.0 mg total loading, gravimetric analysis).

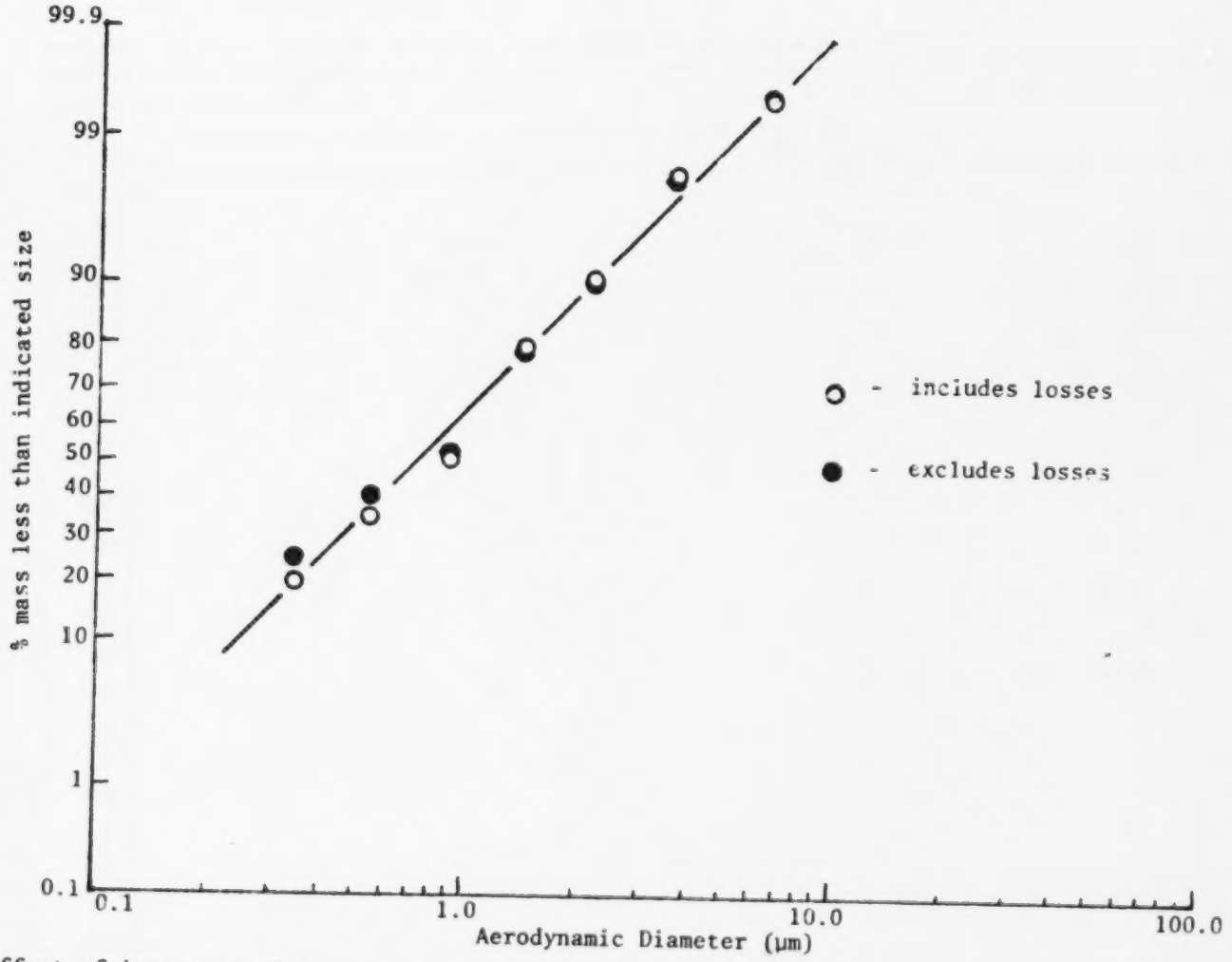


Figure 53. Effect of interstage losses on measured size distribution of polydisperse uranine aerosol sampled using the modified Brink Model B cascade impactor (0.05 cfm, glass fiber collectior surface, 70°F, 30.06 "Hg, 15.0 mg total loading, gravimetric analysis).

## REFERENCES


1. National Council of the Paper Industry for Air and Stream Improvement, Inc., "Procedures for Source Emission Particle Sizing Using Cascade Impactors and Microscopic Sizing Techniques," Atmospheric Quality Improvement Technical Bulletin No 71, May 1974.

2. Calvert, S., C. Lake and R. Parker, "Cascade Impactor Calibration Guidelines," Environmental Protection Technology Series, EPA-600/2-76-118, (NTIS No. PB 252 656), April 1976.

3. Cushing, K.M., G.E. Lacey, J.D. McCain and W.B. Smith, "Particulate Sizing Techniques for Control Device Evaluation: Cascade Impactor Calibrations," Environmental Protection Technology Series, EPA-600/2-76-280, U.S. Environmental Protection Agency, Research Triangle Park, N.C., October 1976.

4. Harris, D.B., "Tentative Procedures for Particle Sizing in Process Streams: Cascade Impactors," Environmental Protection Technology Series, EPA-600/2-76-023 (NTIS No. PB 250 375), February 1976.

5. McCain, J.D., K.M. Cushing and A.N. Bird, Jr., "Field Measurements of Particle Size Distribution with Inertial Sizing Devices," Environmental Protection Technology Series, EPA-650/2-73-035, (NTIS No. PB 226 292), October 1973.

6. Harris, D.B., "Procedures for Cascade Impactor Calibration and Operation in Process Streams," Environmental Protection Technology Series, EPA-600/2-77-004, U.S. Environmental Protection Agency, Research Triangle Park, N.C., January 1977.

7. Smith, W.B., K.M. Cushing, G E. Lacey and J.D. McCain, "Particulate Sizing Techniques for Control Device Evaluation," Environmental Protection Technology Series, EPA-650/2-74-102-a, U.S. Environmental Protection Agency, Research Triangle Park, N.C., August 1975.

8. Smith, W.B., K.M. Cushing and G.E. Lacey, "Andersen Filter Substrate Weight Loss," Environmental Protection Technology Series, EPA-650/2-75-022 (NTIS No. PB 240 720), February 1975.

9. Rao, A.K., An Experimental Study of Inertial Impactors, Doctoral Thesis, University of Minnesota, Minneapolis, Minn., June 1975.

10. Willeke, K., "Performance of the Slotted Impactor," Amer. Ind. Hygiene Assoc. J., 36:683 (1975).

11. May, K.R., "The Cascade Impactor: An Instrument for Sampling Coarse Aerosols," J. Sci. Instr., 22:187, 1945.

12. Marple, V.A., A Fundamental Study of Inertial Impactors, Doctoral Thesis, University of Minnesota, Minneapolis, Minn., December 1970.

13. Ranz, W.E. and J.B. Wong, "Impaction of Dust and Smoke Particles," Ind. and Eng. Chem., 44:1371-81, (1952).

14. Davies, C.N. and M. Aylward, "The Trajectories of Heavy, Solid Particles in a Two Dimensional Jet of Ideal Fluid Impinging Normally Upon a Plate," Proc. Phys. Soc., B64:889 (1951).

15. Mercer, T.T. and H.Y. Chow, "Impaction from Rectangular Jets," J. Coll. and Interface Sci., 27:75 (1968).

16. _____, and R.G. Stafford, "Impaction from Round Jets," Ann. Occup. Hyg., 12:41 (1969).

17. Wilcox, J.D., "Design of a New Five-Stage Cascade Impactor," A.M.A. Arch. Ind. Hyg. and Occup. Med., 7:376 (1953).

18. Fuchs, N.A., The Mechanics of Aerosols, Pergamon Press, New York, (1964).

19. Cooper, D.W. and J.W. Davis, "Cascade Impactors for Aerosols: Improved Data Analysis," Amer. Ind. Hygiene Assoc. J., 33:79 (1972).

20. Mercer, T.T., "The Interpretation of Cascade Impactor Data," Amer. Ind. Hygiene Assoc. J., 26:236 (1965).

21. Natusch, D.F.S. and J.R. Wallace, "Determination of Airborne Particle Size Distributions: Calculation of Cross-Sensitivity and Discreteness Effects in Cascade Impaction," Atmos. Environ. 10:315 (1976).

22. Jordan, D.W., "The Adhesion of Dust Particles," Brit. J. Appl. Phys. Suppl., 3:s194 (1954).

23. Dahneke, B., "The Capture of Aerosol Particles by Surfaces," J. Coll. and Interface Sci., 37:342 (1971).

24. Loffler, F., "The Adhesion of Dust Particles to Fibrous and Particulate Surfaces," Staub-Reinhalt. Luft, 28:29 (1968).

25. Bucchloz, H., "On the Separation of Airborne Matter by Inertia Effect in the Submicron Range," Staub-Reinhalt. Luft, 30:15 (1970).

26. Berner, A., "Practical Experience with a 20-Stage Impactor," Staub-Reinhalt. Luft, 32:1 (1972).

27. Lundgren, D.A., "An Aerosol Sampler for Determination of Particle Concentration of Size and Time," J. Air Poll. Contr. Assoc., 17:225 (1967).

28. Loffler, F., "Blow-off of Particles Collected on Fiber Filters," Filtration and Separation, 9:688 (1972).

29. Winkler, P., "Relative Humidity and the Adhesion of Atmospheric Particles to the Plates of Impactors," Aerosol Science, 5:235 (1974).

30. Willeke, K. and J.J. McFeters, "The Influence of Flow Entry and Collecting Surface on the Impaction Efficiency of Inertial Impactors," J. Coll. and Interface Sci., 53:121 (1975).

31. Felix, G., C.E. Clinard, G.E. Lacey and J.D. McCain, "Inertial Cascade Impactor Substrate Media for Flue Gas Sampling," Interagency Energy-Environmental Research and Development Series, EPA-600/7-77-060, U.S. Environmental Protection Agency, Research Triangle Park, N.C., June 1977.

32. Picknett, R.G., "A New Method for Determining Aerosol Size Distributions from Multistage Sampler Data," Aerosol Science, 3:185 (1972).

33. Berglund, R.N. and B.Y.H. Liu, "Generation of Monodisperse Aerosol Standards," Environ. Sci. and Tech., 7:147 (1973).

34. Green, H.L. and W.R. Lane, Particulate Clouds: Dusts, Smokes and Mists, E. and F.N. Spon. Ltd., London (1957).

35. Whitby, K.T., "Generator for Producing High Concentrations of Small Ions," Rev. Sci. Inst., 32:1351 (1961).

## APPENDIX A

## GUIDE FOR THE USE OF IN-STACK CASCADE IMPACTORS

The guide presented below is not meant to be a complete set of instructions for the field use of in-stack impactors. The information is presented as supplementary material to previously published procedures for the use of in-stack impactors (4,6).

I. Selection of collection surface

A. Spray silicone coating

1. For use at temperatures less than 400°F.
2. Apply the approximate thickness of the size particles which will be caught.
3. Precondition for at least one hour at the temperature at which sampling will occur.

B. Glass fiber

1. For use at temperatures less than approximately 1000°F.
2. Precondition to avoid $SO_2$ uptake (31,8).
3. Precondition for at least one hour at the temperature at which sampling will occur.
4. Measured size distribution mmd could be on the order of 30% greater than actual.
5. Avoid use when sampling "hard" aerosols due to increased bounce related errors.

C. Uncoated aluminum

1. For use at temperatures less than approximately 900°F.
2. Precondition for at least one hour at the temperature at which sampling will occur.
3. Avoid use when sampling oil aerosols or "hard" aerosols due to unstable collection characteristics.

II. Gas sampling rate

A. MK III University of Washington source test cascade impactor

1. $0.25 \text{ cfm} \leq Q < 1.0 \text{ cfm}$ when sampling either oil or hygroscopic type aerosols.

2. 0.25 cfm $\leq$ Q < 0.5 cfm when sampling "hard" aerosols.

B. Sierra Model 226 source test cascade impactor

1. 0.25 cfm $\leq$ Q $\leq$ 1.0 cfm when sampling either oil or hygroscopic type aerosols.

2. 0.25 cfm $\leq$ Q $\leq$ 0.5 cfm when sampling "hard" aerosols.

C. Andersen MK III stack sampler

1. 0.25 cfm $\leq$ Q $\leq$ 1.0 cfm when sampling either oil or hygroscopic type aerosols.

2. 0.25 cfm $\leq$ Q $\leq$ 0.5 cfm when sampling "hard" aerosols.

D. Modified Brink Model B cascade impactor

1. Q < 0.05 cfm when sampling either oil or hygroscopic type aerosols.

2. Q < 0.025 cfm when sampling "hard" aerosols.

E. General selection of flow rate

1. Maintain jet velocities < 75 m/sec when sampling either oil or hygroscopic type aerosols.

2. Maintain jet velocities < 50 m/sec when sampling "hard" aerosols.

3. Choose a flow rate which will provide sizing information over the range of the expected mmd, within the above limits.

III. Stage loadings

A. Hygroscopic type aerosols — 5-7 mg upper limit

B. Oil aerosols — 15 mg upper limit

C. General upper limit

1. Observe back side of nozzle for increased deposition.

2. Observe primary deposits for uniformity.

D. General lower limit

1. Collect at least 10X the error associated with the mass measurement.

IV. Treatment of interstage losses

A. Suggest excluding them from calculations due to errors involved in trying to recover these losses

B. Must include losses as total collected mass if calculating mass loadings of the process stream

V. Treatment of sizing data

Consider that the error associated with a mass measurement is inversely proportional to the mass collected, therefore when constructing the distribution, give greater weight to the data points representing the majority of the collected mass.